Electronic Supplementary Material (ESI) for Chemical Science.

The ON/OFF switching by metal ions of the "Sergeants and Soldiers" chiral amplification effect on helical poly(phenylacetylene)s

Julián Bergueiro, Félix Freire, Edison Wendler, José Manuel Seco,*
*Emilio Quiñoá, Ricardo Riguera**

Department of Organic Chemistry and Center for Research in Biological
Chemistry and Molecular Materials (CIQUS), University of Santiago de
Compostela, E-15782 Santiago de Compostela, Spain

E-mail: ricardo.riguera@usc.es, felix.freire@usc.es

Supporting Information

Contents:

Structures and codes

Monomers

Structure	Code	Structure	Code
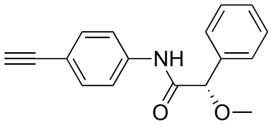	**M01**	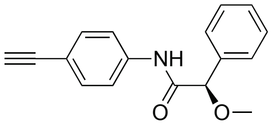	**M02**
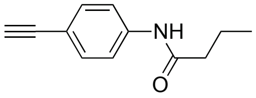	**M03**	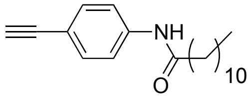	**M04**
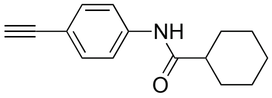	**M05**	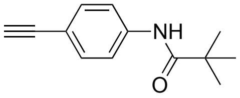	**M06**
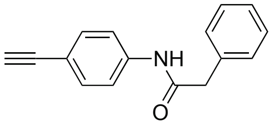	**M07**	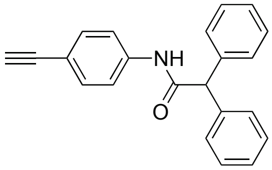	**M08**
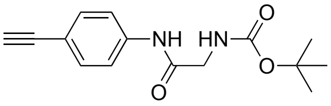	**M09**		

Homopolymers

Structure	Code	Structure	Code
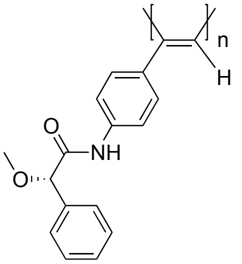	poly-**1**	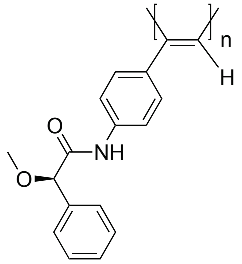	poly-**2**
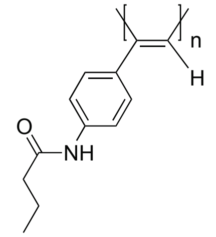	poly-**3**	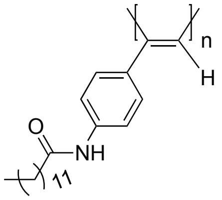	poly-**4**
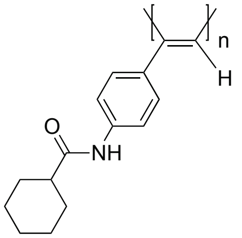	poly-**5**	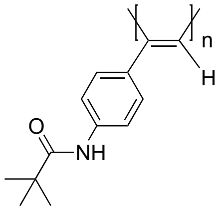	poly-**6**
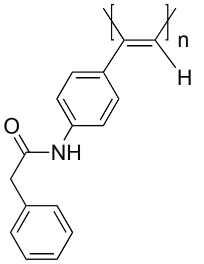	poly-**7**	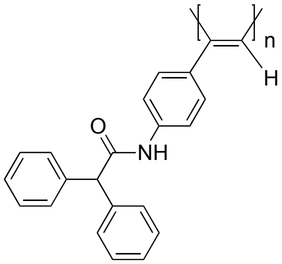	poly-**8**
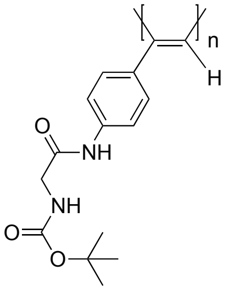	poly-**9**		

Copolymers

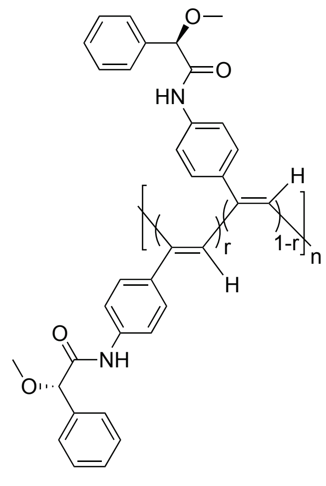	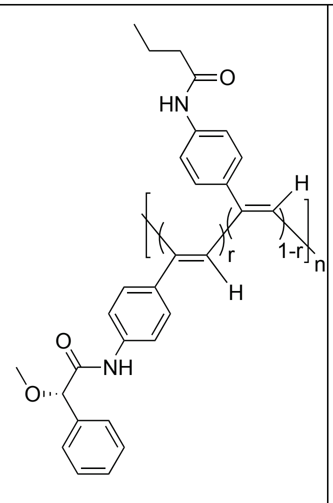	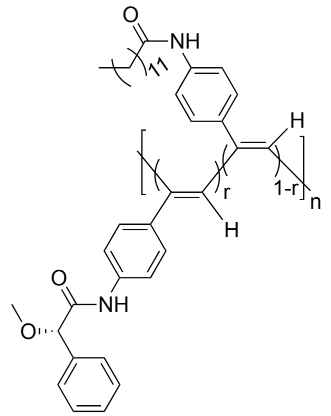	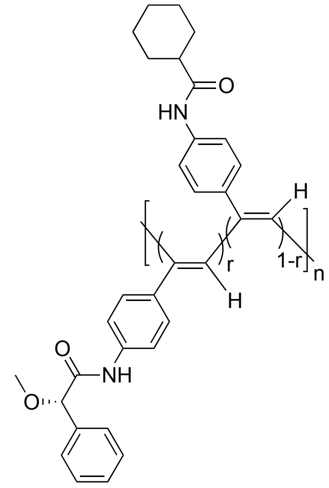
poly(**1**-*co*-**2**)	poly(**1**-*co*-**3**)	poly(**1**-*co*-**4**)	poly(**1**-*co*-**5**)
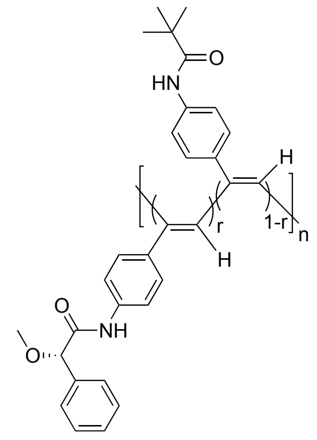	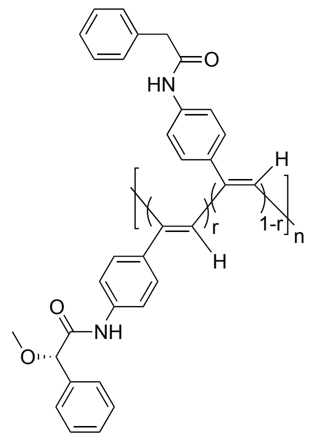	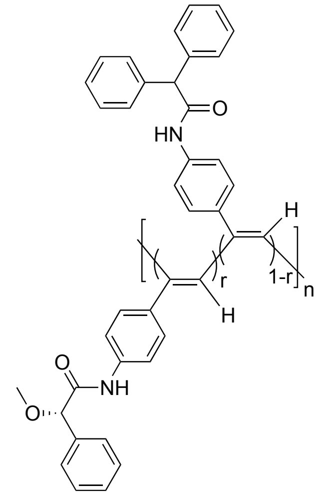	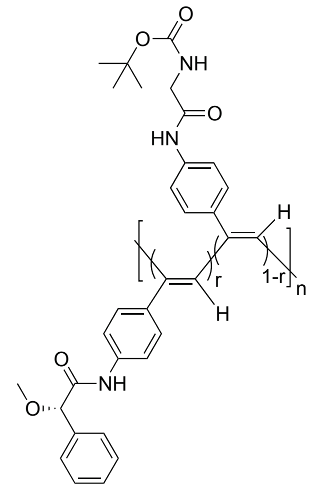
poly(**1**-*co*-**6**)	poly(**1**-*co*-**7**)	poly(**1**-*co*-**8**)	poly(**1**-*co*-**9**)

Synthesis of monomers

Synthesis and spectral data of monomers M01-M02

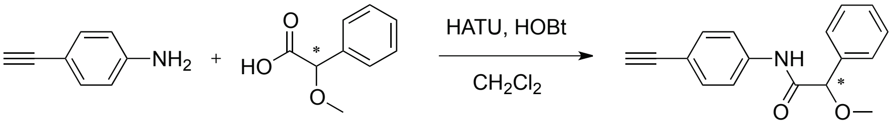

(2-(7-Aza-1H-benzotriazole-1-yl)-1,1,3,3-tetramethyluronium hexafluorophosphate) (AnaSpec. Inc. HATU, 2.3 g, 1.4 equiv.), 1-hydroxybenzotriazole (HOBt, 160 mg, 1.4 equiv.), (*R*)- or (*S*)-α-methoxy-α-phenylacetic acid (Yamakawa Ind, 850 mg, 1.4 equiv.) and diisopropyltriethylamine (DIEA, 207 μL, 1.4 equiv.) were dissolved in 45 mL of CH_2Cl_2, and the mixture was stirred for 10 min to activate the acid. Then, 4-ethynylaniline (Aldrich, 500 mg, 1.0 equiv.) was added and the reaction mixture was stirred for 1 day. The organic layer was washed with water, HCl 1M, water and a saturated solution of $NaHCO_3$. The combined organic layers were dried over anhydrous Na_2SO_4, filtered and the solvent was evaporated at reduced pressure. The crude product was chromatographed on silica gel (70-230 mesh) with hexane/ethyl acetate (7/3) as eluent [980 mg (*R*)-**M01** and 960 mg (*S*)-**M02**], 89% and 87% yield respectively of pure products.

***(R)*-M01 (Figure S1):**

α_D = -15 (*c* = 1.1, $CHCl_3$).

^{1}H NMR (300 MHz, $CDCl_3$) δ(ppm): 3.04 (s, 1H), 3.44 (s, 3H), 4.73 (s, 1H), 7.2-7.5 (m, 7H), 7.54-7.64 (m, 2H), 8.60 (broad s, 1H).

^{13}C NMR (75 MHz, $CDCl_3$) δ(ppm): 57.3, 76.8, 83.3, 83.8, 117.8, 119.3, 127.1, 128.7, 132.9, 136.3, 168.5.

HRMS (ESI) m/z calc. for $C_{18}H_{16}NO_3$ [M + H]: 265.3065, found: 265.2948.

***(S)*-M02 (Figures S2):**

α_D = +15 (*c* = 1.0, $CHCl_3$).

^{1}H NMR (300 MHz, $CDCl_3$) δ(ppm): 3.04 (s, 1H), 3.44 (s, 3H), 4.73 (s, 1H), 7.2-7.5 (m, 7H), 7.54-7.64 (m, 2H), 8.60 (broad s, 1H).

^{13}C NMR (75 MHz, CDCl$_3$) δ(ppm): 57.3, 76.8, 83.3, 83.8, 117.8, 119.3, 127.1, 128.7, 132.9, 136.3, 168.5.

HRMS (ESI) m/z calc. for $C_{18}H_{16}NO_3$ [M + H]: 265.3065, found: 265.3043.

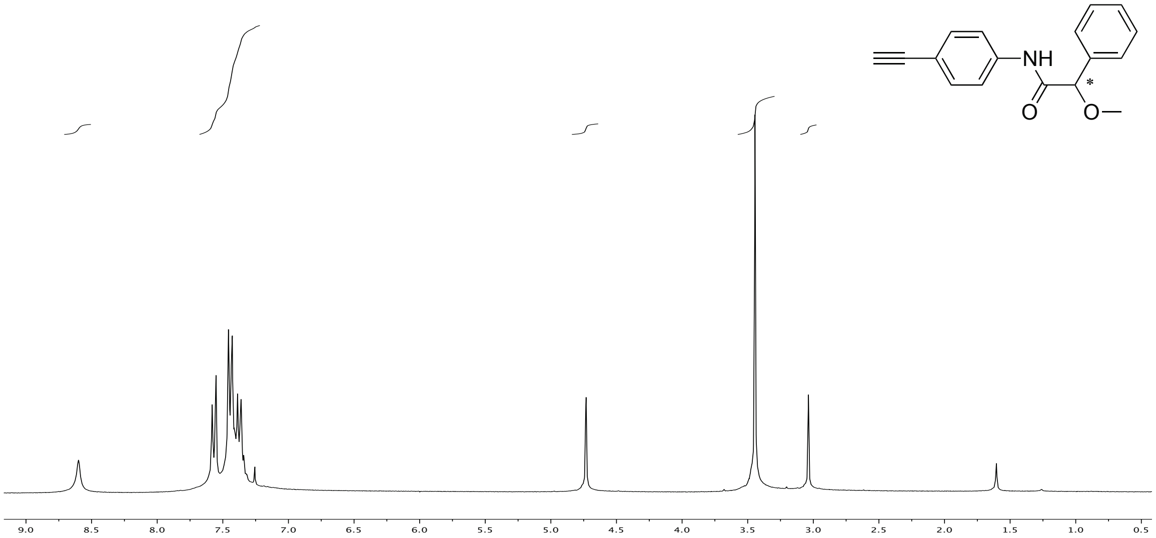

Figure S1. ^{1}H NMR spectrum of **M01** and **M02** (CDCl$_3$, 300 MHz).

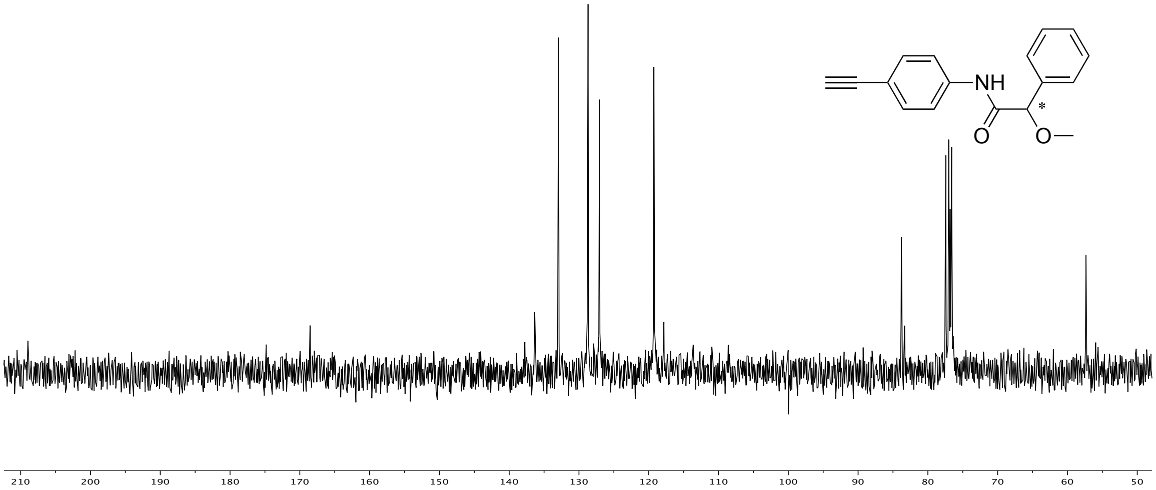

Figure S1. ^{13}C NMR spectrum of **M01** and **M02** (CDCl$_3$, 75 MHz).

General procedure for the synthesis of monomers M03-M09:

(1-Ethyl-3-(3-dimethylaminopropyl)carbodiimide) (AnaSpec. Inc. EDC•HCl, 1.5 equiv.), the corresponding acid (1.3 equiv.) and 4-dimethyaminopyridine (DMAP, 0.1 equiv.) were dissolved in CH_2Cl_2, and the mixture was stirred for 10 min to activate the acid. Then, 4-ethynylaniline (Aldrich, 1.0 equiv.) was added and the reaction mixture was stirred for 1 day. The organic layer was washed with water, HCl 1M, water and a saturated solution of $NaHCO_3$. The combined organic layers were dried over anhydrous Na_2SO_4, filtered and the solvent was evaporated at reduced pressure. The crude product was chromatographed on silica gel (70-230 mesh) with hexane/ethyl acetate (7/3) as eluent.

Synthesis and spectral data of monomer M03:

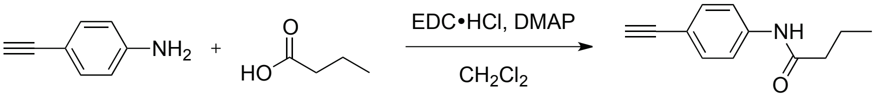

M03

Following the general procedure, EDC•HCl (1.24 g, 6.40 mmol), butyric acid (488.9 mg, 5.44 mmol) and DMAP (52.1 mg, 0.43 mmol) were dissolved in 43 mL of CH_2Cl_2. Next, 4-ethynylaniline (500 mg, 4.27 mmol) was added. After purification, 775.2 mg (97%) of *N*-(4-ethynylphenyl)butyramide (**M03**) were obtained.

^{1}H NMR (300 MHz, $CDCl_3$) δ(ppm): 0. 89 (t, *J* = 7.3 Hz, 3H), 1.6-1.8 (m, 2H), 2.33 (t, *J* = 7.4Hz, 2H),.34 (t, *J* = 7.6 Hz, 2H), 3.03 (s, 1H), 7.4-7.6 (m, 4H).

^{13}C NMR (75 MHz, $CDCl_3$) δ(ppm): 13.7, 19.0, 39.6, 76.7, 83.7, 119.3, 132.9, 138.4, 171.5.

HRMS (ESI) m/z calc. for $C_{12}H_{13}NO$ [M + H]: 188.2457, found: 188.2456.

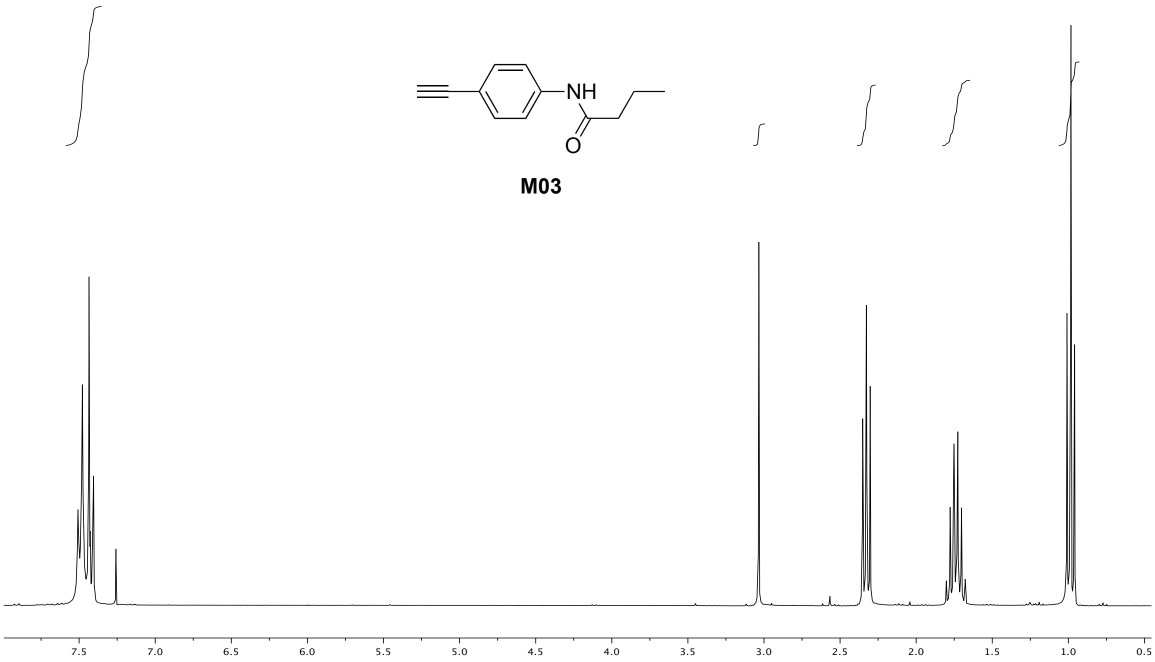

Figure S3. ^{1}H NMR spectrum of **M03** ($CDCl_3$, 300 MHz).

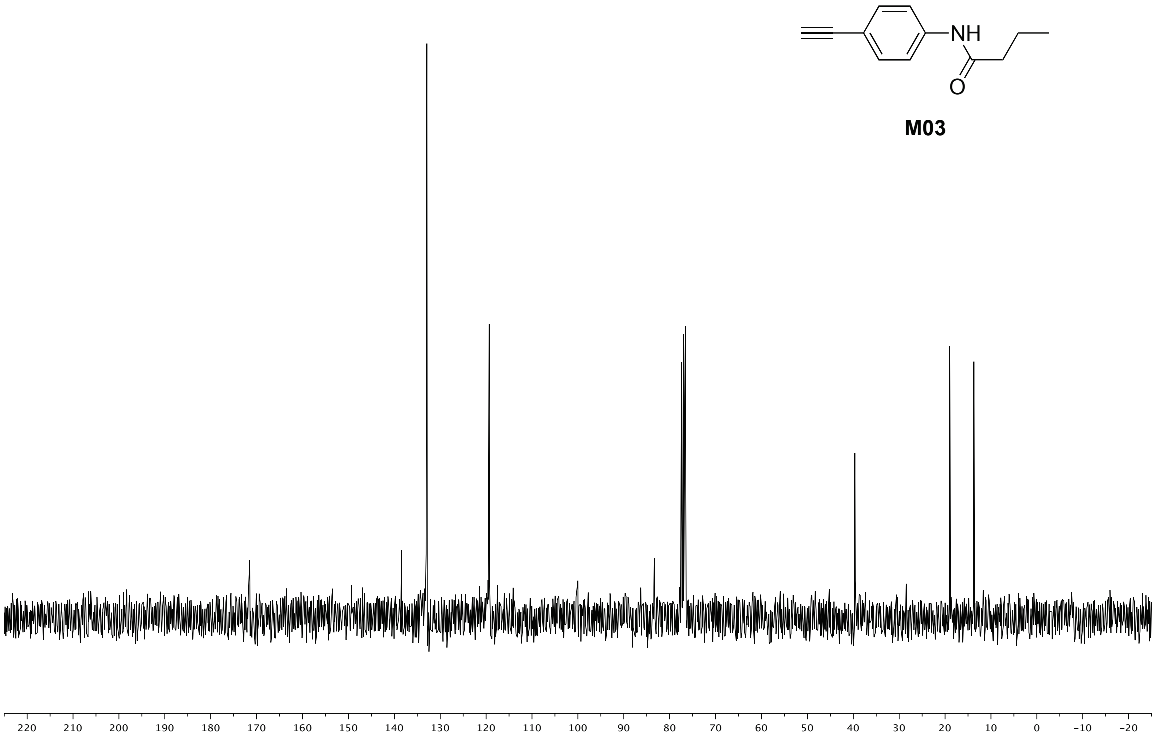

Figure S4. ^{13}C NMR spectrum of **M03** ($CDCl_3$, 75 MHz).

Synthesis and spectral data of monomer M04:

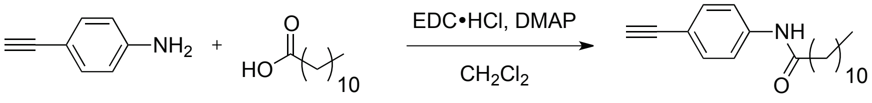

M04

Following the general procedure, EDC•HCl (1.24 g, 6.40 mmol), dodecanoic acid (1111.5 mg, 5.44 mmol) and DMAP (52.1 mg, 0.43 mmol) were dissolved in 43 mL of CH_2Cl_2. Next, 4-ethynylaniline (500 mg, 4.27 mmol) was added. After purification, 1124.7 mg (88%) of *N*-(4-ethynylphenyl)dodecanamide (**M04**) were obtained.

^{1}H NMR (300 MHz, $CDCl_3$) δ(ppm): 0.39 (t, *J* = 7.1 Hz, 3H), 1.2-1.4 (m, 16H), 1.6-1.8 (m, 2H), 2.34 (t, *J* = 7.6 Hz, 2H), 3.03 (s, 1H), 7.33 (broad, s, 1H), 7.4-7.6 (m, 4H).

^{13}C NMR (75 MHz, $CDCl_3$) δ(ppm): 14.1, 22.7, 25.5, 29.3, 29.4, 29.5, 31.9, 37.8, 76.7, 83.4, 98.7, 119.3, 132.9, 138.4.

HRMS (ESI) m/z calc. for $C_{20}H_{29}NO$ [M + H]: 300.4583, found: 300.4580.

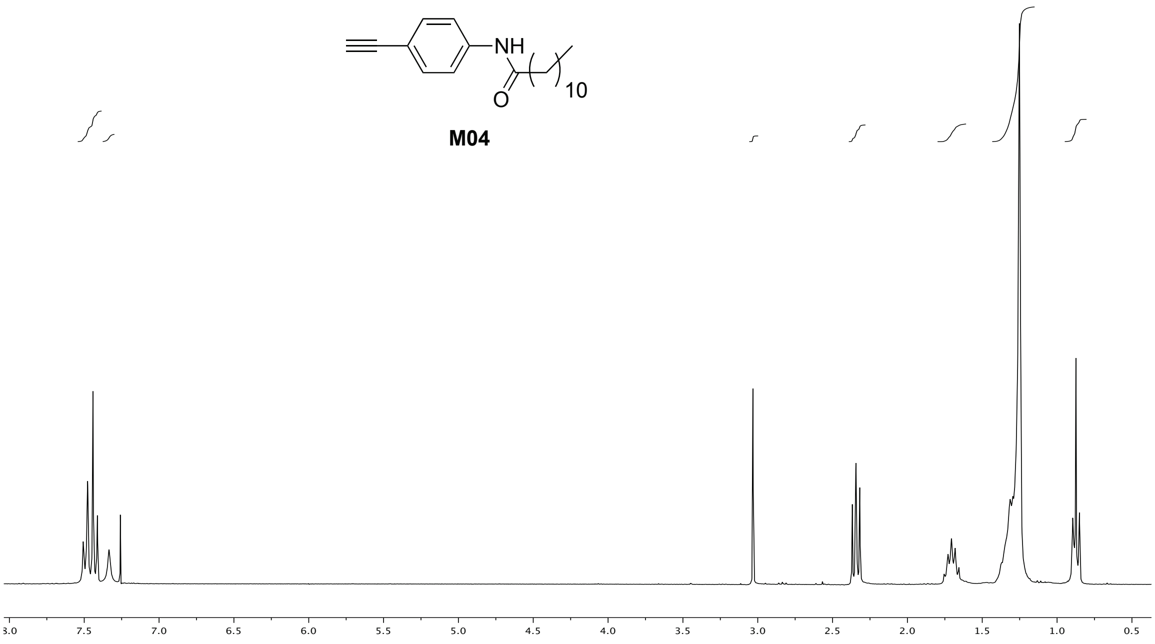

M04

Figure S5. ^{1}H NMR spectrum of **M04** ($CDCl_3$, 300 MHz).

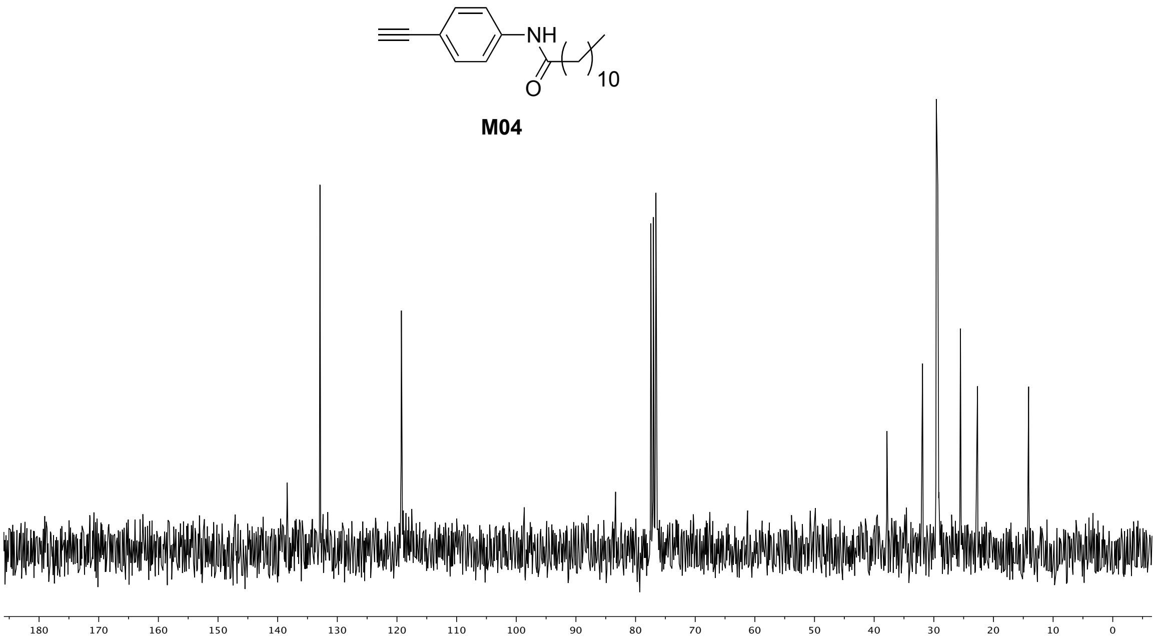

M04

Figure S6. ^{13}C NMR spectrum of **M04** ($CDCl_3$, 75 MHz).

Synthesis and spectral data of monomer M05:

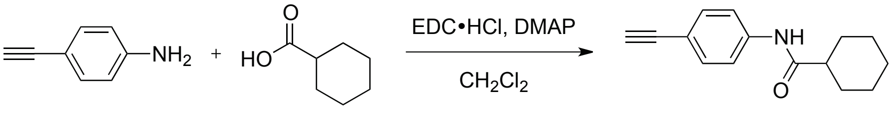

M05

Following the general procedure, EDC•HCl (1.24 g, 6.40 mmol), cyclohexanecarboxylic acid (711.1 mg, 5.44 mmol) and DMAP (52.1 mg, 0.43 mmol) were dissolved in 43 mL of CH_2Cl_2. Next, 4-ethynylaniline (500 mg, 4.27 mmol) was added. After purification, 931.3 mg (96%) of *N*-(4-ethynylphenyl)cyclohexanecarboxamide (**M05**) were obtained.

^{1}H NMR (300 MHz, $CDCl_3$) δ(ppm): 1.2-1.4 (m, 2H), 1.4-1.6 (m, 2H), 1.6-1.9 (m, 2H), 1.8-2.0 (m, 2H), 2.1-2.3 (m, 1H), 3.03 (s, 1H), 7.21 (broad s, 1H), 7.4-7.6 (m, 4H).

^{13}C NMR (75 MHz, $CDCl_3$) δ(ppm): 25.6, 29.6, 46.6, 76.6, 83.4, 100, 119.2, 132.9, 139.3, 159.5.

HRMS (ESI) m/z calc. for $C_{15}H_{18}NO$ [M + H]: 288.1383, found: 288.1374.

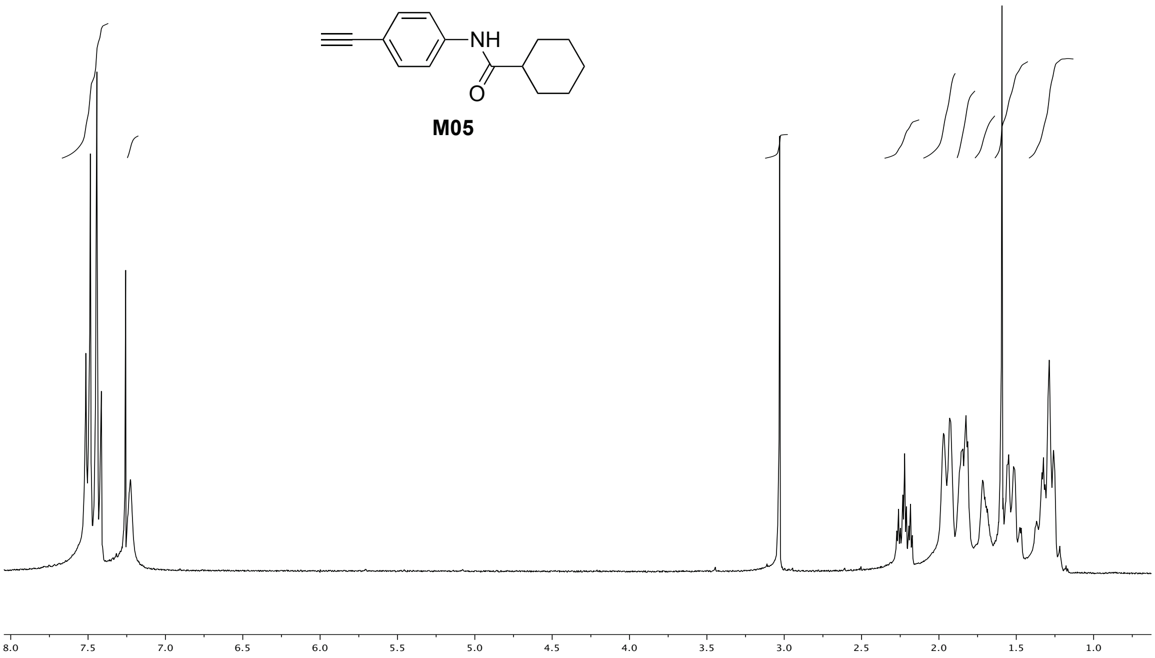

Figure S7. ^{1}H NMR spectrum of **M05** ($CDCl_3$, 300 MHz).

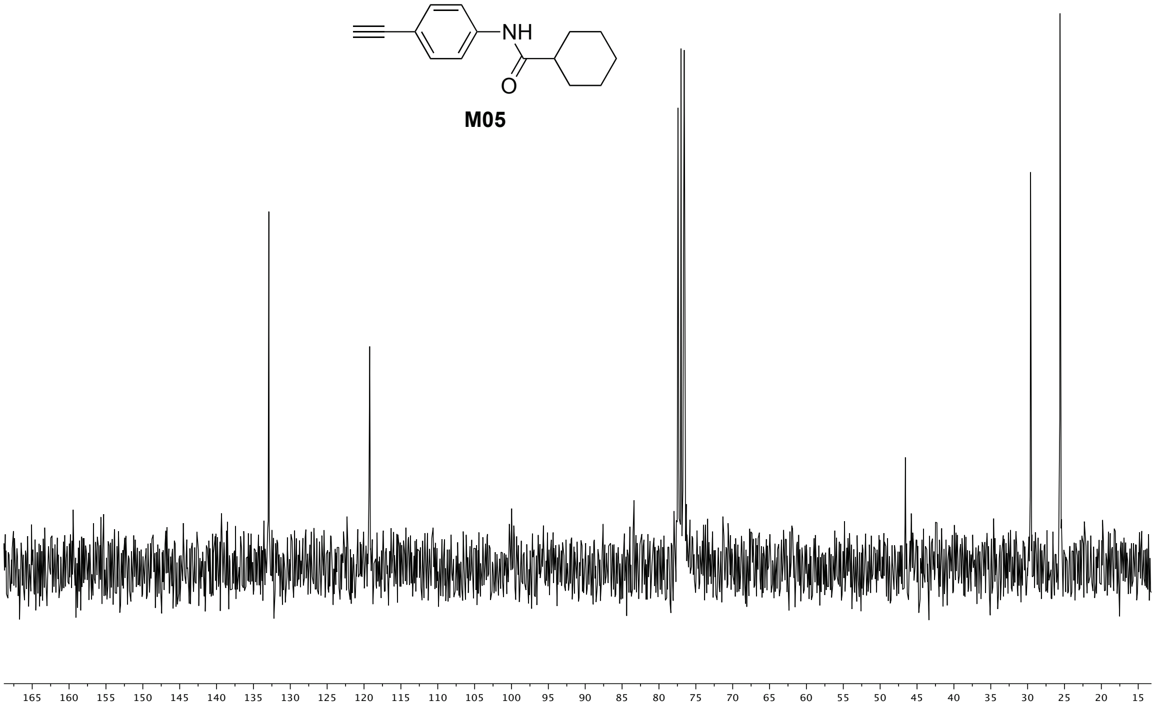

Figure S8. ^{13}C NMR spectrum of **M05** ($CDCl_3$, 75 MHz).

Synthesis and spectral data of monomer M06:

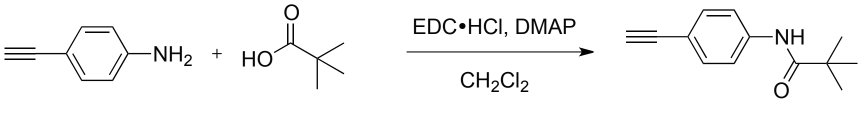

M06

Following the general procedure, EDC•HCl (1.24 g, 6.40 mmol), pivalic acid (566.7 mg, 5.44 mmol) and DMAP (52.1 mg, 0.43 mmol) were dissolved in 43 mL of CH_2Cl_2. Next, 4-ethynylaniline (500 mg, 4.27 mmol) was added. After purification, 790.3 mg (92%) of *N*-(4-ethynylphenyl)pivalamide (**M06**) were obtained.

^{1}H NMR (300 MHz, $CDCl_3$) δ(ppm): 1.30 (s, 9H), 3.03 (s, 1H), 7.38 (broad s, 1H), 7.4-7.6 (m, 4H).

^{13}C NMR (75 MHz, $CDCl_3$) δ(ppm): 26.9, 27.6, 76.6, 83.4, 119.5, 132.9, 138.5, 153.5.

HRMS (ESI) m/z calc. for $C_{13}H_{15}NO$ [M + H]: 202.1231, found: 202.1222.

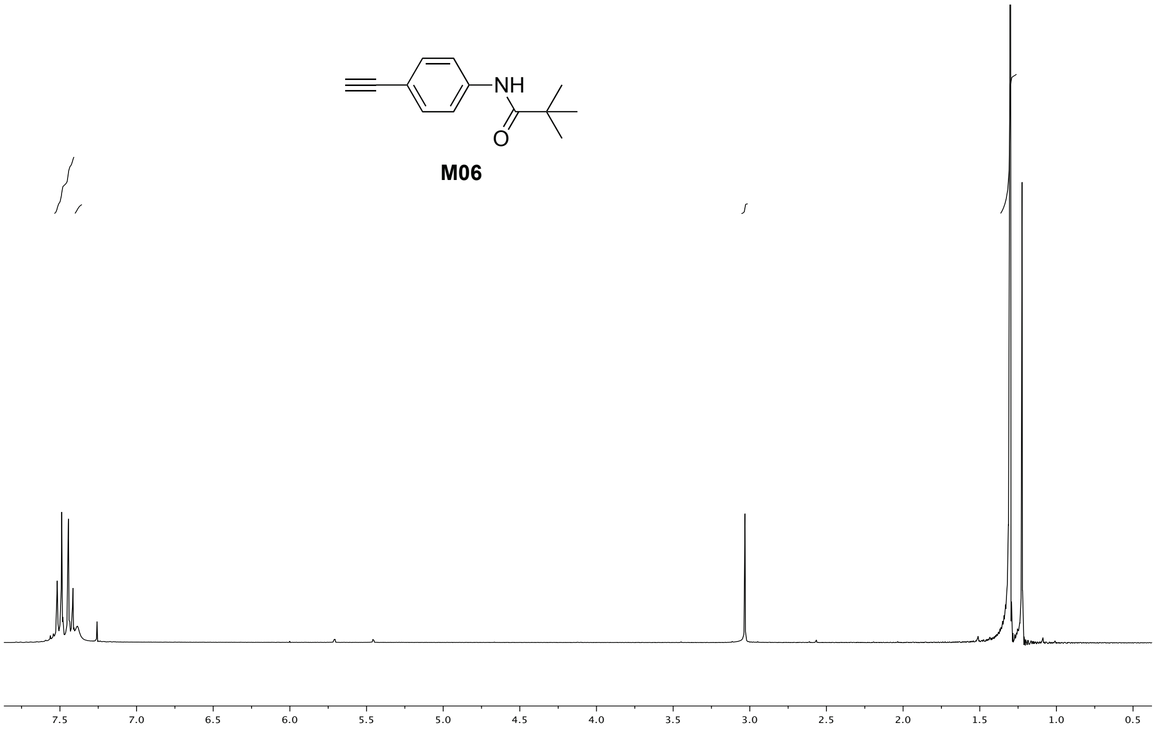

Figure S9. ^{1}H NMR spectrum of **M06** ($CDCl_3$, 300 MHz).

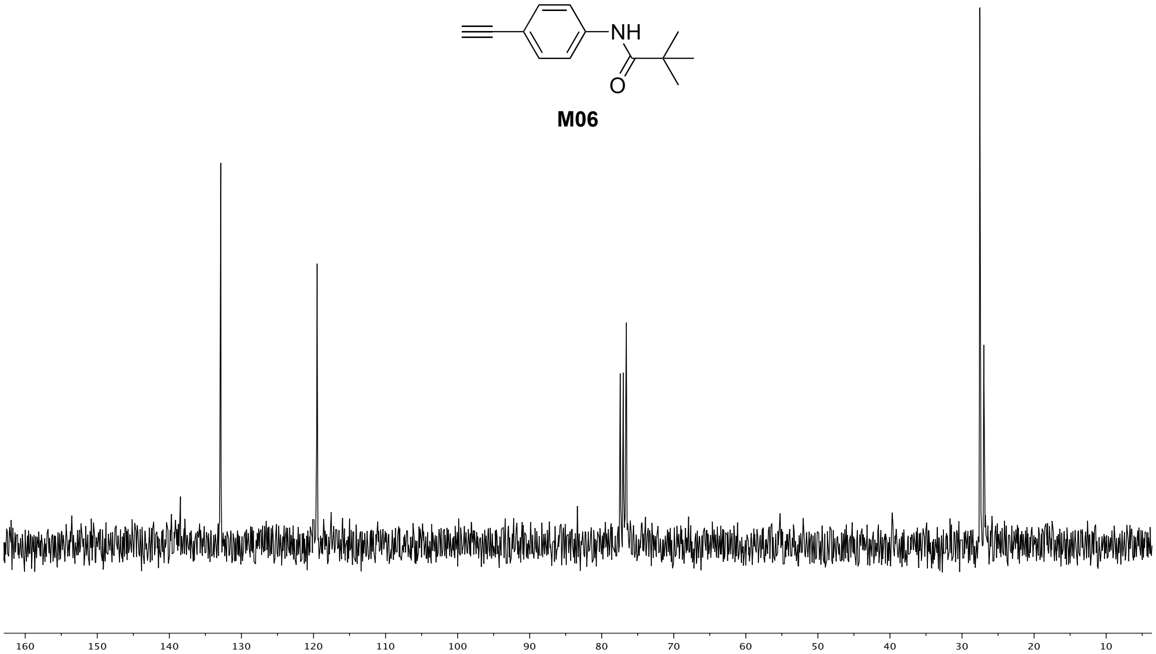

Figure S10. ^{13}C NMR spectrum of **M06** ($CDCl_3$, 75 MHz).

Synthesis and spectral data of monomer M07:

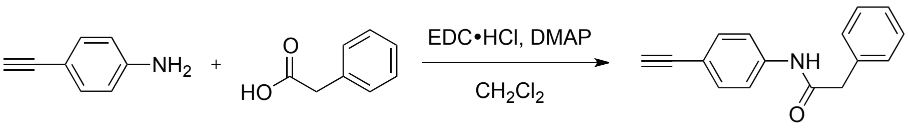

M07

Following the general method, EDC•HCl (1.24 g, 6.40 mmol), 2-phenylacetic acid (755.4 mg, 5.44 mmol) and DMAP (52.1 mg, 0.43 mmol) were dissolved in 43 mL of CH_2Cl_2. Next, 4-ethynylaniline (500 mg, 4.27 mmol) was added. After purification, 964 mg (96%) of *N*-(4-ethynylphenyl)2-phenylacetamide (**M07**) were obtained.

^{1}H NMR (300 MHz, $CDCl_3$) δ(ppm): 3.03 (s, 1H), 3.72 (s, 2H), 7.3-7.5 (m, 10H).

^{13}C NMR (75 MHz, $CDCl_3$) δ(ppm): 44.8, 76.9, 83.9, 117.8, 119.3, 127.8, 129.3, 129.5, 132.9, 134.1, 138.0, 169.2.

HRMS (ESI) m/z calc. for $C_{16}H_{15}NO$ [M + H]: 236.1075, found: 236.1066.

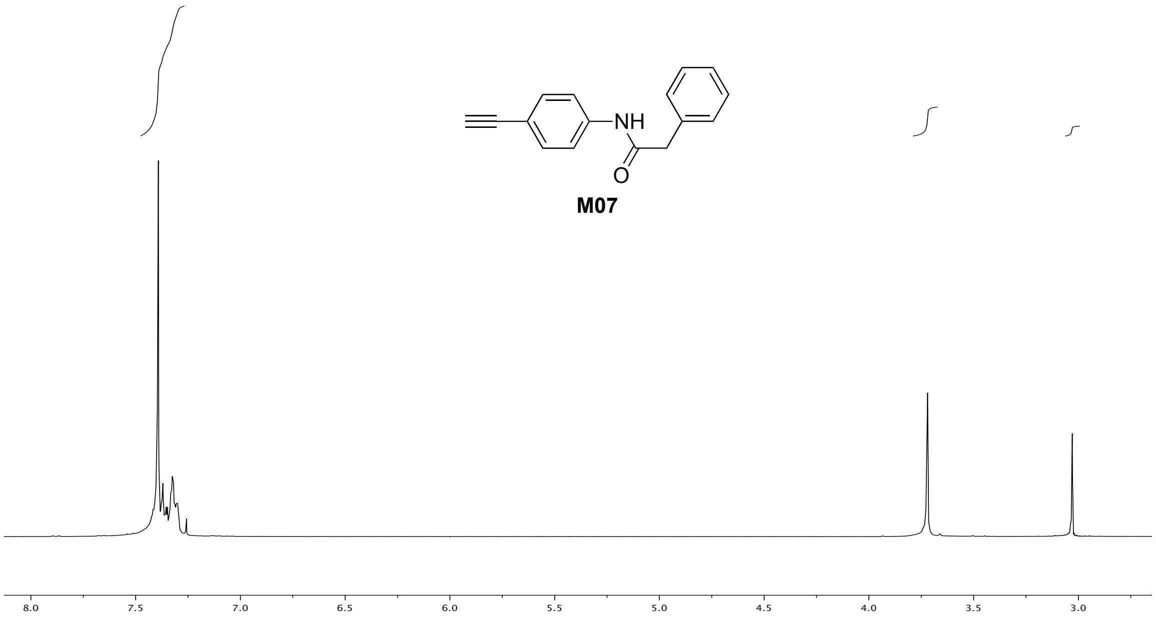

Figure S11. ^{1}H NMR spectrum of **M07** ($CDCl_3$, 300 MHz).

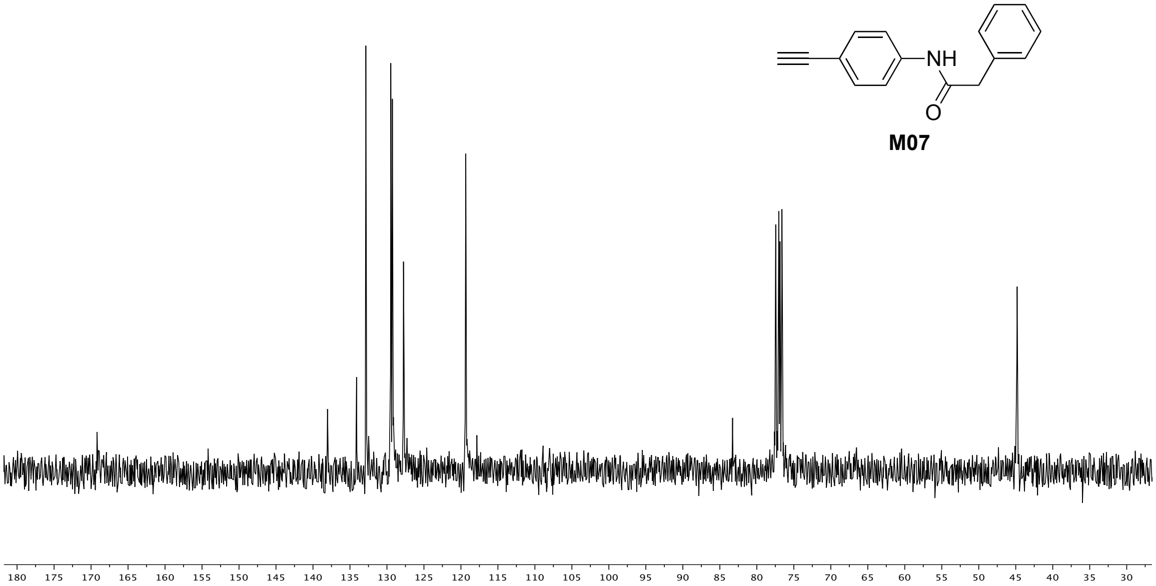

Figure S12. ^{13}C NMR spectrum of **M07** ($CDCl_3$, 75 MHz).

Synthesis and spectral data of monomer M08:

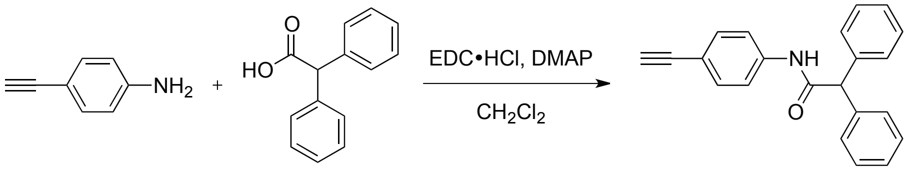

M08

Following the general method, EDC•HCl (1.24 g, 6.40 mmol), 2,2-diphenylacetic acid (1177.6 mg, 5.44 mmol) and DMAP (52.1 mg, 0.43 mmol) were dissolved in 43 mL of CH_2Cl_2. Next, 4-ethynylaniline (500 mg, 4.27 mmol) was added. After purification, 1089.8 mg (82%) of *N*-(4-ethynylphenyl)2,2-diphenylacetamide (**M08**) were obtained.

^{1}H NMR (300 MHz, $CDCl_3$) δ(ppm): 3.04 (s, 1H), 5.06 (s, 1H), 7.2-7.5 (m, 15H).

^{13}C NMR (75 MHz, $CDCl_3$) δ(ppm): 60.0, 76.9, 83.3, 119.4, 127.6, 129.0, 129.2, 132.9, 138.0, 138.8, 170.2.

HRMS (ESI) m/z calc. for $C_{22}H_{17}NO$ [M + H]: 312.1388, found: 312.1380.

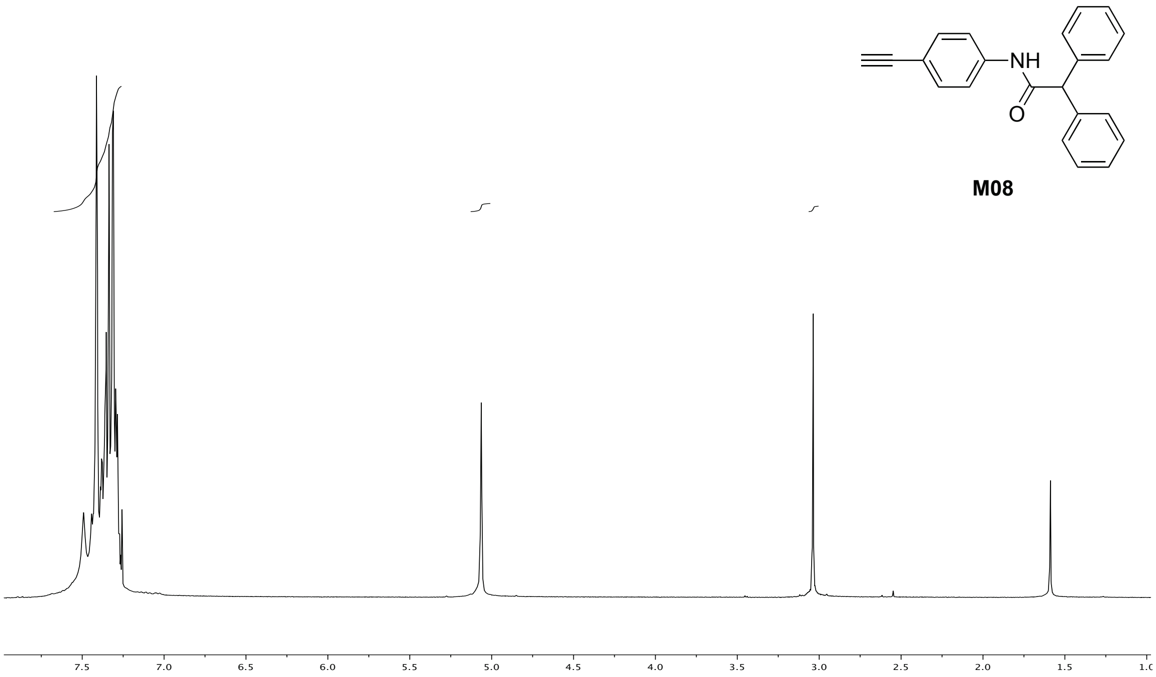

Figure S13. ^{1}H NMR spectrum of **M08** ($CDCl_3$, 300 MHz).

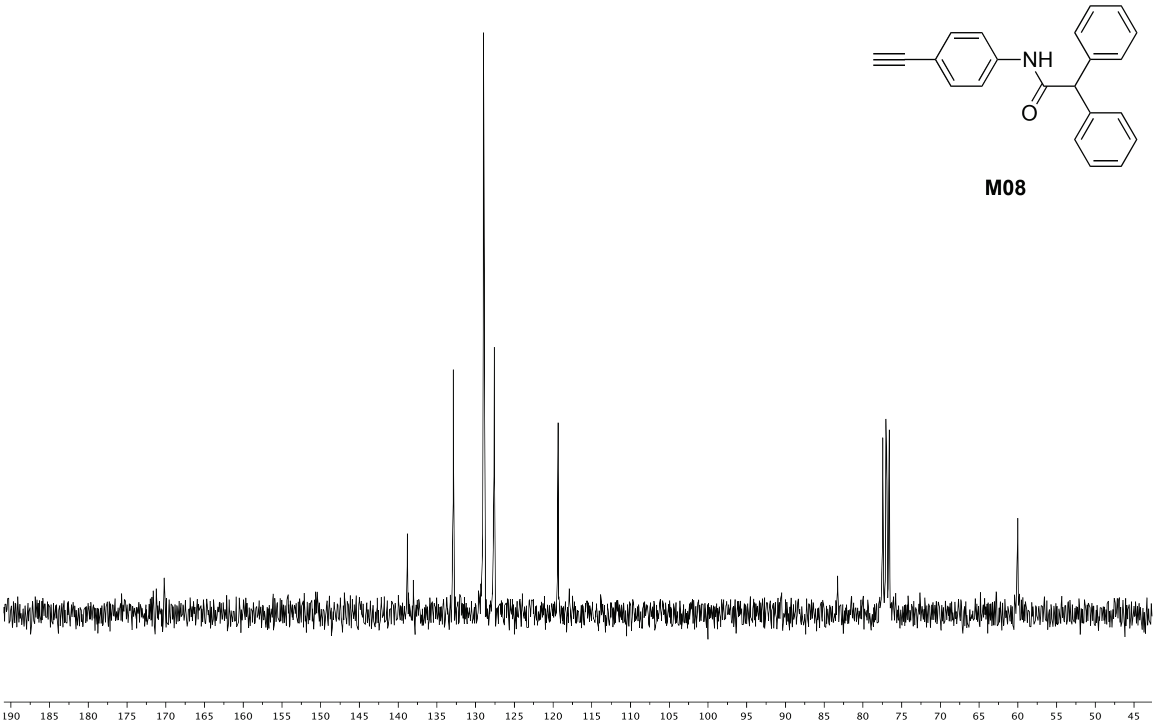

Figure S14. ^{13}C NMR spectrum of **M08** ($CDCl_3$, 75 MHz).

Synthesis and spectral data of monomer M09:

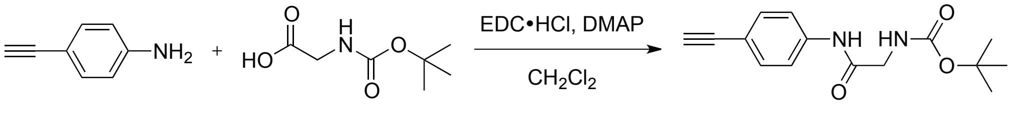

M09

Following the general method, EDC•HCl (1.24 g, 6.40 mmol), 2-((*tert*-butoxycarbonyl)amino)acetic acid (972 mg, 5.44 mmol) and DMAP (52.1 mg, 0.43 mmol) were dissolved in 43 mL of CH_2Cl_2. Next, 4-ethynylaniline (500 mg, 4.27 mmol) was added. After purification, 1101 mg (94%) of *tert*-butyl (2-((4-ethynylphenyl)amino)-2-oxoethyl)carbamate (**M09**) were obtained.

^{1}H NMR (300 MHz, $CDCl_3$) δ(ppm): 1.46 (t, *J* = 9.1 Hz, 9H), 3.04 (s, 1H), 3.93 (d, *J* = 6.3 Hz, 1H), 5.48 (m, 1H), 7.3-7.5 (m, 4H), 8.59 (broad s, 1H).

^{13}C NMR (75 MHz, $CDCl_3$) δ(ppm): 27.9, 28.3, 54.4, 76.8, 100.0, 119.5, 132.9, 139.5, 168.0, 181.2.

HRMS (ESI) m/z calc. for $C_{15}H_{18}N_2O_3$ [M + H]: 275.1396, found: 275.1392.

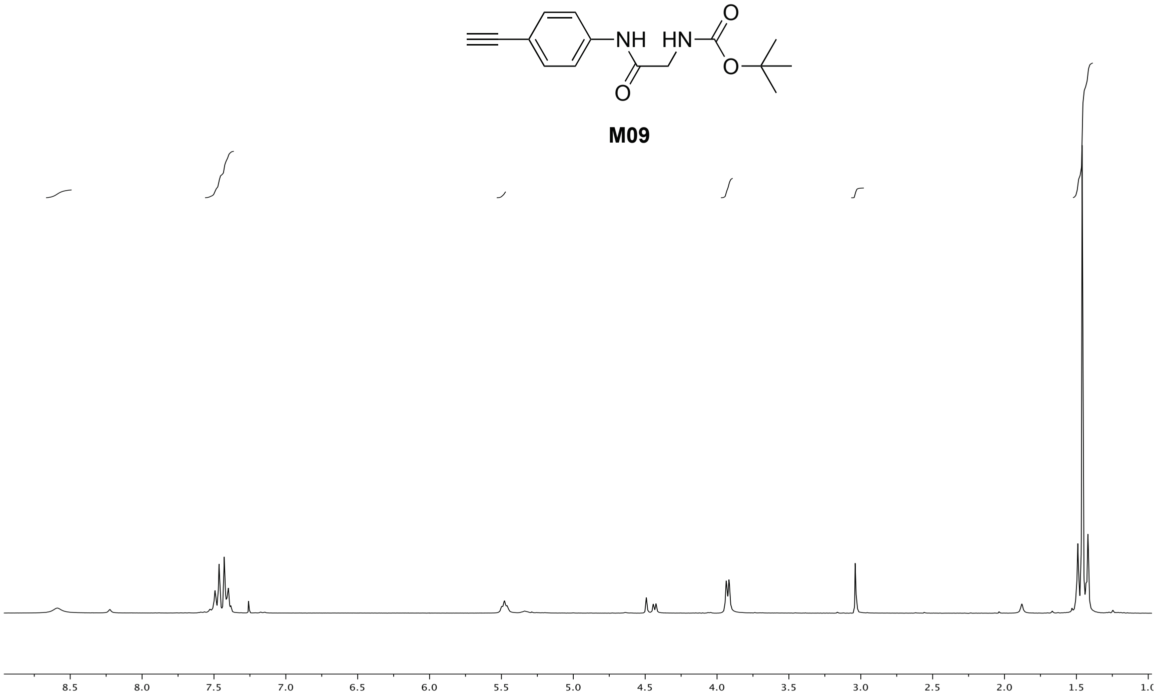

Figure S15. ^{1}H NMR spectrum of **M09** ($CDCl_3$, 300 MHz).

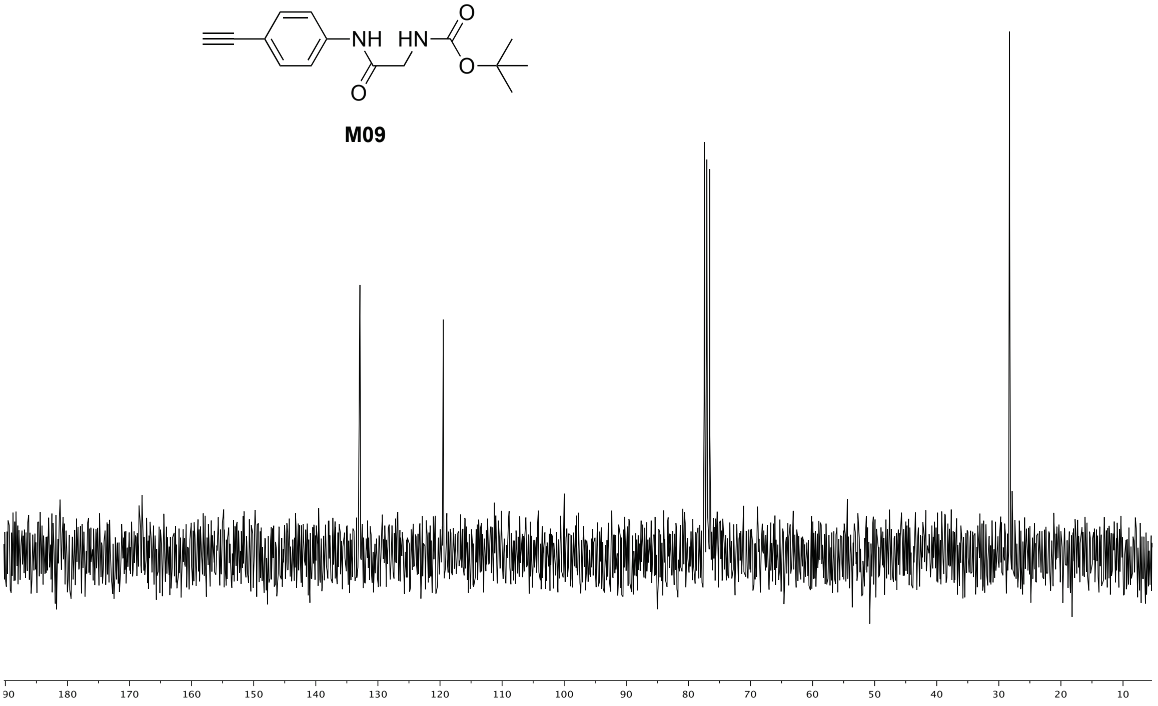

Figure S16. ^{13}C NMR spectrum of **M09** ($CDCl_3$, 75 MHz).

Synthesis of homopolymers (poly-1 to poly-9)

General procedure for polymerization:

The reaction flask (sealed ampoule) was dried under vacuum and argon flushed for three times before the corresponding monomer was added as a solid. Then, the flask was evacuated on a vacuum line and flushed with dry argon (three times). Dry THF was added with a syringe and then triethylamine dropwise. A solution of rhodium norbornadiene chloride dimer, $[Rh(nbd)Cl]_2$, in THF was added at 30° C. The reaction mixture was stirred at 30ºC for 6 h. Then, the resulting polymer was diluted in CH_2Cl_2 and precipitated in a large amount of methanol, centrifuged (2 times) and reprecipitated in hexane and centrifuged again.

The molecular weight (Mn) of all polymers was estimated by SEC with THF as eluent at flow rate 1 ml/min at concentration 0.4 mg/mL using narrow polystyrene standards (PSS) as calibrants.

Synthesis and spectral data of homopolymer poly-1:

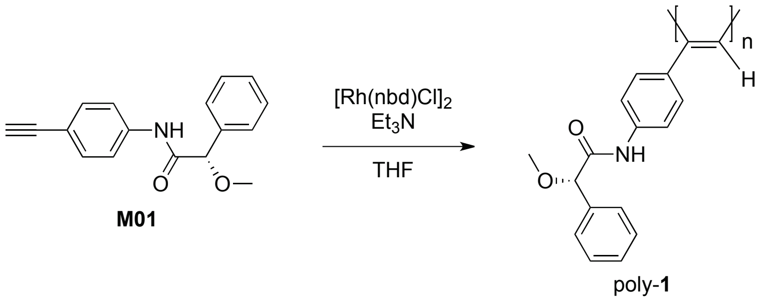

Following the general procedure, reaction of **M01** (100 mg, 0.377 mmol), Et_3N (5 μL, $3.77x10^{-2}$ mmol) and $[Rh(nbd)Cl]_2$ (0.87 mg, $1.89x10^{-3}$ mmol) in THF (750 μL) yielded, after centrifugation, 95 mg (95%) of poly-**1**.

^{1}H NMR (300 MHz, $CDCl_3$, 298 K) *δ*(ppm): 3.20 (s, 3H), 4.64 (s, 1H), 5.71 (s, 1H), 6.55 (s, 1H), 7.04 (s, 1H), 7.1-75 (m, 7H), 8.41(s, 1H).

SEC: Mn = 39607, Mw = 61195, Mp = 60355, Mz = 89611, PDI = 1.55.

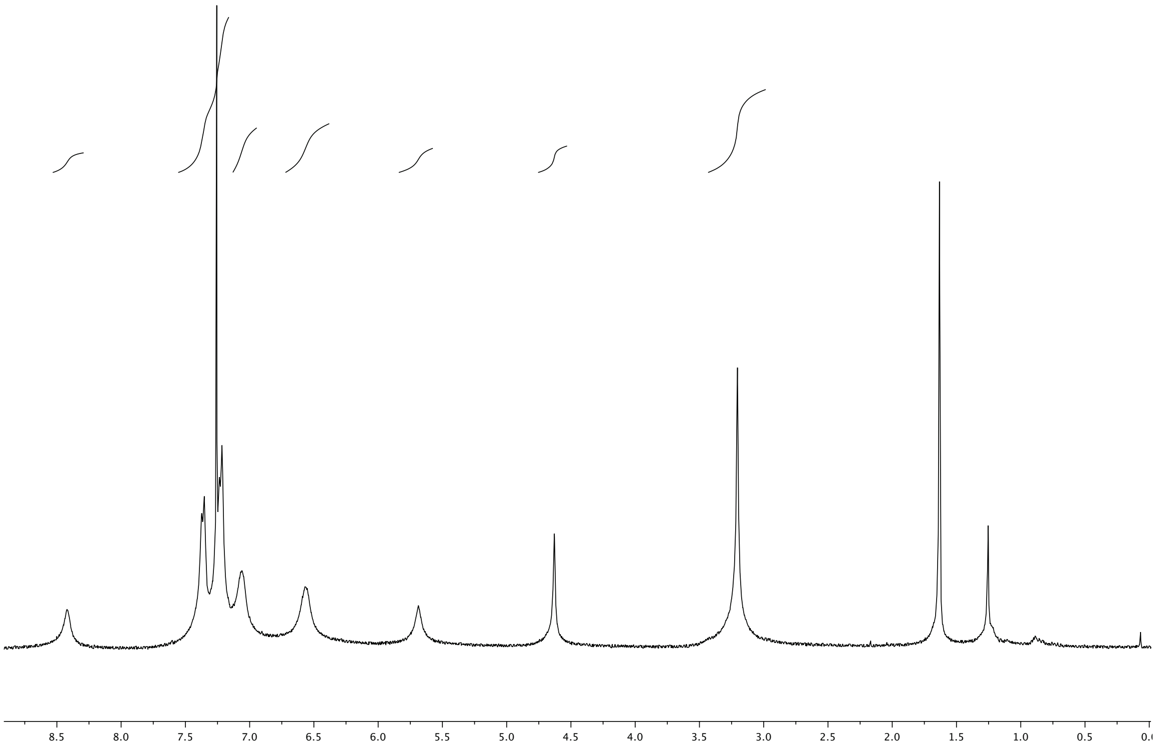

Figure S17. ^{1}H NMR spectrum of poly-**1** ($CDCl_3$, 300 MHz).

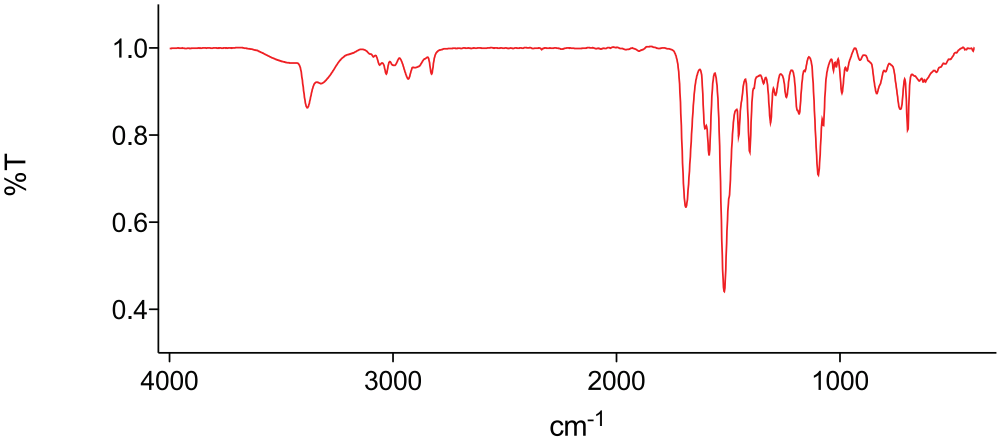

Figure S18. IR spectrum of poly-**1**.

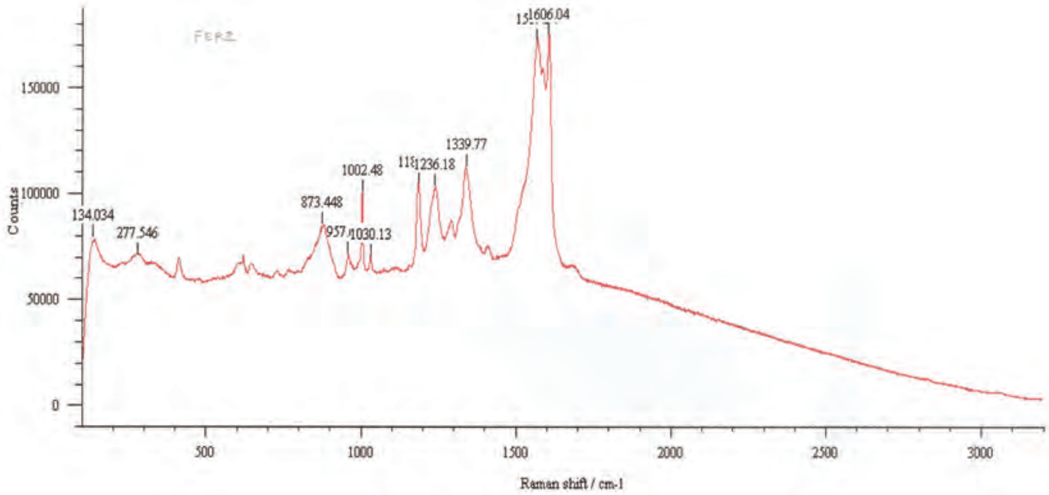

Figure S19. Raman spectrum of poly-**1**.

Synthesis and spectral data of homopolymer poly-2:

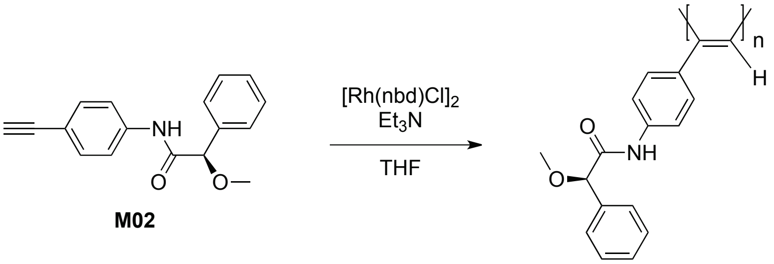

poly-**2**

Following the general procedure, reaction of **M02** (100 mg, 0.377 mmol), Et_3N (5 μL, $3.77x10^{-2}$ mmol) and $[Rh(nbd)Cl]_2$ (0.87 mg, $1.89x10^{-3}$ mmol) in THF (750 μL) yielded, after centrifugation, 93 mg (93%) of poly-**2**.

^{1}H NMR (300 MHz, $CDCl_3$, 298 K) δ(ppm): 3.20 (s, 3H), 4.64 (s, 1H), 5.71 (s, 1H), 6.55 (s, 1H), 7.04 (s, 1H), 7.1-75 (m, 7H), 8.41(s, 1H).

SEC: Mn = 36032, Mw = 58844, Mp = 60315, Mz = 88779, PDI = 1.51.

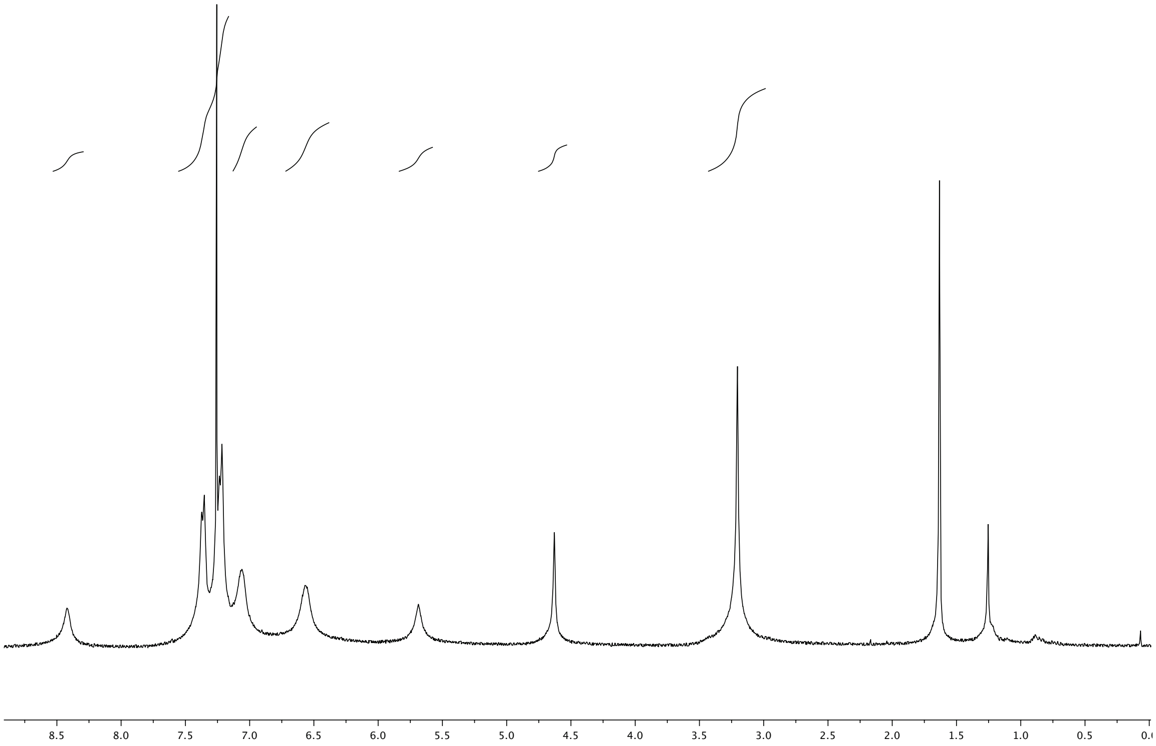

Figure S20. ^{1}H NMR spectrum of poly-**2** ($CDCl_3$, 300 MHz).

Synthesis and spectral data of homopolymer poly-3:

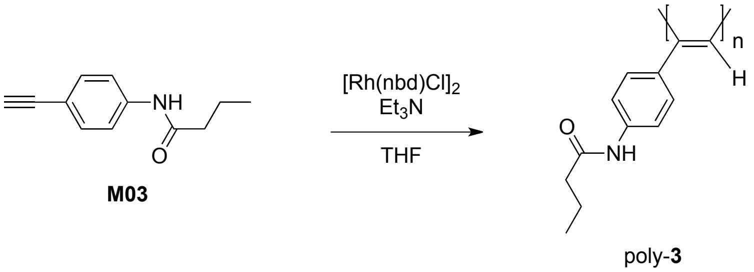

Following the general procedure, reaction of **M03** (102.9 mg, 0.55 mmol), Et_3N (7.7 μL, 5.50x10^{-2} mmol) and $[Rh(nbd)Cl]_2$ (5.6 mg, 5.50x10^{-3} mmol) in THF (1.1 mL) yielded, after centrifugation, 80.3 mg (78%) of poly-**3**.

SEC: Mn = 25177, Mw = 43432, Mp = 47627, Mz = 61219, PDI = 1.72.

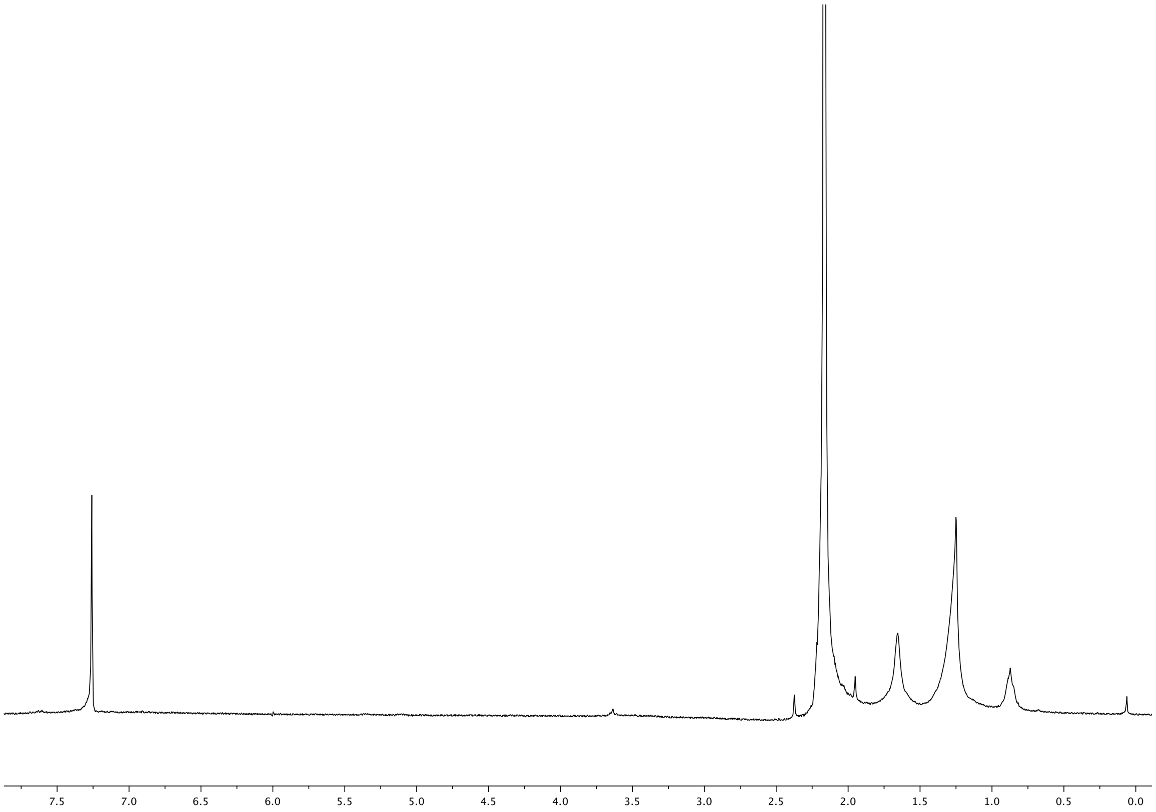

Figure S21. ^{1}H NMR spectrum of poly-**3** ($CDCl_3$, 300 MHz).

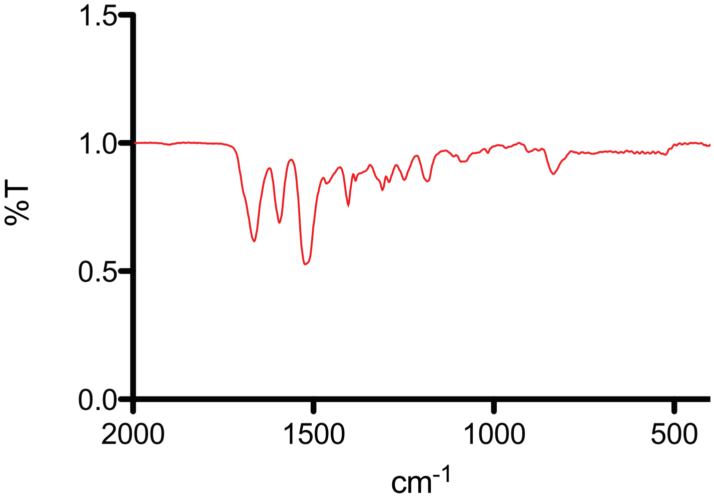

Figure S22. IR spectrum of poly-**3**.

Synthesis and spectral data of homopolymer poly-4:

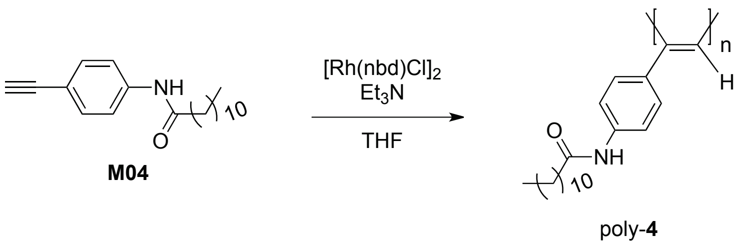

Following the general procedure, reaction of **M04** (105 mg, 0.35 mmol), Et_3N (4.9 μL, 3.50×10^{-2} mmol) and $[Rh(nbd)Cl]_2$ (4.0 mg, 8.70×10^{-3} mmol) in THF (750 μL) yielded, after centrifugation, 40.4 mg (48%) of poly-**4**.

SEC: Mn = 122731, Mw = 227073, Mp = 271176, Mz = 339778, PDI = 1.85.

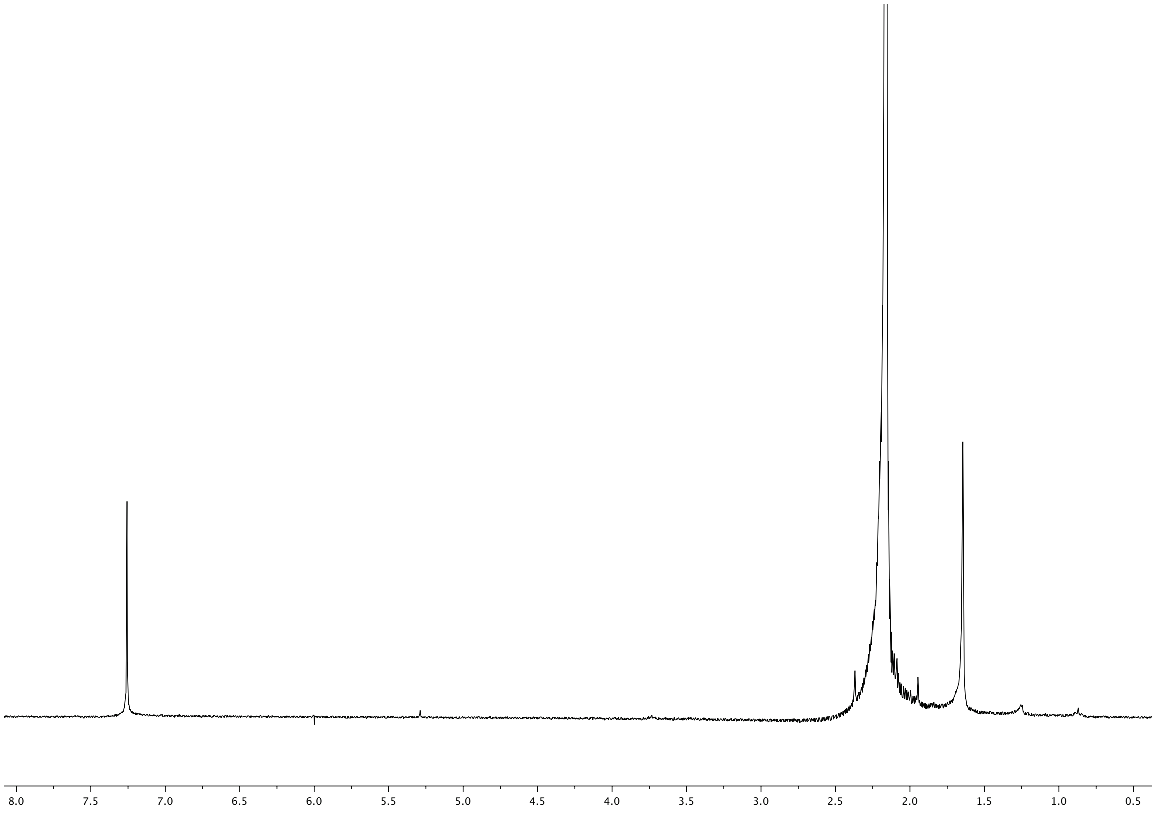

Figure S23. ^1H NMR spectrum of poly-**4** ($CDCl_3$, 300 MHz).

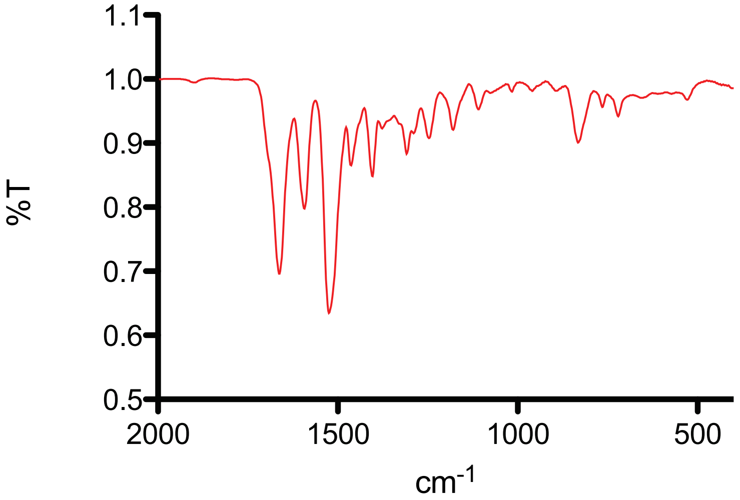

Figure S24. IR spectrum of poly-**4**.

Synthesis and spectral data of homopolymer poly-5:

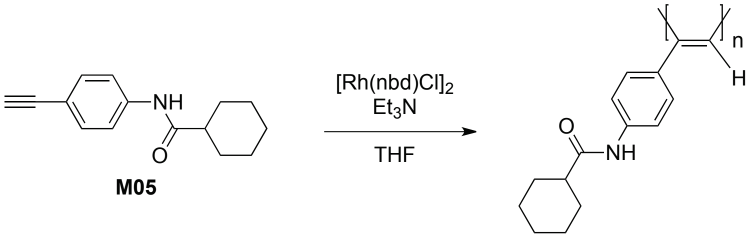

M05

poly-**5**

Following the general procedure, reaction of **M05** (100 mg, 0.44 mmol), Et_3N (6.1 μL, $4.40x10^{-2}$ mmol) and $[Rh(nbd)Cl]_2$ (4 mg, $4.4x10^{-2}$ mmol) in THF (1 mL) yielded, after centrifugation, 67.2 mg (67%) of poly-**5**.

^{1}H NMR (300 MHz, $CDCl_3$, 298 K) *δ*(ppm): 1.23 (broad s, 6H), 1.6-2.5 (m, 4H), 4.2-4.4 (m, 1H), 5.73 (s, 1H), 6.4-7.3 (m, 4H), 7.67 (s, 1H).

SEC: Mn = 3924, Mw = 7516, Mp = 4657, Mz = 20969, PDI = 1.92.

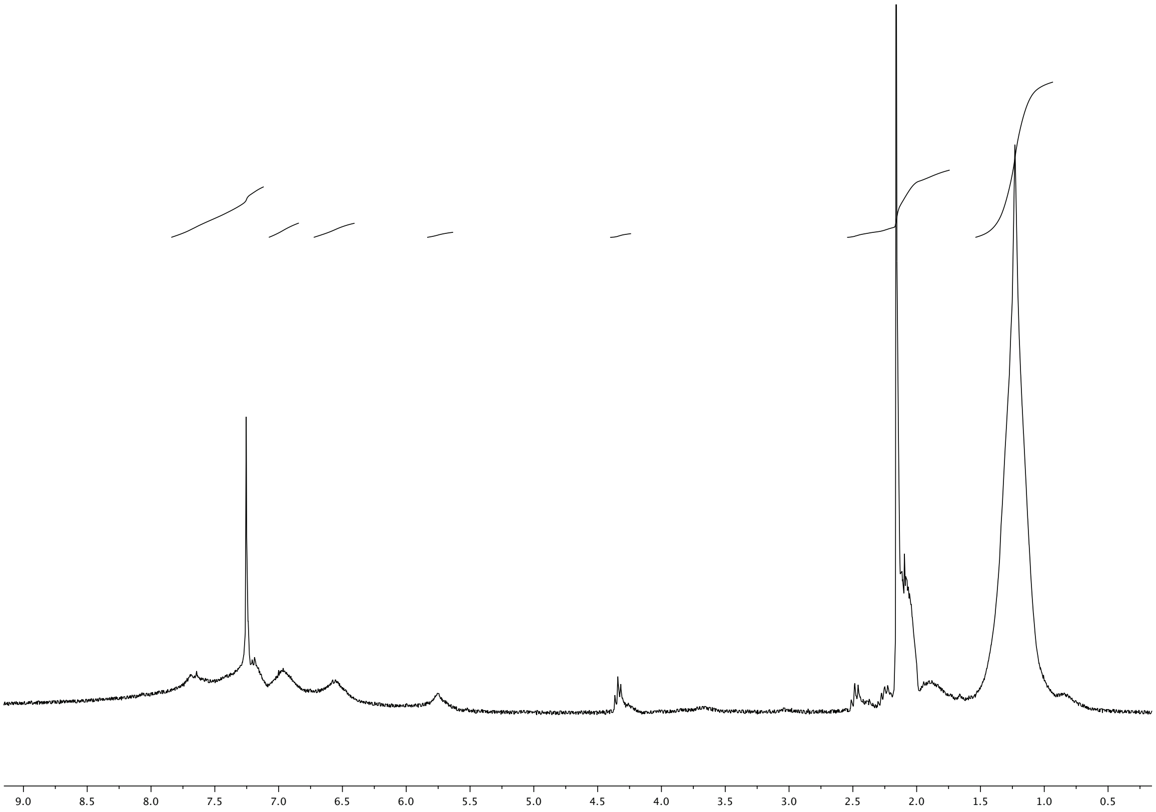

Figure S25. ^{1}H NMR spectrum of poly-**5** ($CDCl_3$, 300 MHz).

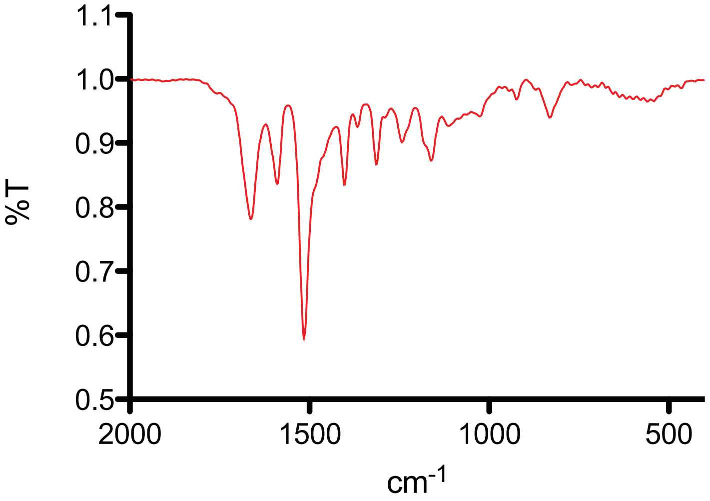

Figure S26. IR spectrum of poly-**5**.

Synthesis and spectral data of homopolymer poly-6:

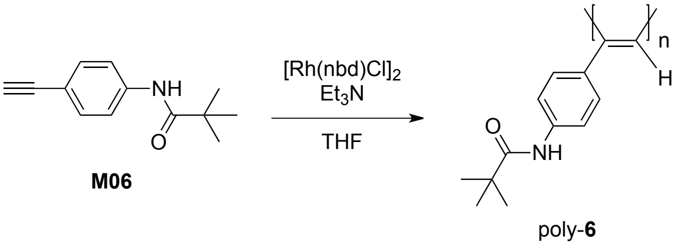

Following the general procedure, reaction of **M06** (100 mg, 0.50 mmol), Et_3N (6.9 μL, 5.0×10^{-2} mmol) and $[Rh(nbd)Cl]_2$ (2.3 mg, 5.0×10^{-3} mmol) in THF (1 mL) yielded, after centrifugation, 60.0 mg (60%) of poly-**6**.

^{1}H NMR (300 MHz, $CDCl_3$, 298 K) *δ*(ppm): 1.0-1.7 (s, 9H), 5.75 (s, 1H), 6.4-7.3 (m, 4H), 7.64 (s, 1H).

SEC: Mn = 3769, Mw = 7002, Mp = 4474, Mz = 17726, PDI = 1.86.

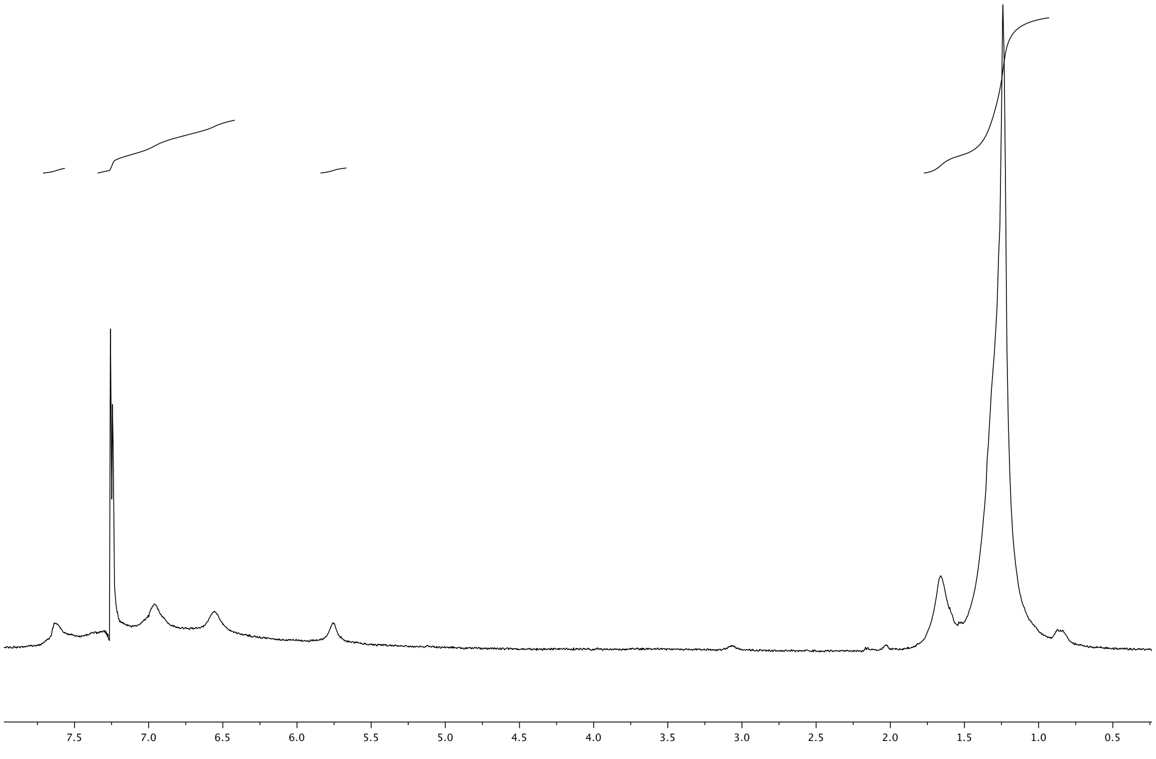

Figure S27. ^{1}H NMR spectrum of poly-**6** ($CDCl_3$, 300 MHz).

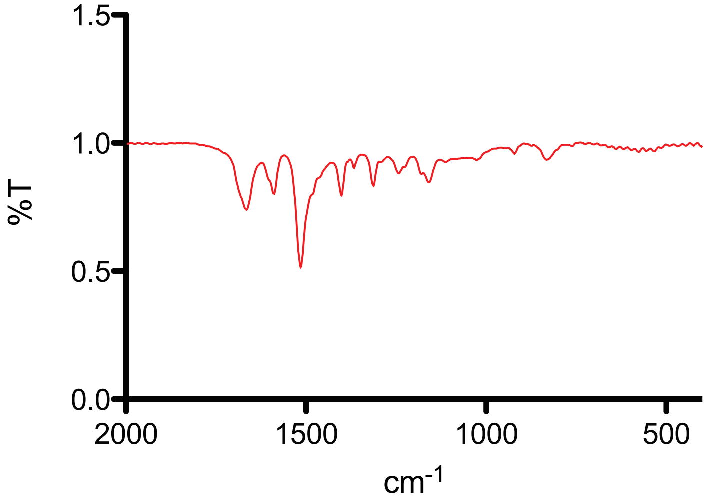

Figure S28. IR spectrum of poly-**6**.

Synthesis and spectral data of homopolymer poly-7:

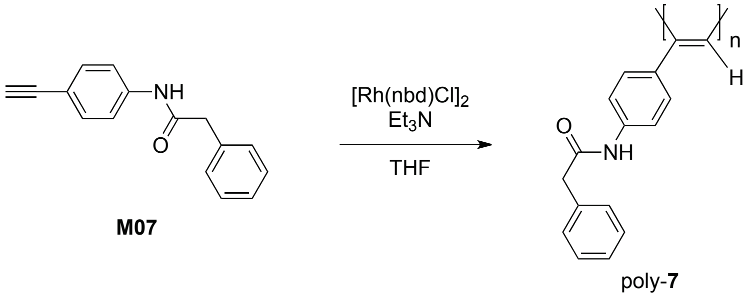

Following the general procedure, reaction of **M07** (100 mg, 0.42 mmol), Et_3N (5.9 μL, 4.25x10^{-2} mmol) and $[Rh(nbd)Cl]_2$ (7.8 mg, 1.70x10^{-2} mmol) in THF (1 mL) yielded, after centrifugation, 88.1 mg (88%) of poly-**7**.

SEC: Mn = 182693, Mw = 126134, Mp = 89816, Mz = 285170, PDI = 1.52.

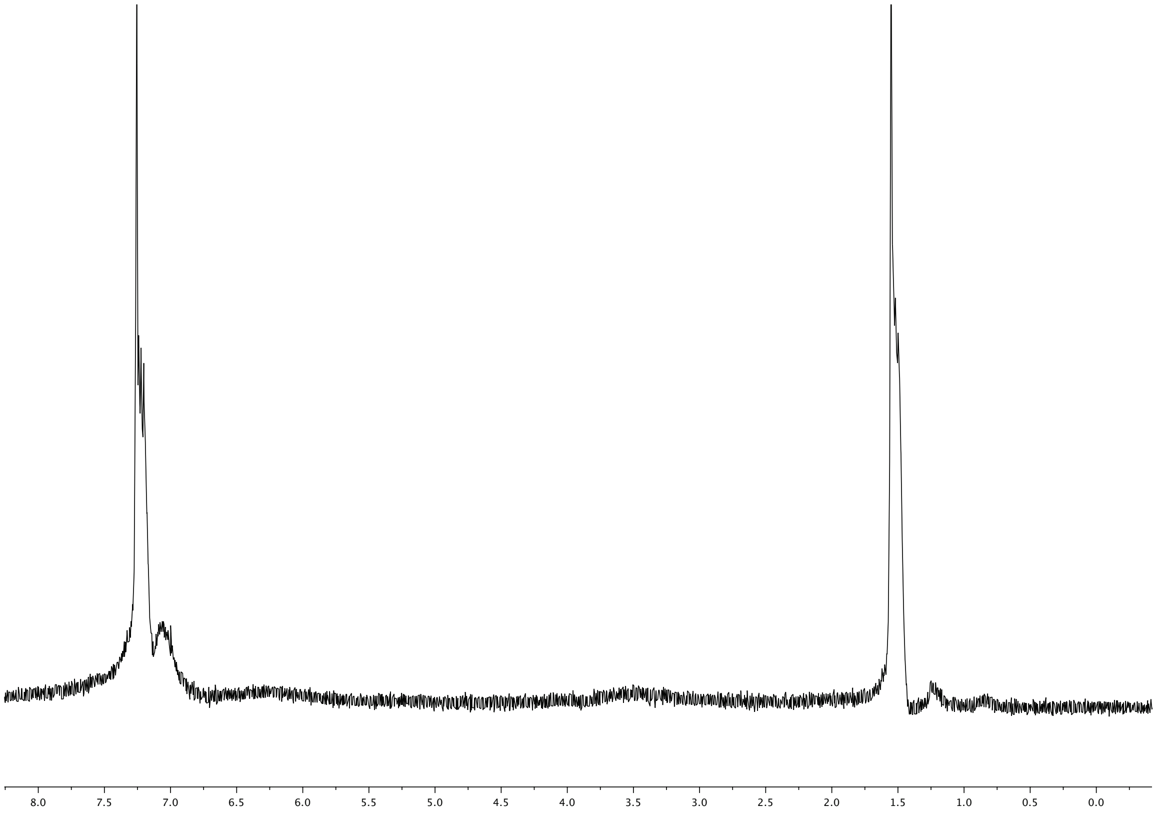

Figure S29. ^{1}H NMR spectrum of poly-**7** ($CDCl_3$, 300 MHz).

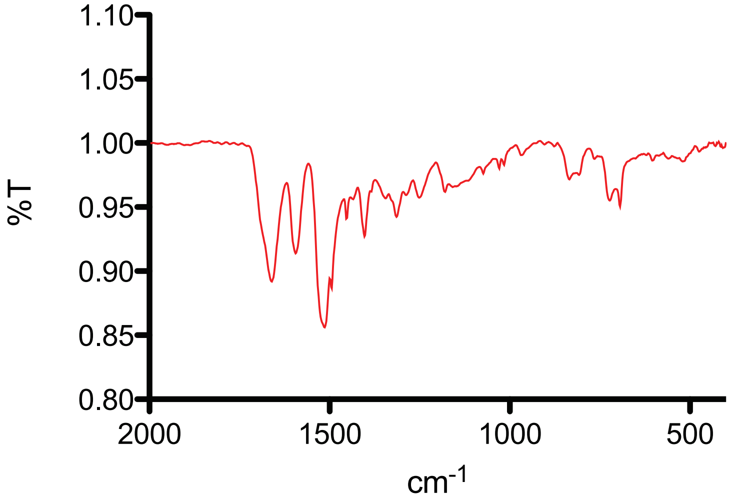

Figure S30. IR spectrum of poly-**7**.

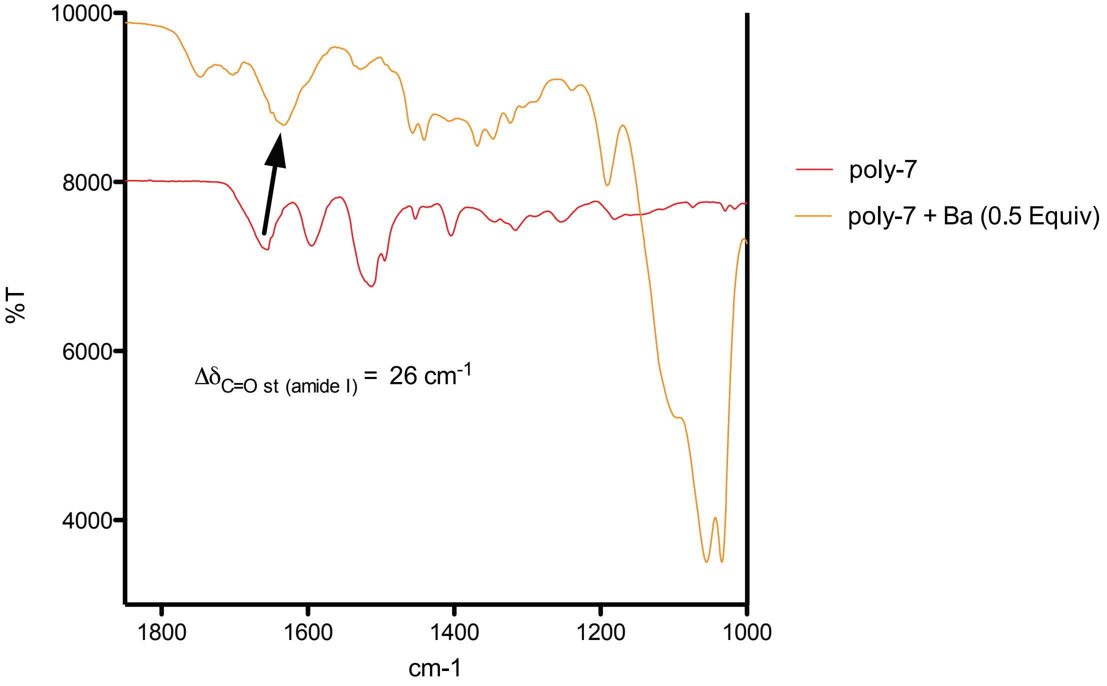

Figure S31. IR spectrum of poly-**7** (red) and poly-**7** with 0.5 equiv. of $Ba(OCl_4)_2$ (orange).

Synthesis and spectral data of homopolymer poly-8:

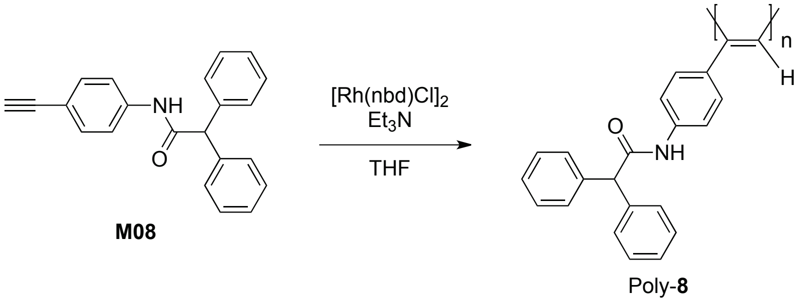

Following the general procedure, reaction of **M08** (100 mg, 0.32 mmol), Et_3N (4.5 μL, 3.21×10^{-2} mmol) and $[Rh(nbd)Cl]_2$ (5.9 mg, 1.29×10^{-2} mmol) in THF (1 mL) yielded, after centrifugation, 80.3 mg (80%) of poly-**8**.

SEC: Mn = 18750, Mw = 33377, Mp = 22423, Mz = 60416, PDI = 1.78.

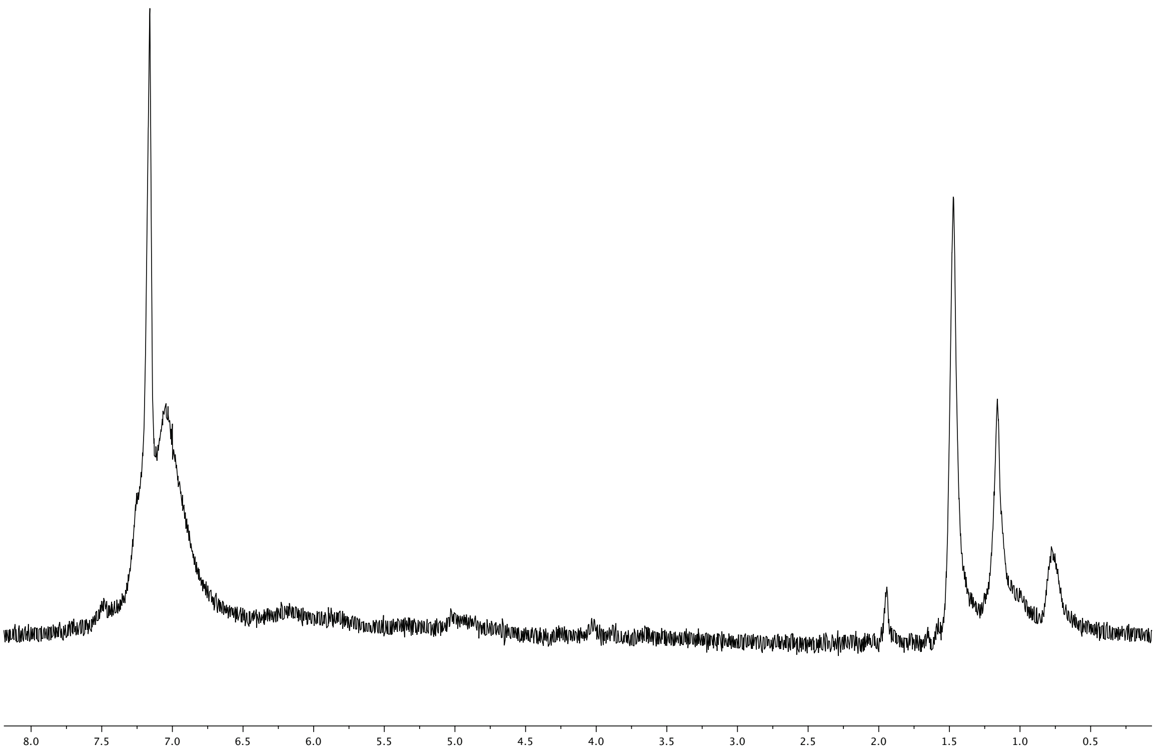

Figure S32. ^{1}H NMR spectrum of poly-**8** ($CDCl_3$, 300 MHz).

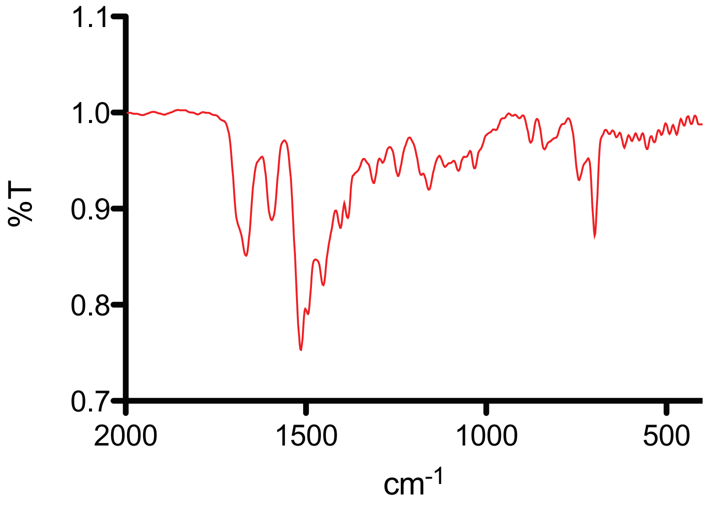

Figure S33. IR spectrum of poly-**8**.

Synthesis and spectral data of homopolymer poly-9:

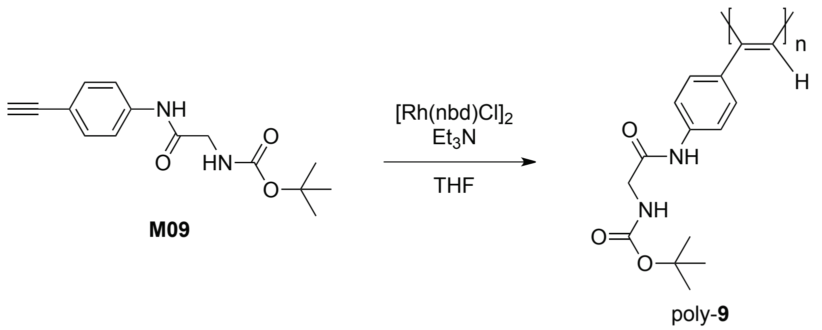

Following the general procedure, reaction of **M09** (100 mg, 0.36 mmol), Et$_3$N (5.1 μL, 3.65x10^{-2} mmol) and [Rh(nbd)Cl]$_2$ (1.7 mg, 3.65x10^{-3} mmol) in THF (1 mL) yielded, after centrifugation, 90 mg (90%) of poly-**9**.

SEC: Mn = 78843, Mw = 124659, Mp = 101306, Mz = 192160, PDI = 1.54.

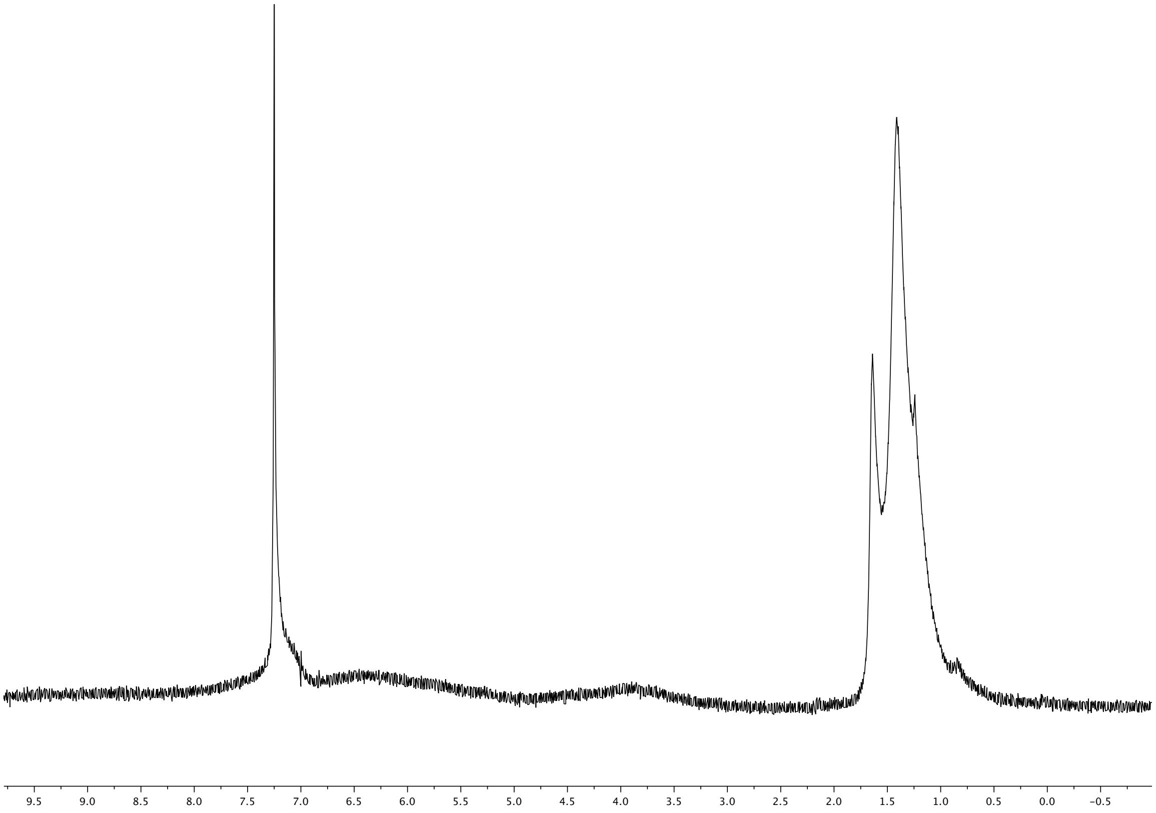

Figure S34. ^{1}H NMR spectrum of poly-**9** (CDCl$_3$, 300 MHz).

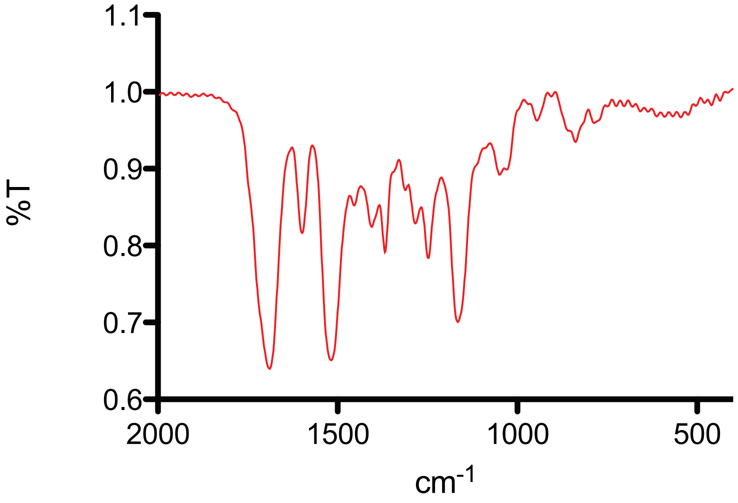

Figure S35. IR spectrum of poly-**9**.

Synthesis of copolymers [poly(1-*co*-3) to poly(1-*co*-9)]

Synthesis of copolymers poly(1-*co*-3):

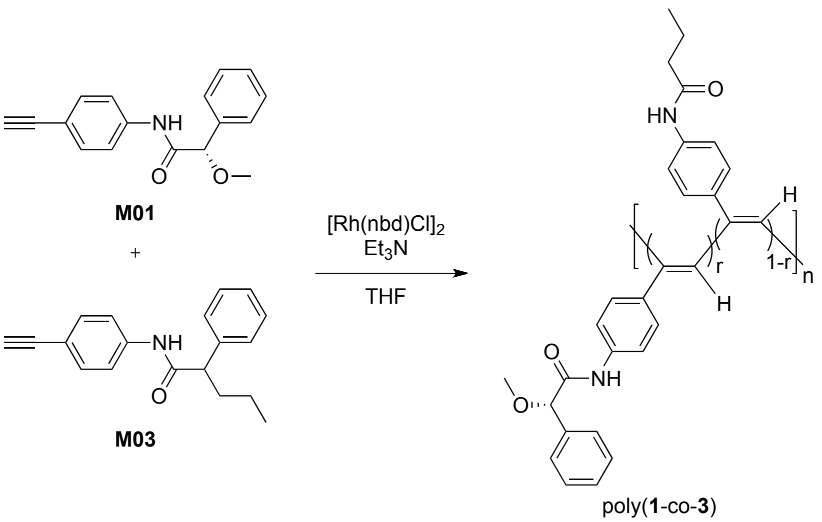

Following the general procedure, the poly(**1**-*co*-**3**) series was synthetized according to the amounts of different reagents (**M01**, **M03**, Et_3N, $[Rh(nbd)Cl]_2$ and THF) reported in Table S1.

Copolymer	**M01** (mg)	**M01** (mmol)	**M03** (mg)	**M03** (mmol)	$[Rh(nbd)Cl]_2$ (mg)	THF (mL)	Et_3N (μL)	Yield (%)
poly($\mathbf{1}_{0.9}$-*co*-$\mathbf{3}_{0.1}$)	95.4	0.36	7.5	$4.0\text{x}10^{-2}$	1.8	0.80	5.6	99
poly($\mathbf{1}_{0.8}$-*co*-$\mathbf{3}_{0.2}$)	84.8	0.32	15	$8.0\text{x}10^{-2}$	1.8	0.80	5.6	92
poly($\mathbf{1}_{0.7}$-*co*-$\mathbf{3}_{0.3}$)	83.5	0.32	25.3	0.14	2.1	0.90	6.3	95
poly($\mathbf{1}_{0.6}$-*co*-$\mathbf{3}_{0.4}$)	71.6	0.27	33.7	0.18	2.1	0.90	6.3	97
poly($\mathbf{1}_{0.5}$-*co*-$\mathbf{3}_{0.5}$)	59.6	0.23	42.1	0.23	2.1	0.90	6.3	95
poly($\mathbf{1}_{0.4}$-*co*-$\mathbf{3}_{0.6}$)	47.7	0.18	50.5	0.27	2.1	0.90	6.3	93
poly($\mathbf{1}_{0.3}$-*co*-$\mathbf{3}_{0.7}$)	39.8	0.15	65.5	0.35	2.3	1	7.0	99
poly($\mathbf{1}_{0.2}$-*co*-$\mathbf{3}_{0.8}$)	26.5	0.1	74.8	0.40	2.3	1	7.0	94
poly($\mathbf{1}_{0.1}$-*co*-$\mathbf{3}_{0.9}$)	13.3	$5\text{x}10^{-2}$	84.2	0.45	5.6	1	5.6	77

Table S 1. Quantities of **M01**, **M03**, base, catalyst and solvent.

Copolymer	Mn	Mw	Mp	Mz	PDI
poly($\mathbf{1}_{0.9}$-*co*-$\mathbf{3}_{0.1}$)	30213	43234	37098	73456	1.43
poly($\mathbf{1}_{0.8}$-*co*-$\mathbf{3}_{0.2}$)	31320	51175	42312	86734	1.63
poly($\mathbf{1}_{0.7}$-*co*-$\mathbf{3}_{0.3}$)	34358	46512	40001	57900	1.35
poly($\mathbf{1}_{0.6}$-*co*-$\mathbf{3}_{0.4}$)	30002	38701	35492	48098	1.29
poly($\mathbf{1}_{0.5}$-*co*-$\mathbf{3}_{0.5}$)	33077	43522	38009	65091	1.32
poly($\mathbf{1}_{0.4}$-*co*-$\mathbf{3}_{0.6}$)	37038	48743	45323	70954	1.32
poly($\mathbf{1}_{0.3}$-*co*-$\mathbf{3}_{0.7}$)	40652	55432	51230	89734	1.36
poly($\mathbf{1}_{0.2}$-*co*-$\mathbf{3}_{0.8}$)	37412	55341	42645	90218	1.48
poly($\mathbf{1}_{0.1}$-*co*-$\mathbf{3}_{0.9}$)	34086	47087	42316	73241	1.38
Mean	34240	47749	41603	72825	1.40

Table S 2. poly(**1-3**) SEC data.

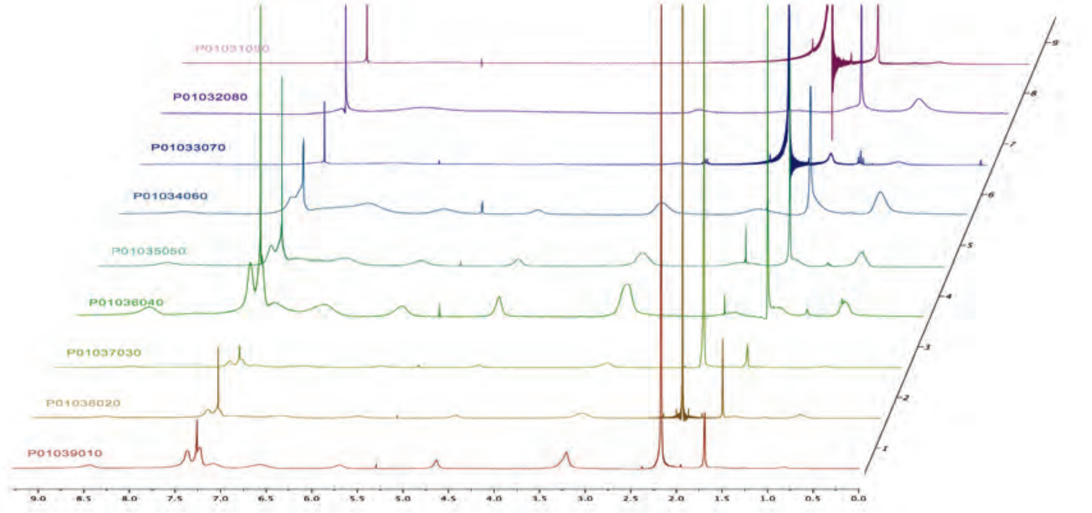

Figure S36. ^{1}H NMR spectra of poly(**1**-*co*-**3**) series (CDCl$_3$, 300 MHz).

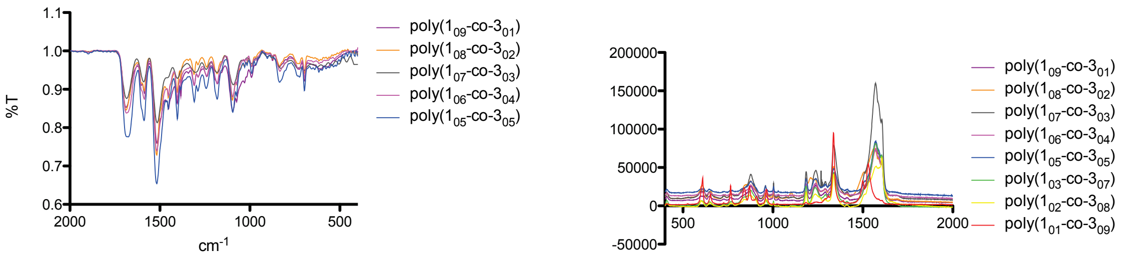

Figure S37. Left: IR and Right: Raman spectra of poly(**1**-*co*-**3**) series.

Synthesis of copolymers poly(1-*co*-4):

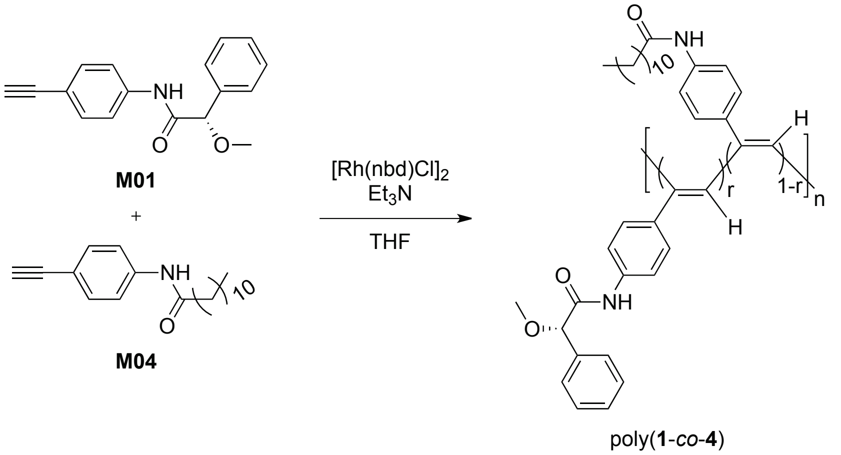

Following the general procedure, the poly(**1**-*co*-**4**) series was synthetized according to the amounts of different reagents (**M01**, **M04**, Et_3N, $[Rh(nbd)Cl]_2$ and THF) reported in Table S 3.

Copolymer	**M01** (mg)	**M01** (mmol)	**M04** (mg)	**M04** (mmol)	$[Rh(nbd)Cl]_2$ (mg)	THF (mL)	Et_3N (μL)	Yield (%)
poly($\mathbf{1}_{0.9}$-*co*-$\mathbf{4}_{0.1}$)	83.5	0.32	10.5	3.5×10^{-2}	1.6	0.75	4.8	88
poly($\mathbf{1}_{0.8}$-*co*-$\mathbf{4}_{0.2}$)	74.2	0.28	20.9	7.0×10^{-2}	1.6	0.75	4.8	82
poly($\mathbf{1}_{0.7}$-*co*-$\mathbf{4}_{0.3}$)	65.0	0.25	31.4	0.11	1.6	0.75	4.8	79
poly($\mathbf{1}_{0.6}$-*co*-$\mathbf{4}_{0.4}$)	55.7	0.21	41.9	0.14	1.6	0.75	4.8	76
poly($\mathbf{1}_{0.5}$-*co*-$\mathbf{4}_{0.5}$)	45.1	0.17	50.9	0.17	1.6	0.75	4.8	71
poly($\mathbf{1}_{0.4}$-*co*-$\mathbf{4}_{0.6}$)	37.1	0.14	62.8	0.21	1.6	0.75	4.8	55
poly($\mathbf{1}_{0.3}$-*co*-$\mathbf{4}_{0.7}$)	27.8	0.11	73.3	0.25	1.6	0.75	4.8	46
poly($\mathbf{1}_{0.2}$-*co*-$\mathbf{4}_{0.8}$)	18.5	7×10^{-2}	83.8	0.28	4.0	0.90	4.8	54
poly($\mathbf{1}_{0.1}$-*co*-$\mathbf{4}_{0.9}$)	9.3	3.5×10^{-2}	94.2	0.32	4.0	0.90	4.8	43

Table S 3. Quantities of **M01**, **M04**, base, catalyst and solvent.

Copolymer	Mn	Mw	Mp	Mz	PDI
poly($\mathbf{1}_{0.9}$-*co*-$\mathbf{4}_{0.1}$)	30111	43229	41293	65332	1.44
poly($\mathbf{1}_{0.8}$-*co*-$\mathbf{4}_{0.2}$)	35426	50932	47628	88654	1.44
poly($\mathbf{1}_{0.7}$-*co*-$\mathbf{4}_{0.3}$)	31984	45382	42394	75664	1.42
poly($\mathbf{1}_{0.6}$-*co*-$\mathbf{4}_{0.4}$)	33285	49986	47345	87465	1.50
poly($\mathbf{1}_{0.5}$-*co*-$\mathbf{4}_{0.5}$)	30100	44309	41002	64598	1.47
poly($\mathbf{1}_{0.4}$-*co*-$\mathbf{4}_{0.6}$)	29783	37645	36392	63221	1.26
poly($\mathbf{1}_{0.3}$-*co*-$\mathbf{4}_{0.7}$)	36487	49281	47392	70298	1.35
poly($\mathbf{1}_{0.2}$-*co*-$\mathbf{4}_{0.8}$)	33298	50392	48728	79384	1.51
poly($\mathbf{1}_{0.1}$-*co*-$\mathbf{4}_{0.9}$)	32182	46237	45983	77345	1.44
Mean	32517	46377	44240	74662	1.43

Table S 4 poly(**1-4**) SEC data.

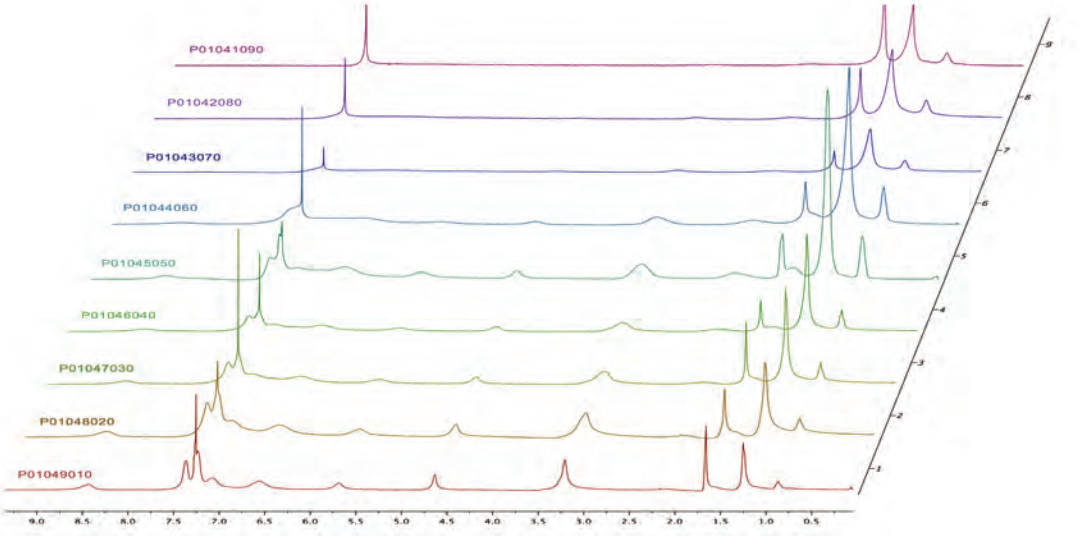

Figure S38. ^{1}H NMR spectra of poly(**1**-*co*-**4**) series (CDCl$_3$, 300 MHz).

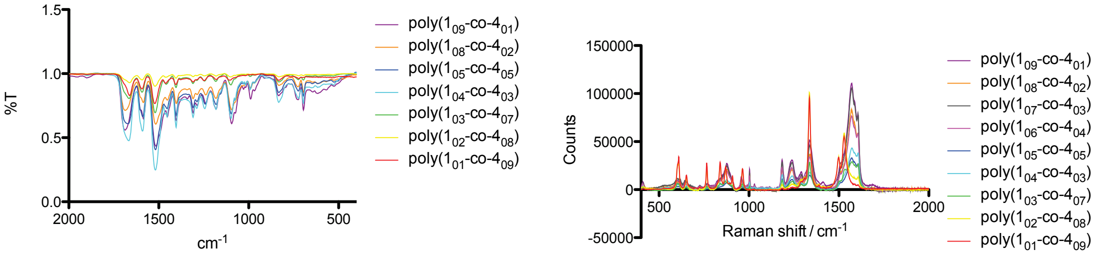

Figure S39. Left: IR and Right: Raman spectra of poly(**1**-*co*-**4**) series.

Synthesis of copolymers poly(1-*co*-5):

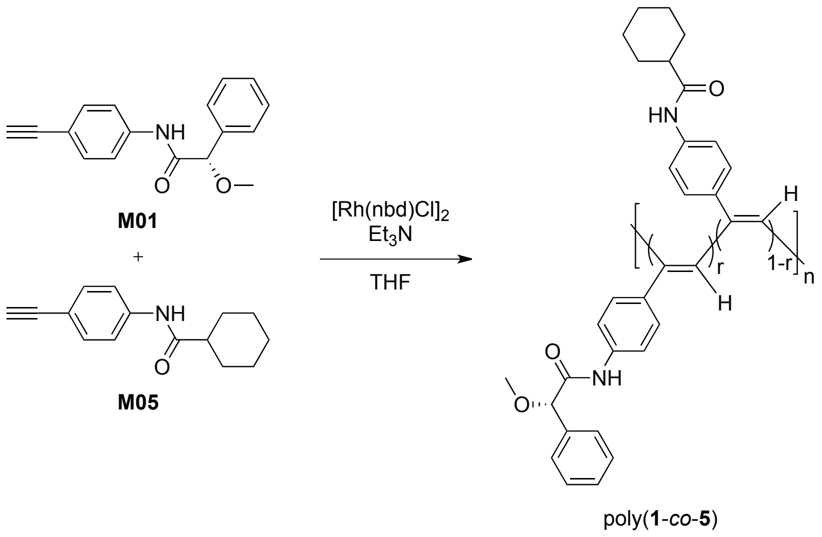

Following the general procedure, the poly(**1**-*co*-**5**) series was synthetized according to the amounts of different reagents (**M01**, **M05**, Et_3N, $[Rh(nbd)Cl]_2$ and THF) reported in Table S 5.

Copolymer	**M01** (mg)	**M01** (mmol)	**M05** (mg)	**M05** (mmol)	$[Rh(nbd)Cl]_2$ (mg)	THF (mL)	Et_3N (μL)	Yield (%)
poly($\mathbf{1}_{0.9}$-*co*-$\mathbf{5}_{0.1}$)	119.4	0.45	11.4	$5x10^{-2}$	1.2	1.2	7.0	80
poly($\mathbf{1}_{0.8}$-*co*-$\mathbf{5}_{0.2}$)	106.1	0.4	22.7	0.1	1.2	1.2	7.0	80
poly($\mathbf{1}_{0.7}$-*co*-$\mathbf{5}_{0.3}$)	92.9	0.35	34.1	0.15	1.2	1.2	7.0	81
poly($\mathbf{1}_{0.6}$-*co*-$\mathbf{5}_{0.4}$)	79.6	0.3	45.5	0.2	1.2	1.2	7.0	84
poly($\mathbf{1}_{0.5}$-*co*-$\mathbf{5}_{0.5}$)	66.3	0.25	56.8	0.25	1.2	1.2	7.0	84
poly($\mathbf{1}_{0.4}$-*co*-$\mathbf{5}_{0.6}$)	53.1	0.2	68.2	0.3	1.2	1.2	7.0	86
poly($\mathbf{1}_{03}$-*co*-$\mathbf{5}_{0.7}$)	39.8	0.15	79.6	0.35	1.2	1.3	7.0	85
poly($\mathbf{1}_{0.2}$-*co*-$\mathbf{5}_{0.8}$)	26.5	0.1	90.9	0.4	1.2	1.3	7.0	80
poly($\mathbf{1}_{0.1}$-*co*-$\mathbf{5}_{0.9}$)	13.3	$5x10^{-2}$	102.3	0.45	1.2	1.3	7.0	72

Table S 5. Quantities of **M01**, **M05**, base, catalyst and solvent.

Copolymer	Mn	Mw	Mp	Mz	PDI
poly(**1**$_{0.9}$-*co*-**5**$_{0.1}$)	30429	52696	58906	79619	1.73
poly(**1**$_{0.8}$-*co*-**5**$_{0.2}$)	28481	51188	57286	74388	1.80
poly(**1**$_{0.7}$-*co*-**5**$_{0.3}$)	33482	48394	50605	78300	1.45
poly(**1**$_{0.6}$-*co*-**5**$_{0.4}$)	30921	43745	44348	57686	1.41
poly(**1**$_{0.5}$-*co*-**5**$_{0.5}$)	23648	35304	35984	47813	1.49
poly(**1**$_{0.4}$-*co*-**5**$_{0.6}$)	19048	28819	27769	41425	1.51
poly(**1**$_{0.3}$-*co*-**5**$_{0.7}$)	13262	26831	22178	30958	1.63
poly(**1**$_{0.2}$-*co*-**5**$_{0.8}$)	15464	24114	22922	34116	1.56
poly(**1**$_{0.1}$-*co*-**5**$_{0.9}$)	13234	23425	20938	35423	1.77
Mean	23107	37168	37881	53303	1.59

Table S 6 poly(**1-5**) SEC data.

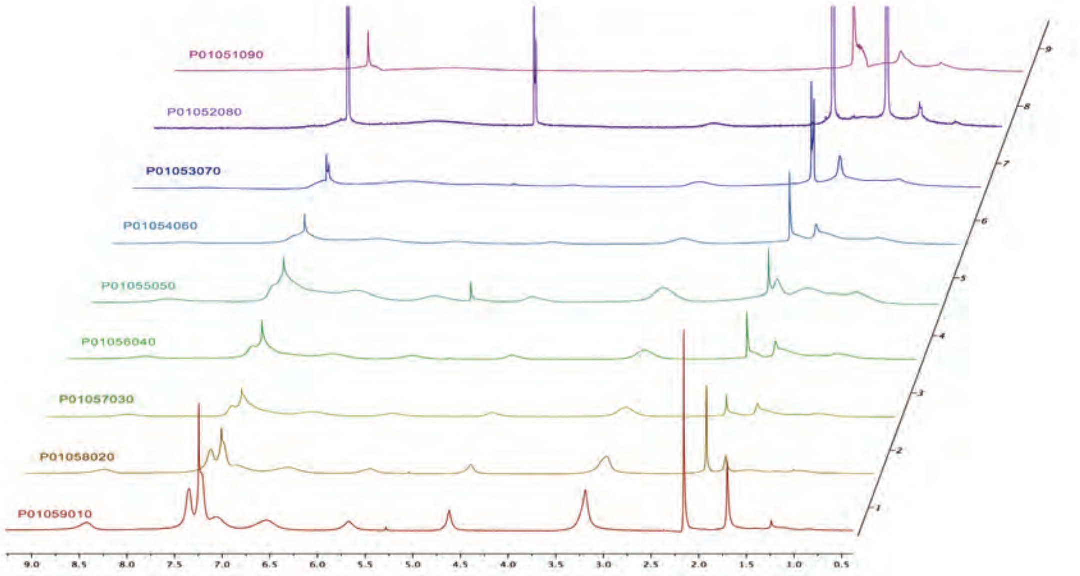

Figure S40. ^{1}H NMR spectra of poly(**1**-*co*-**5**) series ($CDCl_3$, 300 MHz).

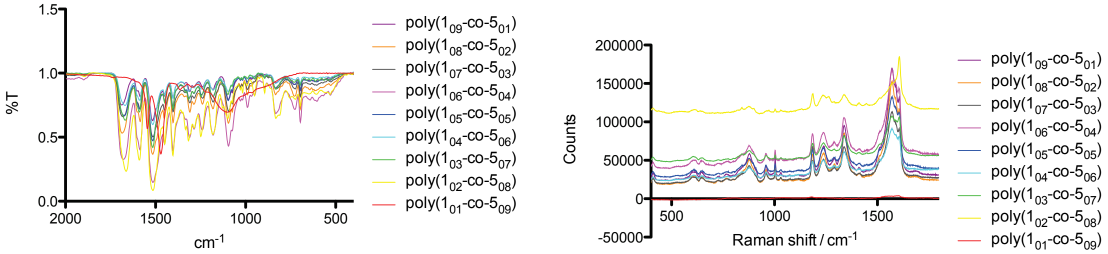

Figure S41. Left: IR and Right: Raman spectra of poly(**1**-*co*-**5**) series.

Synthesis of copolymers poly(1-*co*-6):

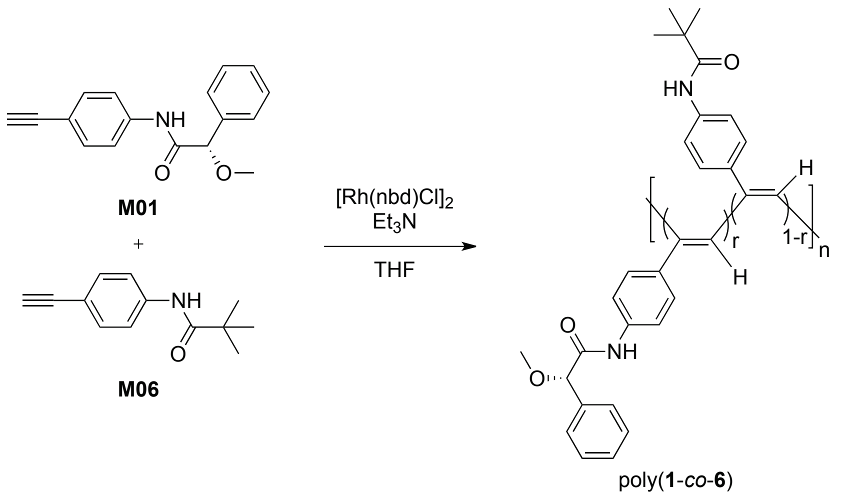

Following the general procedure, the poly(**1**-*co*-**6**) series was synthetized according to the amounts of different reagents (**M01**, **M06**, Et_3N, $[Rh(nbd)Cl]_2$ and THF) reported in Table S 7.

Copolymer	**M01** (mg)	**M01** (mmol)	**M06** (mg)	**M06** (mmol)	$[Rh(nbd)Cl]_2$ (mg)	THF (mL)	Et_3N (μL)	Yield (%)
poly($\mathbf{1}_{0.9}$-*co*-$\mathbf{6}_{0.1}$)	119.4	0.45	10.1	$5x10^{-2}$	1.3	1.04	7.0	65
poly($\mathbf{1}_{0.8}$-*co*-$\mathbf{6}_{0.2}$)	106.1	0.4	20.1	0.1	1.4	1.07	7.0	63
poly($\mathbf{1}_{0.7}$-*co*-$\mathbf{6}_{0.3}$)	92.9	0.35	30.2	0.15	1.5	1.10	7.0	64
poly($\mathbf{1}_{0.6}$-*co*-$\mathbf{6}_{0.4}$)	79.6	0.3	40.3	0.2	1.6	1.13	7.0	59
poly($\mathbf{1}_{0.5}$-*co*-$\mathbf{6}_{0.5}$)	66.3	0.25	50.3	0.25	1.7	1.17	7.0	60
poly($\mathbf{1}_{0.4}$-*co*-$\mathbf{6}_{0.6}$)	53.1	0.2	60.4	0.3	1.8	1.20	7.0	53
poly($\mathbf{1}_{0.3}$-*co*-$\mathbf{6}_{0.7}$)	39.8	0.15	70.4	0.35	2.0	1.23	7.0	55
poly($\mathbf{1}_{0.2}$-*co*-$\mathbf{6}_{0.8}$)	26.5	0.1	80.5	0.4	2.1	1.27	7.0	50
poly($\mathbf{1}_{0.1}$-*co*-$\mathbf{6}_{0.9}$)	13.3	$5x10^{-2}$	90.6	0.45	2.2	1.30	7.0	48

Table S 7. Quantities of **M01**, **M06**, base, catalyst and solvent.

Copolymer	Mn	Mw	Mp	Mz	PDI
poly($\mathbf{1}_{0.9}$-*co*-$\mathbf{6}_{0.1}$)	22304	26940	27309	43928	1.21
poly($\mathbf{1}_{0.8}$-*co*-$\mathbf{6}_{0.2}$)	21457	26548	28457	51245	1.24
poly($\mathbf{1}_{0.7}$-*co*-$\mathbf{6}_{0.3}$)	25487	32154	31245	45785	1.26
poly($\mathbf{1}_{0.6}$-*co*-$\mathbf{6}_{0.4}$)	24517	33284	32458	47865	1.36
poly($\mathbf{1}_{0.5}$-*co*-$\mathbf{6}_{0.5}$)	26548	35687	34785	52011	1.34
poly($\mathbf{1}_{0.4}$-*co*-$\mathbf{6}_{0.6}$)	25487	34574	32154	65487	1.36
poly($\mathbf{1}_{0.3}$-*co*-$\mathbf{6}_{0.7}$)	21548	30258	31547	57888	1.40
poly($\mathbf{1}_{0.2}$-*co*-$\mathbf{6}_{0.8}$)	20154	29658	28997	48754	1.47
poly($\mathbf{1}_{0.1}$-*co*-$\mathbf{6}_{0.9}$)	21548	28657	28874	47586	1.33
Mean	23227	28640	275826	51172	1.33

Table S 8 poly(**1**-**6**) SEC data.

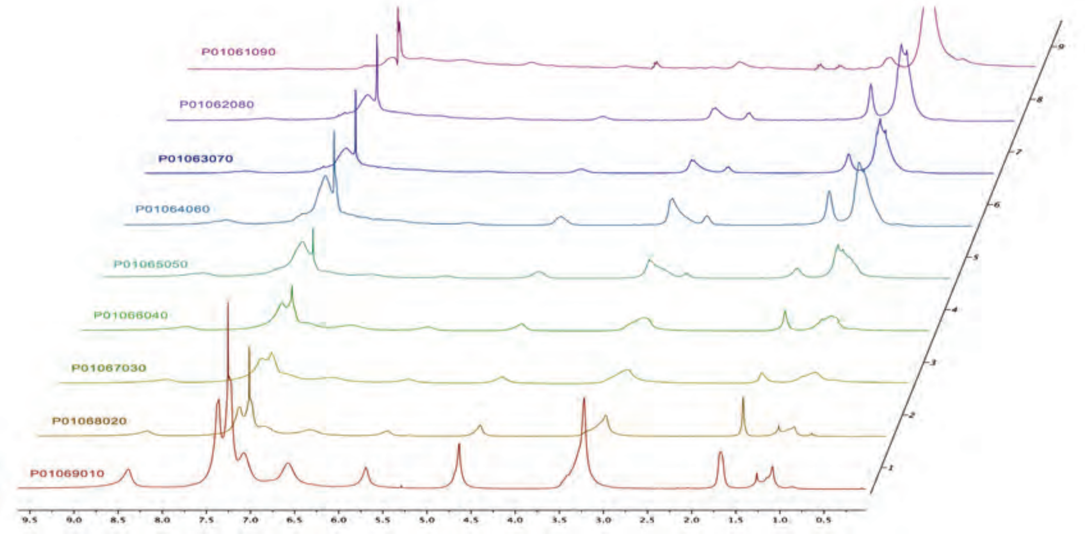

Figure S42. ^{1}H NMR spectra of poly(**1**-*co*-**6**) series (CDCl$_3$, 300 MHz).

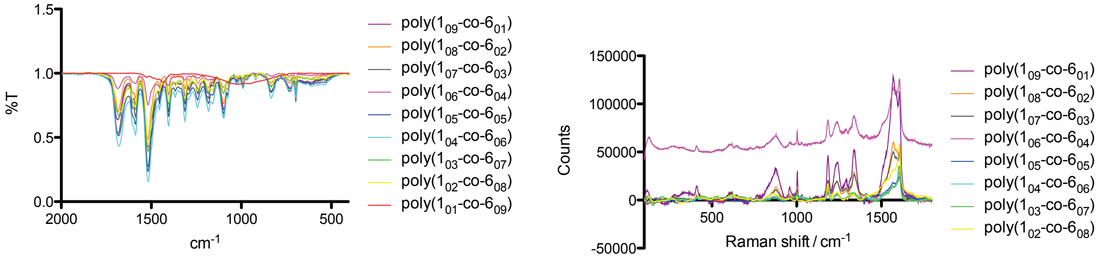

Figure S43. Left: IR and Right: Raman spectra of poly(**1**-*co*-**6**) series.

Synthesis of copolymers poly(1-*co*-7):

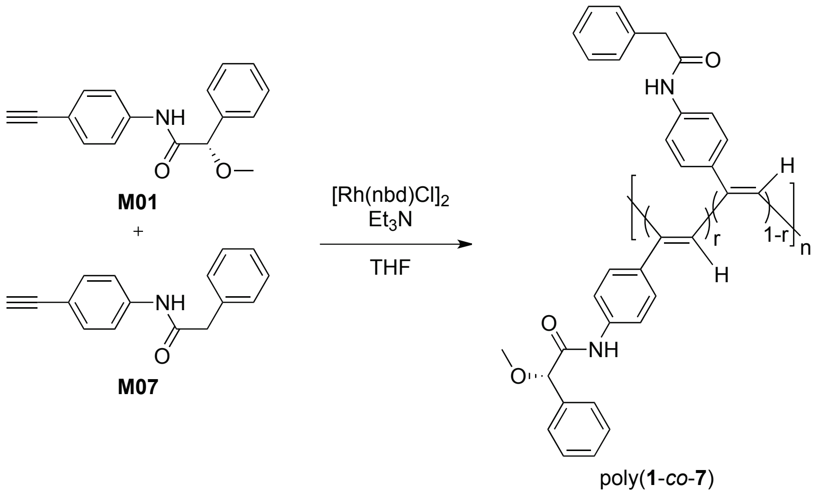

Following the general procedure, the poly(**1**-*co*-**7**) series was synthetized according to the amounts of different reagents (**M01**, **M07**, Et_3N, $[Rh(nbd)Cl]_2$ and THF) reported in Table S 9.

Copolymer	**M01** (mg)	**M01** (mmol)	**M07** (mg)	**M07** (mmol)	$[Rh(nbd)Cl]_2$ (mg)	THF (mL)	Et_3N (μL)	Yield (%)
poly(**1**$_{0.9}$-*co*-**7**$_{0.1}$)	119.4	0.45	11.7	5×10^{-2}	2.0	1.43	7.0	91
poly(**1**$_{0.8}$-*co*-**7**$_{0.2}$)	106.1	0.4	23.5	0.1	2.7	1.53	7.0	89
poly(**1**$_{0.7}$-*co*-**7**$_{0.3}$)	92.9	0.35	35.3	0.15	3.6	1.63	7.0	89
poly(**1**$_{0.6}$-*co*-**7**$_{0.4}$)	79.6	0.3	47.0	0.2	4.4	1.74	7.0	89
poly(**1**$_{0.5}$-*co*-**7**$_{0.5}$)	66.3	0.25	58.8	0.25	5.2	1.84	7.0	88
poly(**1**$_{0.4}$-*co*-**7**$_{0.6}$)	53.1	0.2	70.6	0.3	6.0	1.94	7.0	89
poly(**1**$_{0.3}$-*co*-**7**$_{0.7}$)	39.8	0.15	82.3	0.35	6.8	2.05	7.0	89
poly(**1**$_{0.2}$-*co*-**7**$_{0.8}$)	26.5	0.1	94.1	0.4	7.6	2.15	7.0	59
poly(**1**$_{0.1}$-*co*-**7**$_{0.9}$)	13.3	5×10^{-2}	105.9	0.45	8.4	2.25	7.0	51

Table S 9. Quantities of **M01**, **M07**, base, catalyst and solvent.

Copolymer	Mn	Mw	Mp	Mz	PDI
poly($\mathbf{1}_{0.9}$-*co*-$\mathbf{7}_{0.1}$)	38691	55378	45238	78907	1.43
poly($\mathbf{1}_{0.8}$-*co*-$\mathbf{7}_{0.2}$)	38320	61195	55937	93709	1.59
poly($\mathbf{1}_{0.7}$-*co*-$\mathbf{7}_{0.3}$)	44258	68845	62412	103311	1.56
poly($\mathbf{1}_{0.6}$-*co*-$\mathbf{7}_{0.4}$)	41350	63055	54180	94134	1.52
poly($\mathbf{1}_{0.5}$-*co*-$\mathbf{7}_{0.5}$)	40581	62071	50908	93831	1.53
poly($\mathbf{1}_{0.4}$-*co*-$\mathbf{7}_{0.6}$)	42860	67300	53695	104156	1.57
poly($\mathbf{1}_{0.3}$-*co*-$\mathbf{7}_{0.7}$)	51510	67579	54128	88780	1.31
poly($\mathbf{1}_{0.2}$-*co*-$\mathbf{7}_{0.8}$)	44478	63487	50888	90218	1.43
poly($\mathbf{1}_{0.1}$-*co*-$\mathbf{7}_{0.9}$)	42805	63722	55703	92673	1.49
Mean	42761	63625	53677	93302	1.49

Table S 10 poly(**1**-**7**) SEC data.

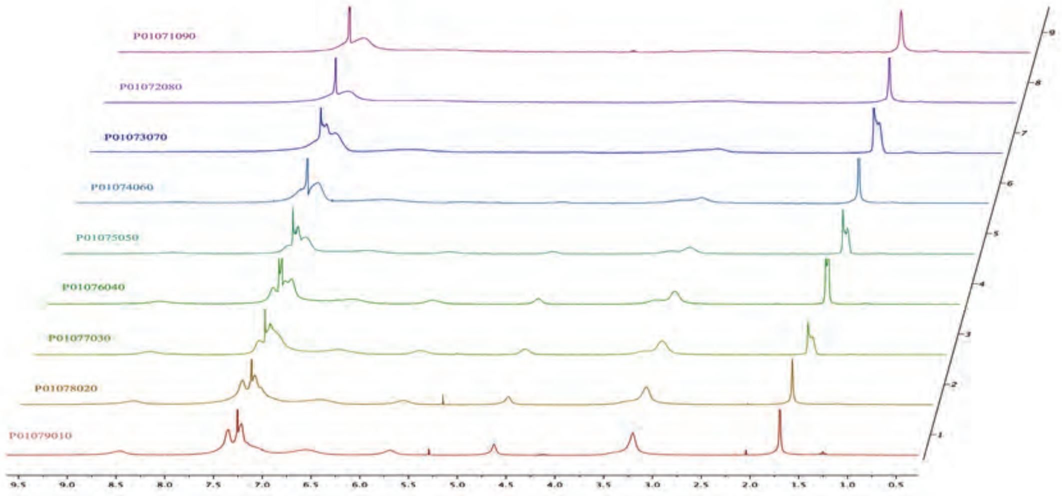

Figure S44. ^{1}H NMR spectra of poly(**1**-*co*-**7)** series ($CDCl_3$, 300 MHz).

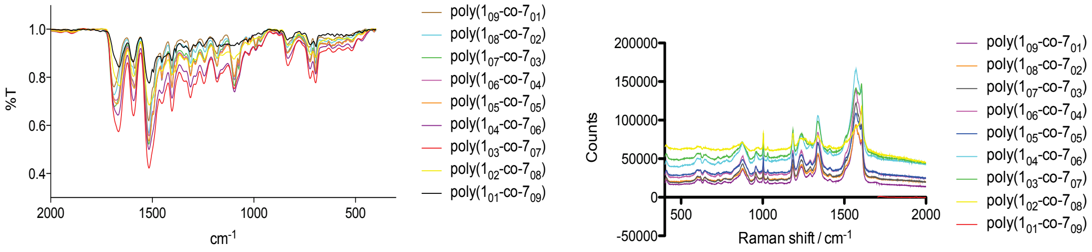

Figure S45. Left: IR and Right: Raman spectra of poly(**1**-*co*-**7**) series.

Synthesis of copolymers poly(**1**-*co*-8):

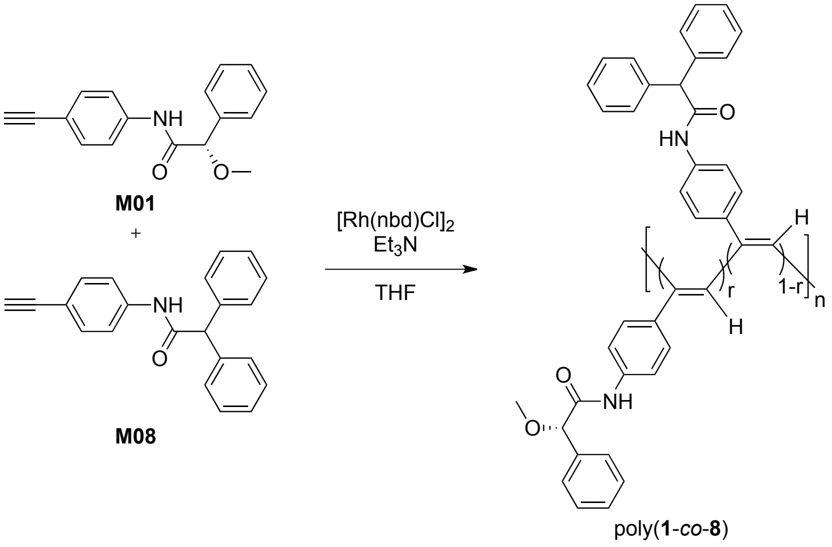

Following the general procedure, the poly(**1**-*co*-**8**) series was synthetized according to the amounts of different reagents (**M01**, **M08**, Et_3N, $[Rh(nbd)Cl]_2$ and THF) reported in Table S 11.

Copolymer	**M01** (mg)	**M01** (mmol)	**M08** (mg)	**M08** (mmol)	$[Rh(nbd)Cl]_2$ (mg)	THF (mL)	Et_3N (μL)	Yield (%)
poly(**1**$_{0.9}$-*co*-**8**$_{0.1}$)	119.4	0.45	15.6	5×10^{-2}	2.0	1.50	7.0	80
poly(**1**$_{0.8}$-*co*-**8**$_{0.2}$)	106.1	0.4	31.1	0.1	2.8	1.68	7.0	83
poly(**1**$_{0.7}$-*co*-**8**$_{0.3}$)	92.9	0.35	46.7	0.15	3.6	1.86	7.0	84
poly(**1**$_{0.6}$-*co*-**8**$_{0.4}$)	79.6	0.3	62.3	0.2	4.4	2.04	7.0	84
poly(**1**$_{0.5}$-*co*-**8**$_{0.5}$)	66.3	0.25	77.9	0.25	5.2	2.22	7.0	89
poly(**1**$_{0.4}$-*co*-**8**$_{0.6}$)	53.1	0.2	93.4	0.3	6.0	2.40	7.0	86
poly(**1**$_{0.3}$-*co*-**8**$_{0.7}$)	39.8	0.15	109.0	0.35	6.8	2.60	7.0	87
poly(**1**$_{0.2}$-*co*-**8**$_{0.8}$)	26.5	0.1	124.6	0.4	7.6	2.76	7.0	61
poly(**1**$_{0.1}$-*co*-**8**$_{0.9}$)	13.3	5×10^{-2}	140.1	0.45	8.4	2.94	7.0	65

Table S 11. Quantities of **M01**, **M08**, base, catalyst and solvent.

Copolymer	Mn	Mw	Mp	Mz	PDI
poly(**1**$_{0.9}$-*co*-**8**$_{0.1}$)	33799	50245	42358	75848	1.49
poly(**1**$_{0.8}$-*co*-**8**$_{0.2}$)	38547	52147	48578	85766	1.35
poly(**1**$_{0.7}$-*co*-**8**$_{0.3}$)	29674	52221	44157	78596	1.76
poly(**1**$_{0.6}$-*co*-**8**$_{0.4}$)	26587	47584	45784	65878	1.79
poly(**1**$_{0.5}$-*co*-**8**$_{0.5}$)	28514	43257	41241	77444	1.52
poly(**1**$_{0.4}$-*co*-**8**$_{0.6}$)	25554	48887	43255	80125	1.91
poly(**1**$_{0.3}$-*co*-**8**$_{0.7}$)	22000	37548	36215	65245	1.70
poly(**1**$_{0.2}$-*co*-**8**$_{0.8}$)	21522	36222	35255	57485	1.68
poly(**1**$_{0.1}$-*co*-**8**$_{0.9}$)	22110	35475	32154	51245	1.60
Mean	27590	49014	41000	70848	1.64

Table S 5 poly(**1**-**8**) SEC data.

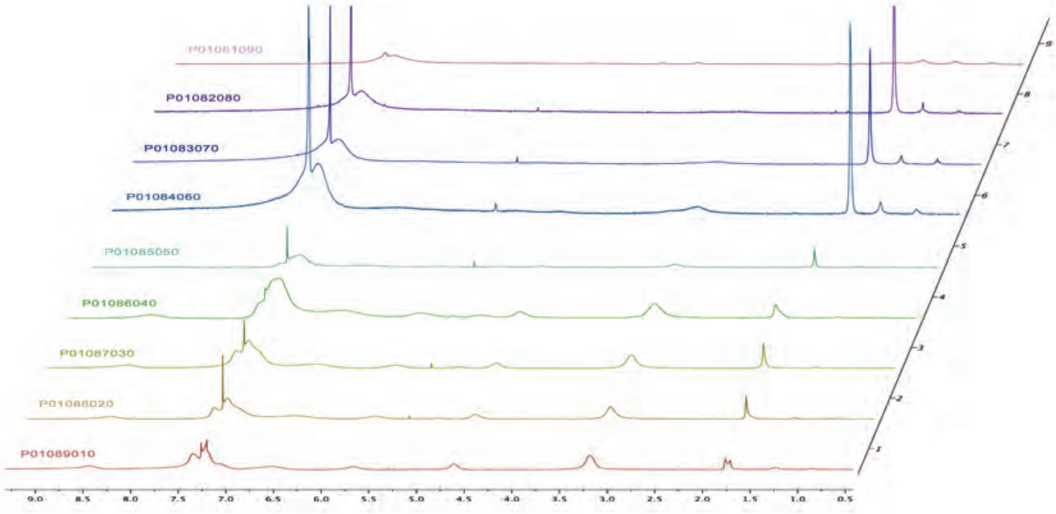

Figure S46. ^{1}H NMR spectra of poly(**1**-*co*-**8**) series ($CDCl_3$, 300 MHz).

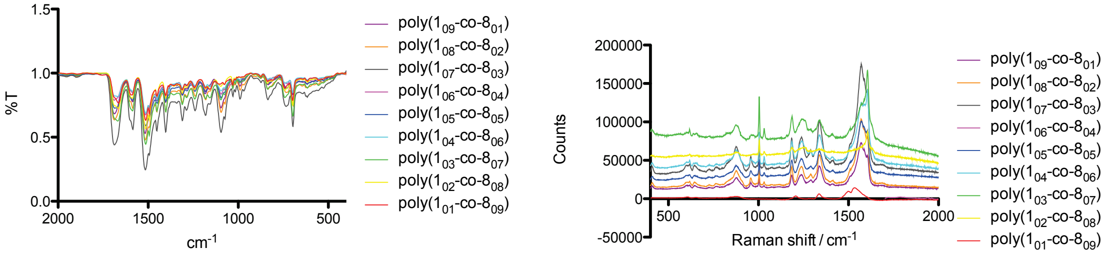

Figure S47. Left: IR and Right: Raman spectra of poly(**1**-*co*-**8**) series.

Synthesis of copolymers poly(1-*co*-9):

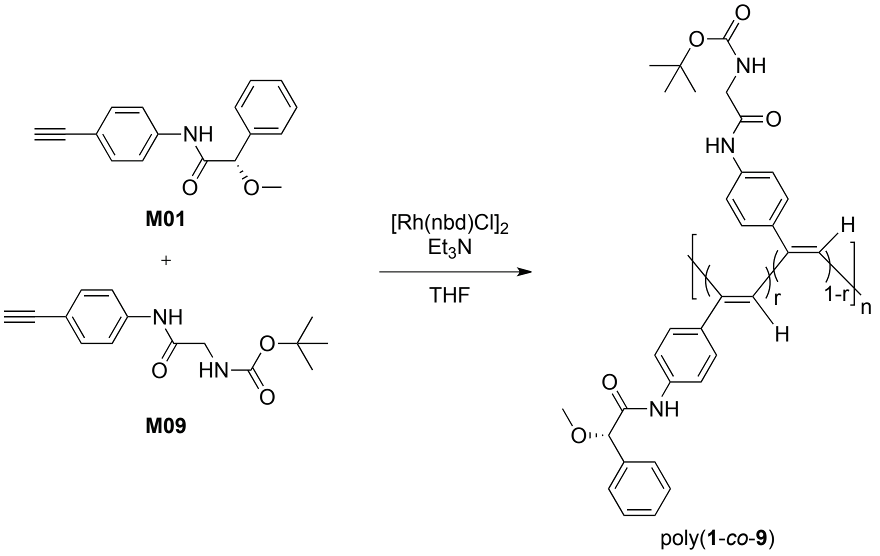

Following the general procedure, the poly(**1**-*co*-**9**) series was synthetized according to the amounts of different reagents (**M01**, **M09**, Et$_3$N, [Rh(nbd)Cl]$_2$ and THF) reported in Table S 13.

Copolymer	**M01** (mg)	**M01** (mmol)	**M09** (mg)	**M09** (mmol)	[Rh(nbd)Cl]$_2$ (mg)	THF (mL)	Et$_3$N (μL)	Yield (%)
poly(**1**$_{0.9}$-*co*-**9**$_{0.1}$)	119.4	0.45	13.7	5x10^{-2}	1.3	1.33	7.0	97
poly(**1**$_{0.8}$-*co*-**9**$_{0.2}$)	106.1	0.4	27.4	0.1	1.4	1.34	7.0	90
poly(**1**$_{0.7}$-*co*-**9**$_{0.3}$)	92.9	0.35	41.2	0.15	1.5	1.34	7.0	90
poly(**1**$_{0.6}$-*co*-**9**$_{0.4}$)	79.6	0.3	54.9	0.2	1.6	1.35	7.0	91
poly(**1**$_{0.5}$-*co*-**9**$_{0.5}$)	66.3	0.25	68.6	0.25	1.7	1.35	7.0	97
poly(**1**$_{0.4}$-*co*-**9**$_{0.6}$)	53.1	0.2	82.3	0.3	1.8	1.35	7.0	93
poly(**1**$_{0.3}$-*co*-**9**$_{0.7}$)	39.8	0.15	96.0	0.35	2.0	1.36	7.0	96
poly(**1**$_{0.2}$-*co*-**9**$_{0.8}$)	26.5	0.1	109.7	0.4	2.1	1.36	7.0	95
poly(**1**$_{0.1}$-*co*-**9**$_{0.9}$)	13.3	5x10^{-2}	123.4	0.45	2.2	1.37	7.0	93

Table S 13. Quantities of **M01**, **M09**, base, catalyst and solvent.

Copolymer	Mn	Mw	Mp	Mz	PDI
poly($\mathbf{1}_{0.9}$-*co*-$\mathbf{9}_{0.1}$)	16045	25198	19127	38372	1.52
poly($\mathbf{1}_{0.8}$-*co*-$\mathbf{9}_{0.2}$)	31241	43566	44838	56804	1.40
poly($\mathbf{1}_{0.7}$-*co*-$\mathbf{9}_{0.3}$)	31610	44205	43862	58165	1.40
poly($\mathbf{1}_{0.6}$-*co*-$\mathbf{9}_{0.4}$)	36199	54673	55260	75097	1.51
poly($\mathbf{1}_{0.5}$-*co*-$\mathbf{9}_{0.5}$)	44352	65134	64460	88846	1.47
poly($\mathbf{1}_{0.4}$-*co*-$\mathbf{9}_{0.6}$)	40382	74439	72750	123050	1.84
poly($\mathbf{1}_{0.3}$-*co*-$\mathbf{9}_{0.7}$)	27619	57166	58384	90767	2.06
poly($\mathbf{1}_{0.2}$-*co*-$\mathbf{9}_{0.8}$)	39318	75618	84049	120613	1.92
poly($\mathbf{1}_{0.1}$-*co*-$\mathbf{9}_{0.9}$)	25053	50991	47118	90122	2.04
Mean	32424	54554	54427	82426	1,68

Table S 6 poly(**1**-**9**) SEC data.

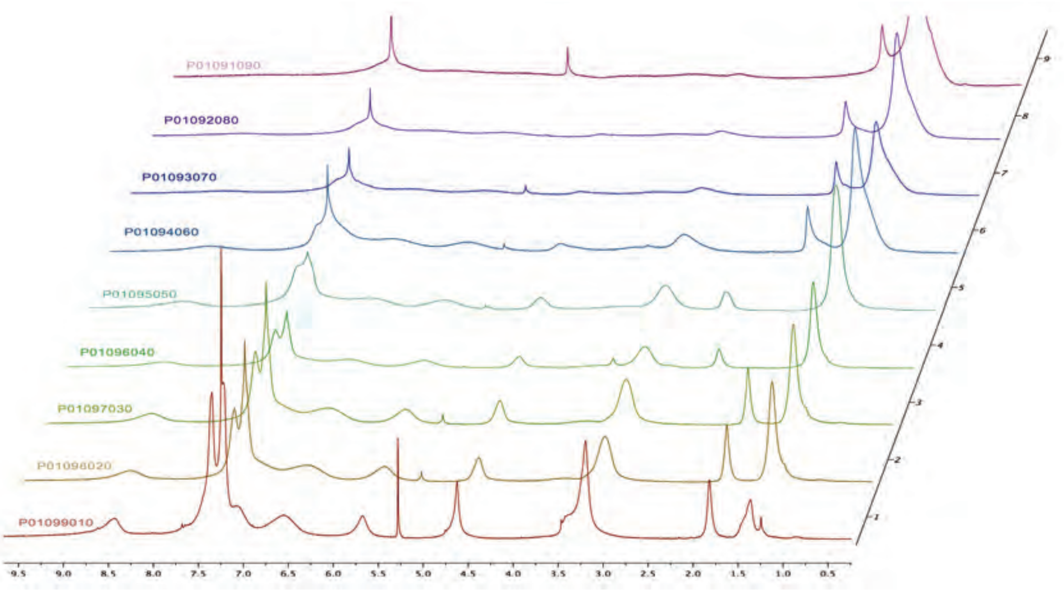

Figure S48. ^{1}H NMR spectra of poly(**1**-*co*-**9**) series (CDCl$_3$, 300 MHz).

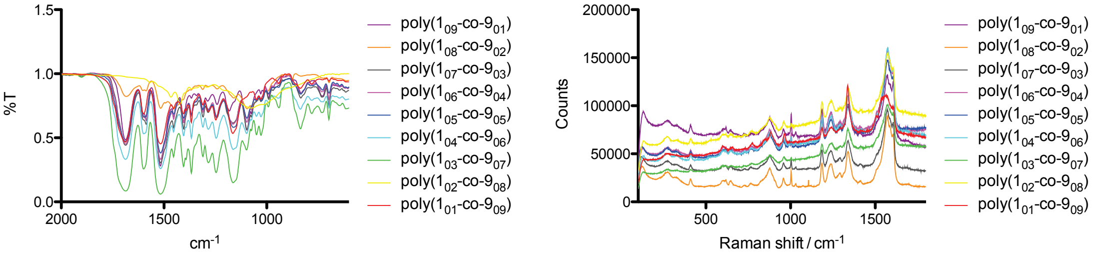

Figure S49. Left: IR and Right: Raman spectra of poly(**1**-*co*-**9**) series.

Determination of the monomer reactivity ratios in copolymerizations

To estimate the monomer reactivity ratios in the copolymerizations of poly(**1**-*co*-**7**) (r1 and r7), and in poly(**1**-*co*-**8**) (r1 and r8), the copolymerizations of **M01** with **M07** and **M01** with **M08** at varying monomer feed ratios were carried out and were terminated at low conversions by adding, in both cases, a solution of HCl 0,05 M in THF (5 mL) 5 seconds after the catalyst addition. Subsequently, a solution of NaOH 0,05 M in THF (5 mL) was added followed by MeOH (10 mL) containing a small amount of conc. HCl. The resulting poly(**1**-*co*-**7**) and poly(**1**-*co*-**8**) were collected by centrifugation, and dried in vacuo at room temperature overnight. The copolymer compositions were determined from their ^{1}H NMR spectra (Figure S50) and the results are summarized in Table S15. The copolymer compositions are almost similar to the corresponding monomer feed ratios. For the determination of r1 and r7, and r1 and r8, the Kelen-Tüdös method was used.[i],[ii] In this method, the following equation is employed:

$$\eta = \left(r_1 + \frac{r_7(r_8)}{\alpha}\right)\xi - \frac{r_7(r_8)}{\alpha}$$

Where η and ξ are expressed as $G/(\alpha+H)$ and $H/(\alpha+H)$, respectively, by using G and H, which are defined as $G = F(f-1)/f$ and F^2/f, respectively, with F and f representing the molar ratios of monomers in the feed and the molar ratios in the copolymers. α is a parameter defined as $\alpha = (F_{\text{min}}\bullet F_{\text{max}})^{0,5}$, where F_{min} and F_{max} correspond to the lowest and highest values of F, respectively. A plot of η versus ξ affords a straight line (Figure S51). The intercept at $\xi = 0$ and $\xi = 1$ gives –r7(or r8)/α and r1, respectively. The estimated monomer reactivity ratios for **M01–M07** copolymer are r1 = 1.0166 and r7 = 1.0195 and those for **M01–M08** copolymer are r1 = 1.0647 and r8 = 1.052. The products of the monomer reactivity ratios (r1r7 and r1r8) for the copolymerizations of **M01** with **M07** and **M01** with **M08** are 1,0364 and 1,1201, respectively, suggesting that the monomer distributions in the copolymers are mostly random.

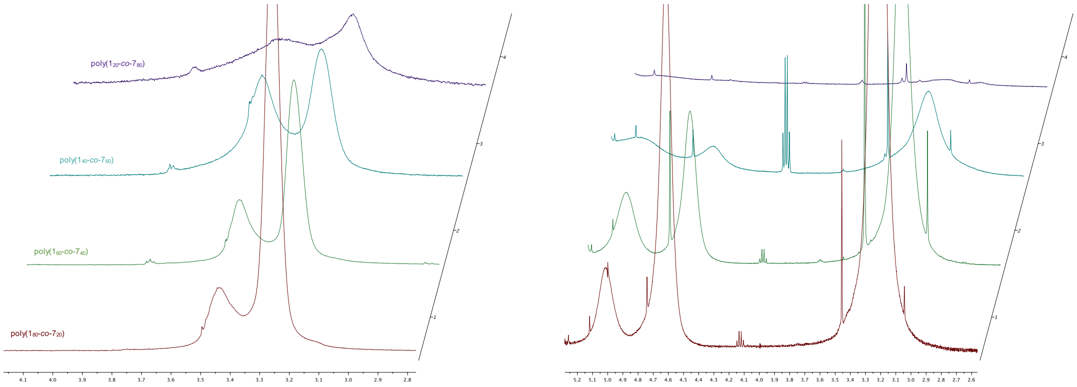

Figure S50. ^{1}H NMR spectra of copolymerizations at low conversion of poly($\mathbf{1}_{0.8}$-*co*-$\mathbf{7}_{0.2}$), poly($\mathbf{1}_{0.6}$-*co*-$\mathbf{7}_{0.4}$), poly($\mathbf{1}_{0.4}$-*co*-$\mathbf{7}_{0.6}$) and poly($\mathbf{1}_{0.2}$-*co*-$\mathbf{7}_{0.8}$) (Left) and poly($\mathbf{1}_{0.8}$-*co*-$\mathbf{8}_{0.2}$), poly($\mathbf{1}_{0.6}$-*co*-$\mathbf{8}_{0.4}$), poly($\mathbf{1}_{0.4}$-*co*-$\mathbf{8}_{0.6}$) and poly($\mathbf{1}_{0.2}$-*co*-$\mathbf{8}_{0.8}$) (Right)

	Monomer	Polymer	
Run	*F*	yield (%)[a]	*f* [b]
poly($\mathbf{1}_{0.8}$-*co*-$\mathbf{7}_{0.2}$)	0.8	26	0.7986
poly($\mathbf{1}_{0.6}$-*co*-$\mathbf{7}_{0.4}$)	0.6	29	0.5989
poly($\mathbf{1}_{0.4}$-*co*-$\mathbf{7}_{0.6}$)	0.4	28	0.3975
poly($\mathbf{1}_{0.2}$-*co*-$\mathbf{7}_{0.8}$)	0.2	27	0.1978
poly($\mathbf{1}_{0.8}$-*co*-$\mathbf{8}_{0.2}$)	0.8	32	0.7972
poly($\mathbf{1}_{0.6}$-*co*-$\mathbf{8}_{0.4}$)	0.6	28	0.5945
poly($\mathbf{1}_{0.4}$-*co*-$\mathbf{8}_{0.6}$)	0.4	28	0.4001
poly($\mathbf{1}_{0.2}$-*co*-$\mathbf{8}_{0.8}$)	0.2	24	0.1913

[a] Insoluble fraction in MeOH. [b] Determined by integration in the ^{1}H NMR spectra of the copolymers

Table S 15. *F* and *f* molar fractions and conversions of poly(**1**-*co*-**7**) and poly(**1**-*co*-**8**) series.

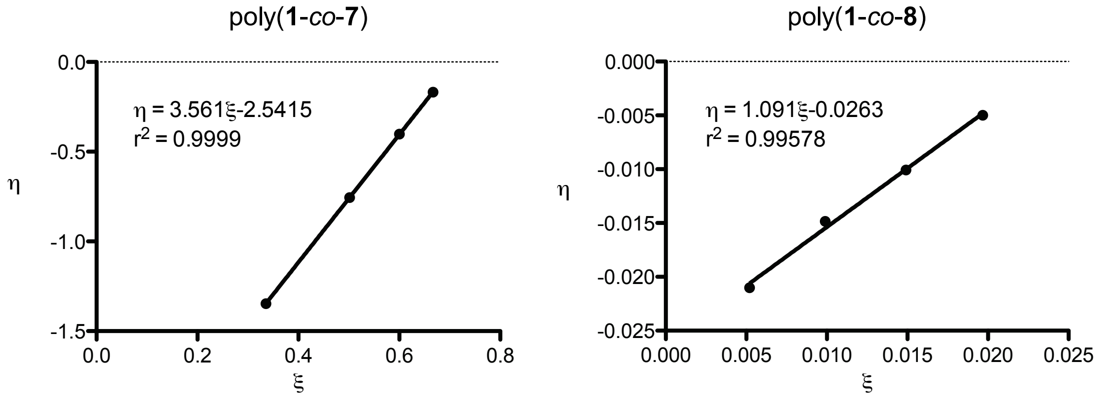

Figure S51. Kelen-Tüdös plots for the copolymerization of poly(**1**-*co*-**7**) and poly(**1**-*co*-**8**)

The *cis-transoidal* stereoregularity was determined by ^{1}H NMR (vinyl proton resonance at around 5.7-5.8 ppm) and Raman Resonances (785 nm).[iii] The peak at 1567 cm^{-1} is assigned to C=C bond stretching in the *cis* polyacetylene overlap with that of the phenyl ring. The peak at 1340 cm^{-1} is assigned to the *cis* C-C bond coupled with the single bond connecting the main chain and phenyl ring. The peak at 1003 cm^{-1} is assigned to the C-H bond deformation of the *cis* form (Figure S).[iv]

Raman spectra was performed in a FT-Raman BRUKER (FRA 106) equipped by Nd:Yag laser (350 mW, 1.064 nm excitation wavelength).

CD/UV studies and chiral amplification mechanism

All CD measurements were performed in HPLC grade $CHCl_3$ filtered in basic alumina in 0.1 and/or 0.2 mg/mL concentration of polymer. Optimum $M(ClO_4)_x$ concentration was previously determined.[v],[vi]

The percentage of CD signal was determined at the wavelength of the maximum in the two regions of the exciton (340-350 nm and 380-400 nm). These values were related to the UV spectra to avoid concentration differences in CD measurements using the following equation: $\%\mathrm{CD} = \frac{\%g_{340-350}+\%g_{380-400}}{2}$, where $\%g_x = \frac{g_x}{g(poly-1)_x}\times 100$ and $g_x = \frac{CDsignal_x}{UVsignal_x}$.

Chiral amplification in poly(1-*co*-3) with divalent metal ions

a)

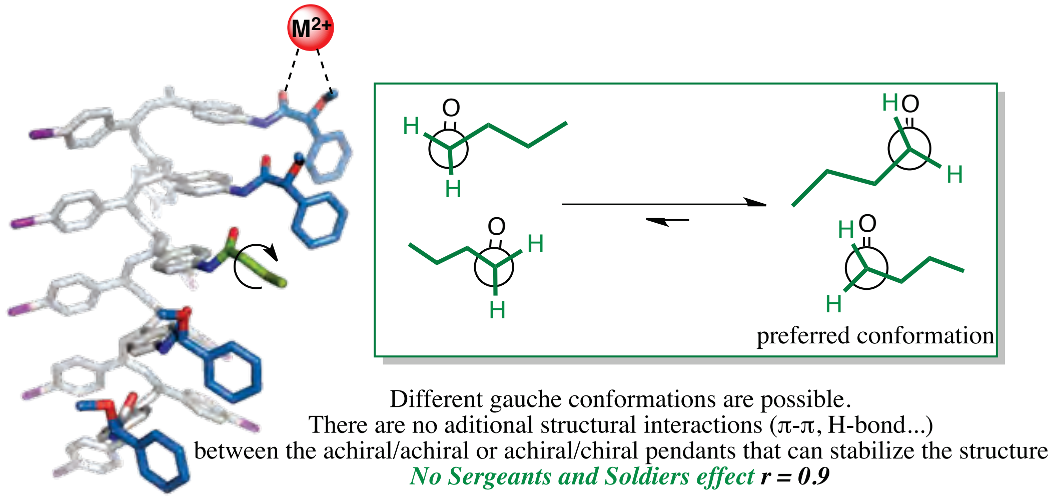

Different gauche conformations are possible.
There are no aditional structural interactions (π-π, H-bond...)
between the achiral/achiral or achiral/chiral pendants that can stabilize the structure
No Sergeants and Soldiers effect ***r = 0.9***

3/1 helical structure generated by the MPA pendant groups

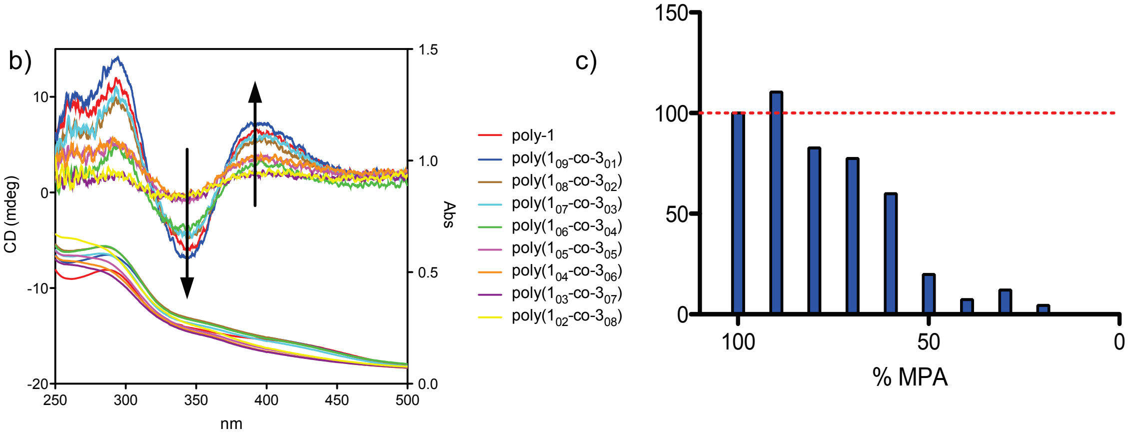

Figure S52. a) Structural effect of replacing MPA pendants by monomer **03** **i**n poly(**1**-*co*-**3**) and interaction with Ba^{2+}. b) CD and UV spectra. c) % of CD signal compared to poly-**1** in a solution of the poly(**1**-*co*-**3**) series (mru)/Ba^{2+} ratio of 1.0/0.5 (mol/mol) in $CDCl_3$ [poly(**1**-*co*-**3**)] = 0.1 mg/mL].

Chiral amplification in poly(1-*co*-3) with monovalent metal ions

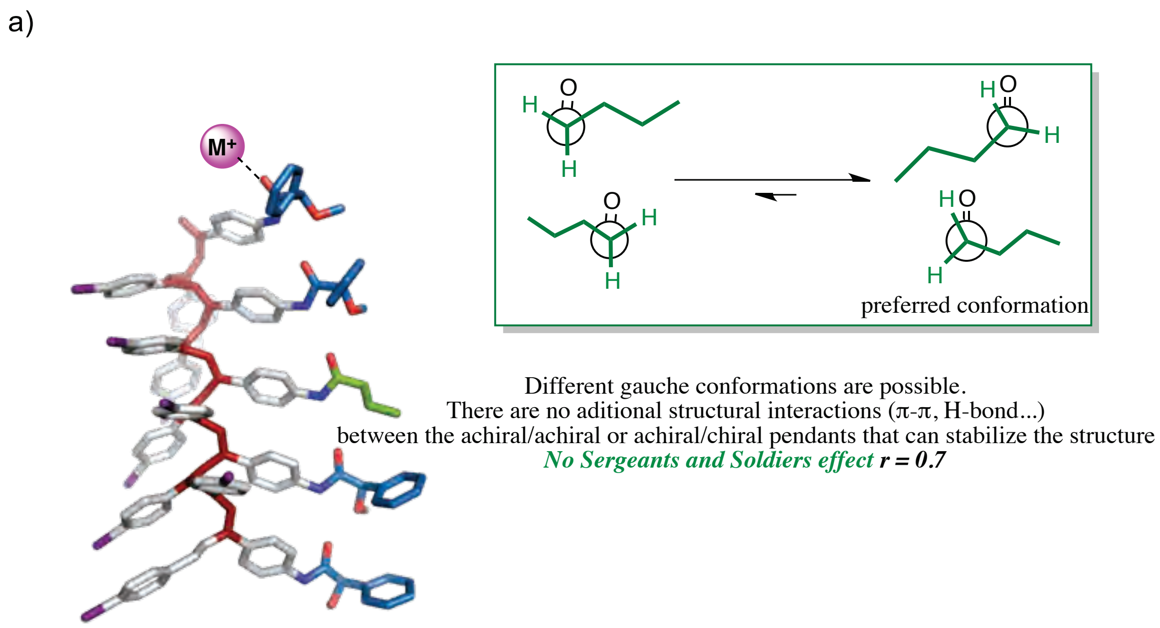

Different gauche conformations are possible.
There are no aditional structural interactions (π-π, H-bond...)
between the achiral/achiral or achiral/chiral pendants that can stabilize the structure
No Sergeants and Soldiers effect r = 0.7

3/1 helical structure generated by the MPA pendant groups

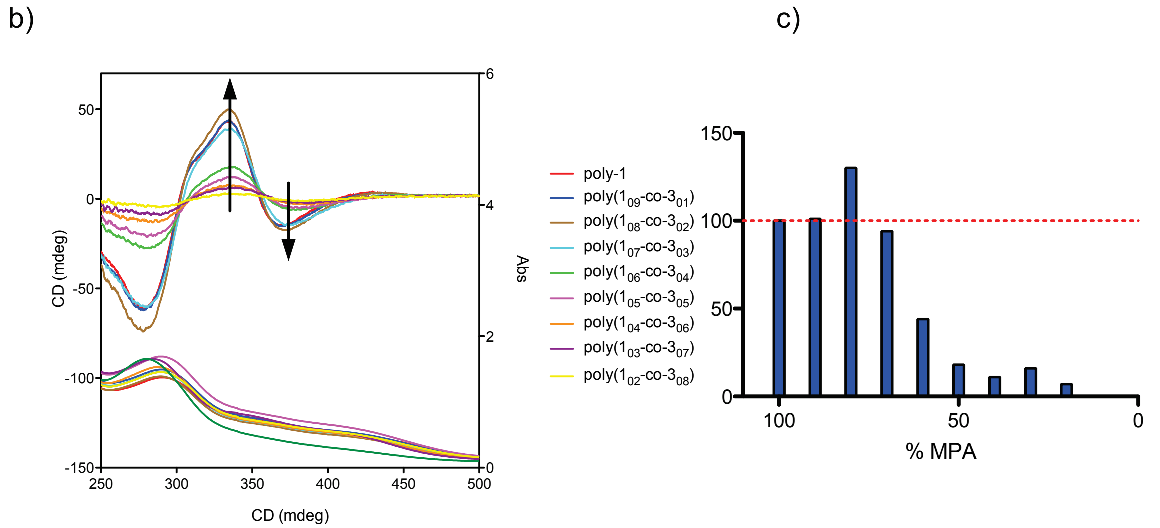

Figure S53. a) Structural effect of replacing MPA pendants by monomer **03 i**n poly(**1**-*co*-**3**) and interaction with Li^+. b) CD and UV spectra. c) % of CD signal compared to poly-**1** in a solution of the poly(**1**-*co*-**3**) series (mru)/Li^+ ratio of 1.0/0.5 (mol/mol) in $CDCl_3$ [poly(**1**-*co*-**3**)] = 0.1 mg/mL].

Chiral amplification in poly(1-*co*-4) with divalent metal ions

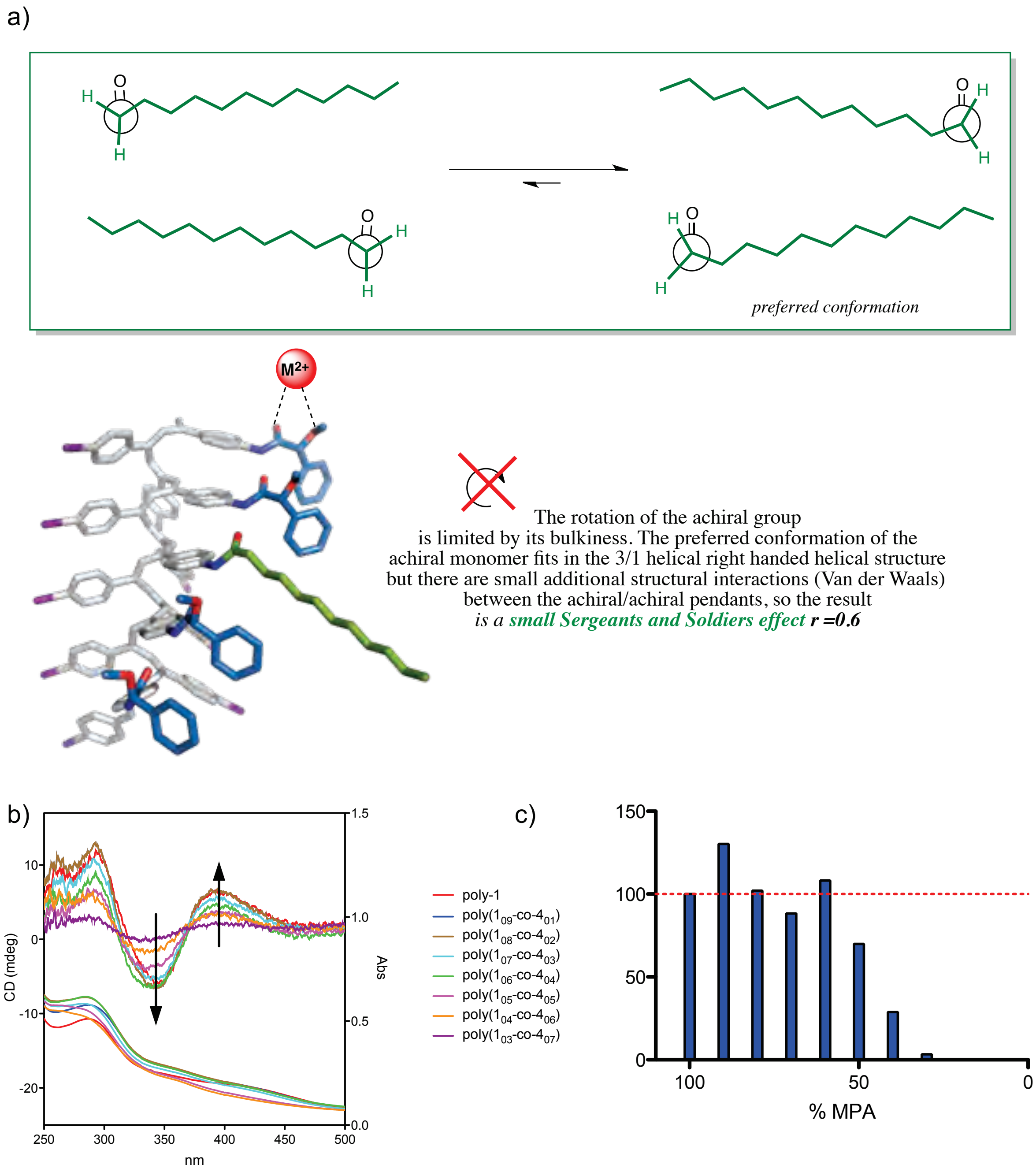

Figure S54. a) Structural effect of replacing MPA pendants by monomer **04 i**n poly(**1**-*co*-**4**) and interaction with Ba^{2+}. b) CD and UV spectra. c) % of CD signal compared to poly-**1** in a solution of the poly(**1**-*co*-**4**) series (mru)/Ba^{2+} ratio of 1.0/0.5 (mol/mol) in $CDCl_3$ [poly(**1**-*co*-**4**)] = 0.1 mg/mL].

Chiral amplification in poly(1-*co*-4) with monovalent metal ions

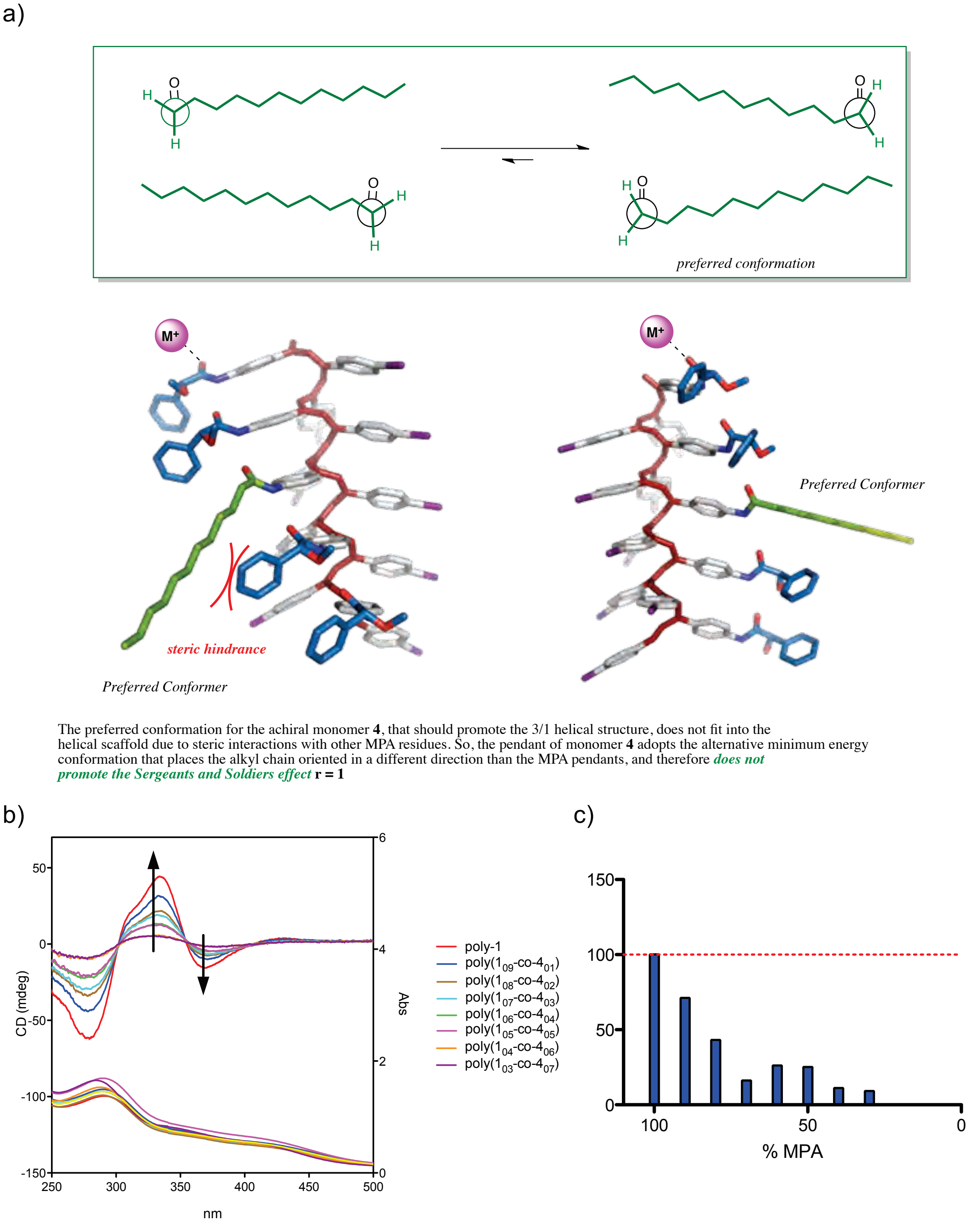

The preferred conformation for the achiral monomer **4**, that should promote the 3/1 helical structure, does not fit into the helical scaffold due to steric interactions with other MPA residues. So, the pendant of monomer **4** adopts the alternative minimum energy conformation that places the alkyl chain oriented in a different direction than the MPA pendants, and therefore ***does not promote the Sergeants and Soldiers effect*** **r = 1**

Figure S55. a) Structural effect of replacing MPA pendants by monomer **04** **i**n poly(**1**-*co*-**4**) and interaction with Li$^+$. b) CD and UV spectra. c) % of CD signal compared to poly-**1** in of a solution of the poly(**1**-*co*-**4**) series (mru/Li$^+$ ratio of 1.0/0.5 (mol/mol) in CDCl$_3$ [poly(**1**-*co*-**4**)] = 0.1 mg/mL].

Chiral amplification in poly(1-*co*-5) with divalent metal ions

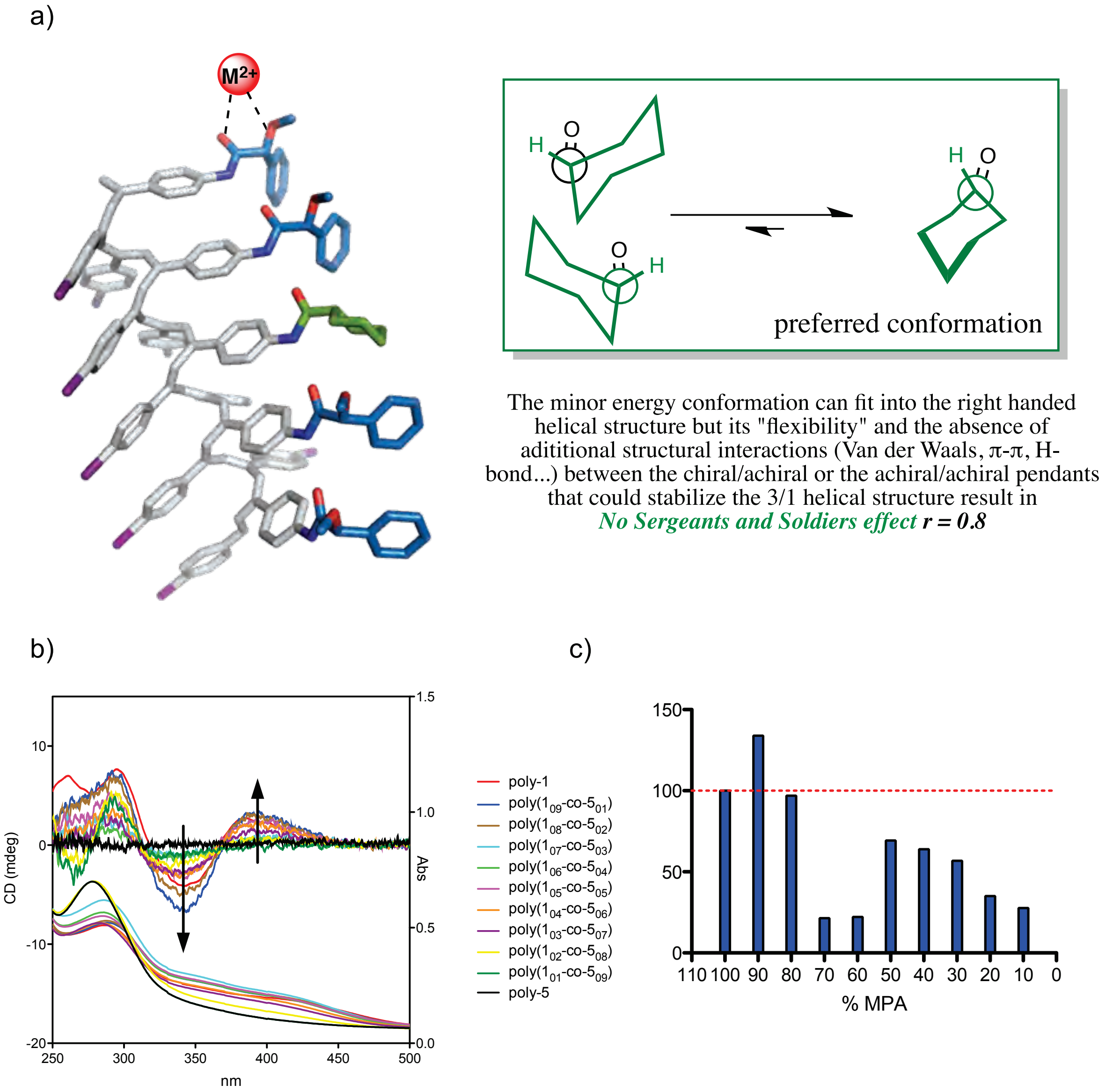

The minor energy conformation can fit into the right handed helical structure but its "flexibility" and the absence of adititional structural interactions (Van der Waals, π-π, H-bond...) between the chiral/achiral or the achiral/achiral pendants that could stabilize the 3/1 helical structure result in ***No Sergeants and Soldiers effect r = 0.8***

Figure S56. a) Structural effect of replacing MPA pendants by monomer **05 i**n poly(**1**-*co*-**5**) and interaction with Ba^{2+}. b) CD and UV spectra. c) % of CD signal compared to poly-**1** in a solution of the poly(**1**-*co*-**5**) series (mru)/Ba^{2+} ratio of 1.0/0.5 (mol/mol) in $CDCl_3$ [poly(**1**-*co*-**5**)] = 0.1 mg/mL].

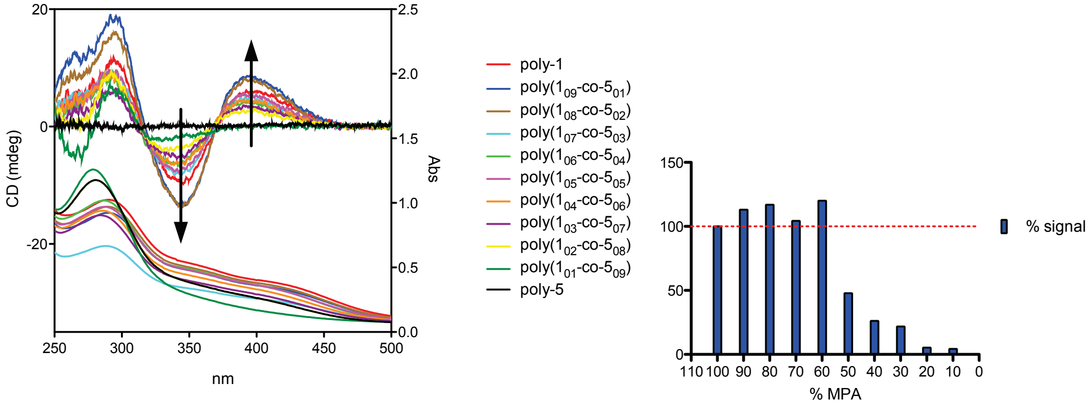

Figure S57. Left: CD and UV spectra and Right: % of CD signal compared to poly-**1** in a solution of the poly(**1**-*co*-**5**) series (mru)/Ba^{2+} ratio of 1.0/0.5 (mol/mol) in $CDCl_3$ [poly(**1**-*co*-**5**)] = 0.2 mg/mL].

Chiral amplification in poly(**1**-*co*-**5**) with monovalent metal ions

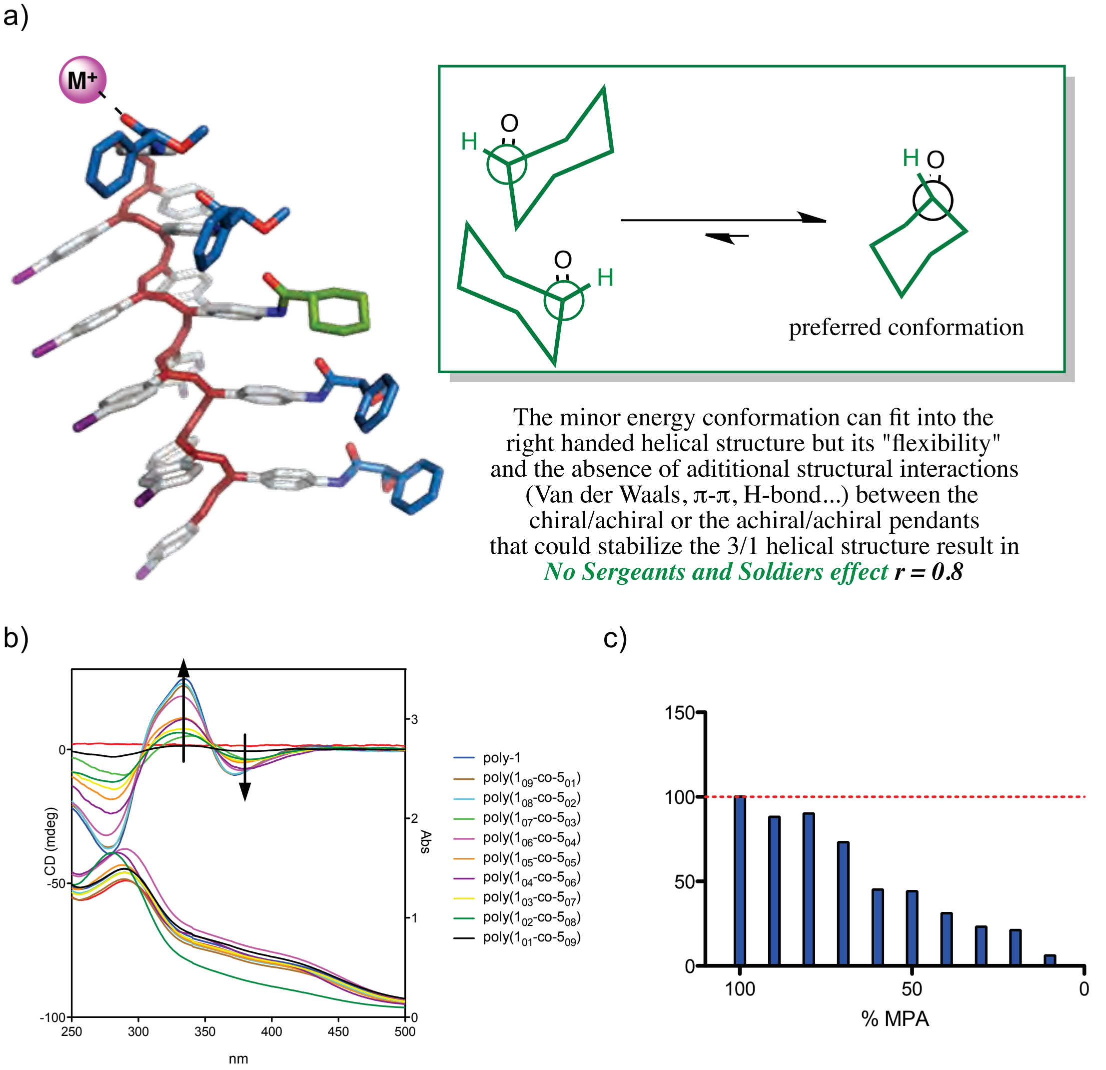

The minor energy conformation can fit into the right handed helical structure but its "flexibility" and the absence of aditiitional structural interactions (Van der Waals, π-π, H-bond...) between the chiral/achiral or the achiral/achiral pendants that could stabilize the 3/1 helical structure result in ***No Sergeants and Soldiers effect* r = 0.8**

Figure S58.) Structural effect of replacing MPA pendants by monomer **05 i**n poly(**1**-*co*-**5**) and interaction with Li$^+$. b) CD and UV spectra. c) % of CD signal compared to poly-**1** in a solution of the poly(**1**-*co*-**5**) series (mru)/Li$^+$ ratio of 1.0/0.5 (mol/mol) in $CDCl_3$ [poly(**1**-*co*-**5**)] = 0.1 mg/mL].

Chiral amplification in poly(1-*co*-6) with divalent metal ions

a)

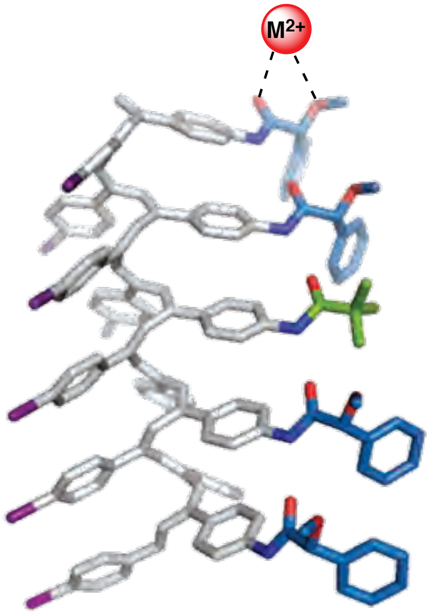

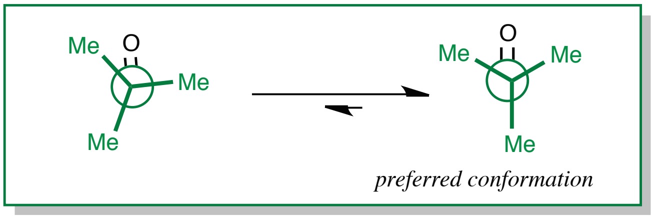

The rotation of the achiral group
is limited by its bulkiness. The preferred conformation of the
achiral monomer fits in the 3/1 right-handed helical structure
but there are no additional structural features
that can stabilize the structure with this pendant, so the result
is a ***small Sergeants and Soldiers effect r =0.6***

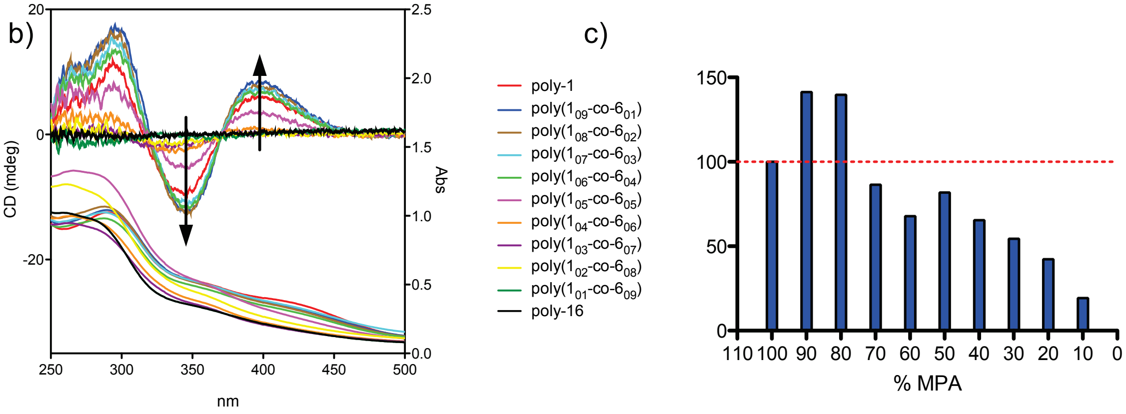

Figure S59. a) Structural effect of replacing MPA pendants by monomer **06 i**n poly(**1**-*co*-**6**) and interaction with Ba^{2+} b) CD and UV spectra and c) % of CD signal compared to poly-**1** in of a solution of the poly(**1**-*co*-**6**) series (mru)/Ba^{2+} ratio of 1.0/0.5 (mol/mol) in $CDCl_3$. [poly(**1**-*co*-**6**)] = 0.1 mg/mL].

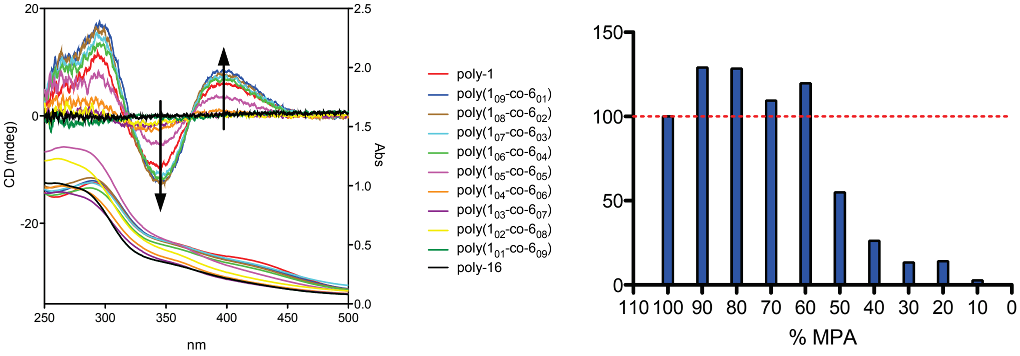

Figure S60. Left: CD and UV spectra and Right: % of CD signal compared to poly-**1** in of a solution of the poly(**1**-*co*-**6**) series (mru)/Ba^{2+} ratio of 1.0/0.5 (mol/mol) in CDCl$_3$. [poly(**1**-*co*-**6**)] = 0.2 mg/mL].

Chiral amplification in poly(1-*co*-6) with monovalent metal ions

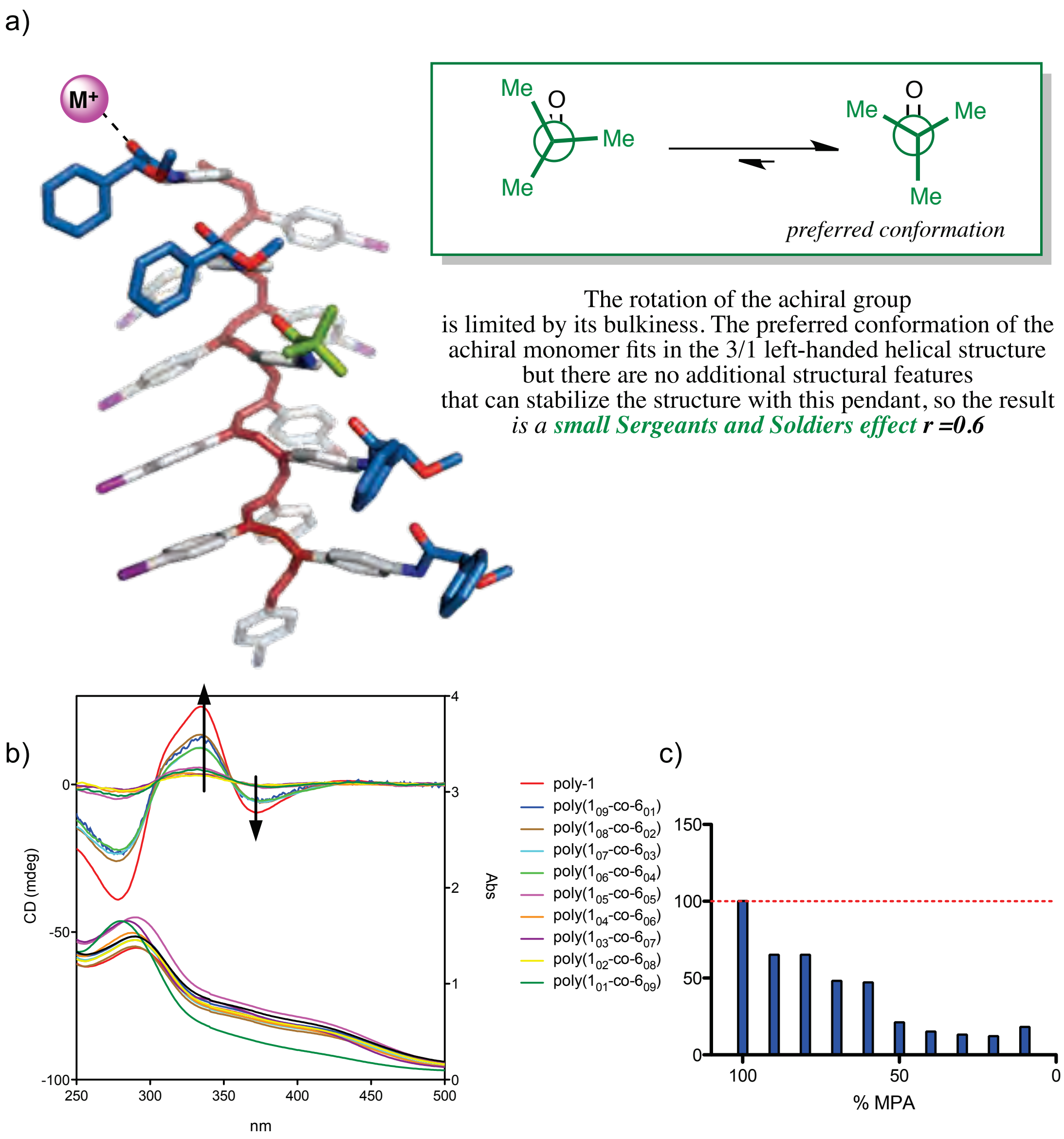

The rotation of the achiral group is limited by its bulkiness. The preferred conformation of the achiral monomer fits in the 3/1 left-handed helical structure but there are no additional structural features that can stabilize the structure with this pendant, so the result *is a* ***small Sergeants and Soldiers effect r =0.6***

Figure S61. a) Structural effect of replacing MPA pendants by monomer **06 i**n poly(**1**-*co*-**6**) and interaction with Li$^+$. b) CD and UV spectra. c) CD signal compared to poly-**1** in of a solution of the poly(**1**-*co*-**6**) series (mru)/Li$^+$ ratio of 1.0/0.5 (mol/mol) in CDCl$_3$. [poly(**1**-*co*-**6**)] = 0.1 mg/mL].

Chiral amplification in poly(**1**-*co*-**7**) with divalent metal ions

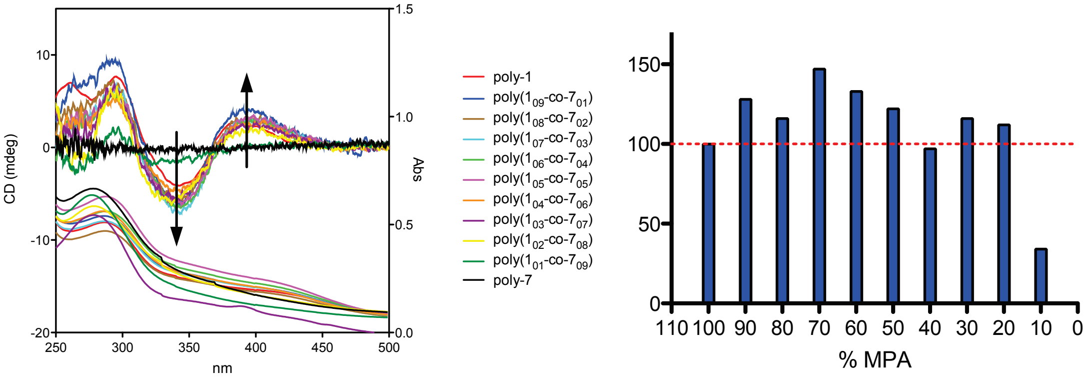

Figure S62. Left: CD and UV spectra and Right: % of CD signal compared to poly-**1** in of a solution of the poly(**1**-*co*-**7**) series (mru)/Ba^{2+} ratio of 1.0/0.5 (mol/mol) in CDCl$_3$. [poly(**1**-*co*-**7**)] = 0.1 mg/mL].

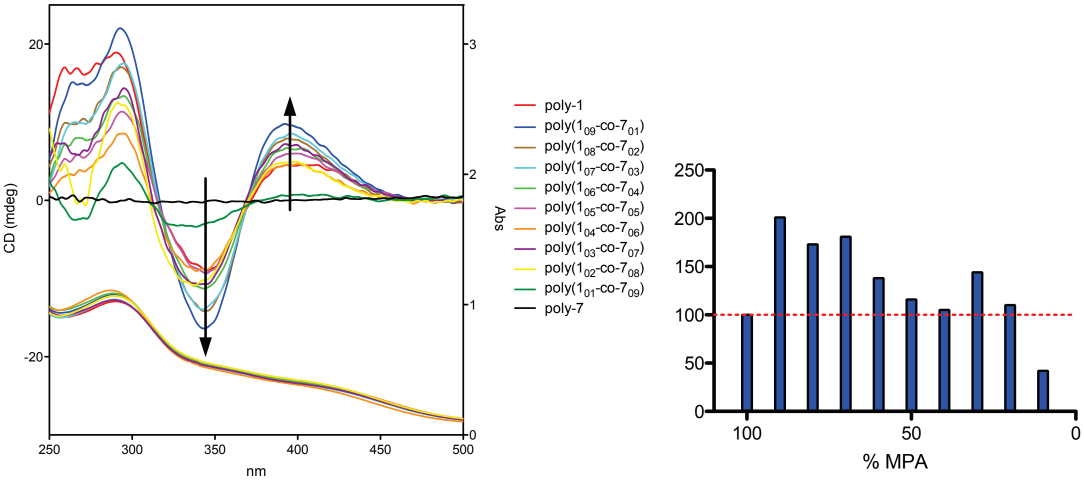

Figure S63. Left: CD and UV spectra and Right: % of CD signal compared to poly-**1** in of a solution of the poly(**1**-*co*-**7**) series (mru)/Ba^{2+} ratio of 1.0/0.5 (mol/mol) in CDCl$_3$. [poly(**1**-*co*-**7**)] = 0.2 mg/mL].

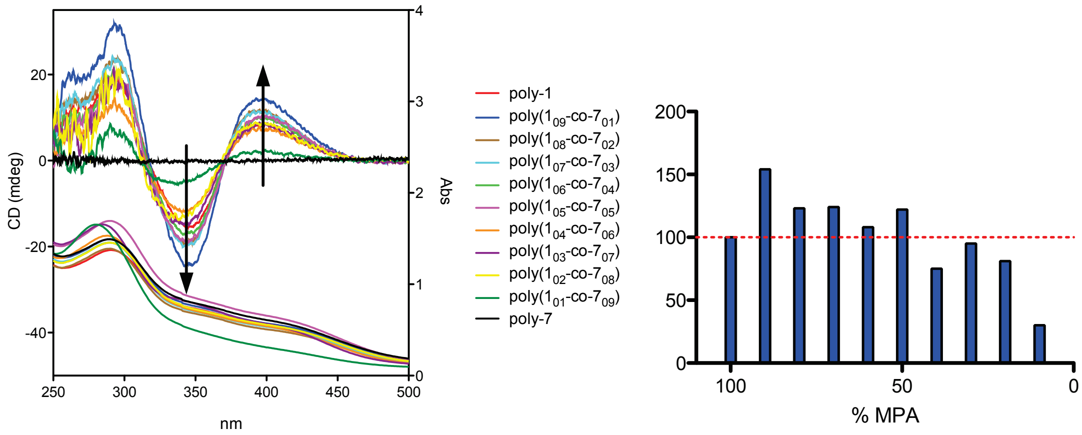

Figure S64. Left: CD and UV spectra and Right: % of CD signal compared to poly-**1** in of a solution of the poly(**1**-*co*-**7**) series (mru)/Ba^{2+} ratio of 1.0/0.5 (mol/mol) in CDCl$_3$. [poly(**1**-*co*-**7**)] = 0.3 mg/mL].

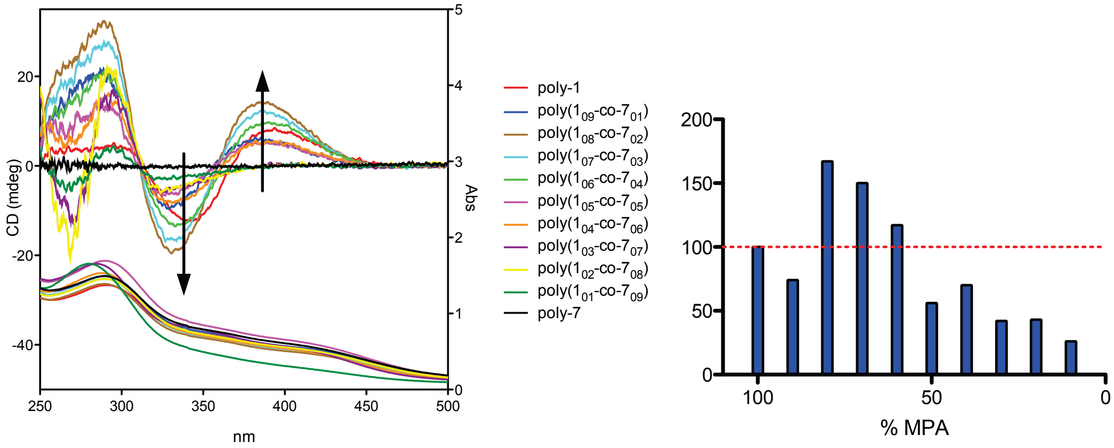

Figure S65. Left: CD and UV spectra and Right: % of CD signal compared to poly-**1** in of a solution of the poly(**1**-*co*-**7**) series (mru)/Ca^{2+} ratio of 1.0/0.5 (mol/mol) in CDCl$_3$. [poly(**1**-*co*-**7**)] = 0.3 mg/mL].

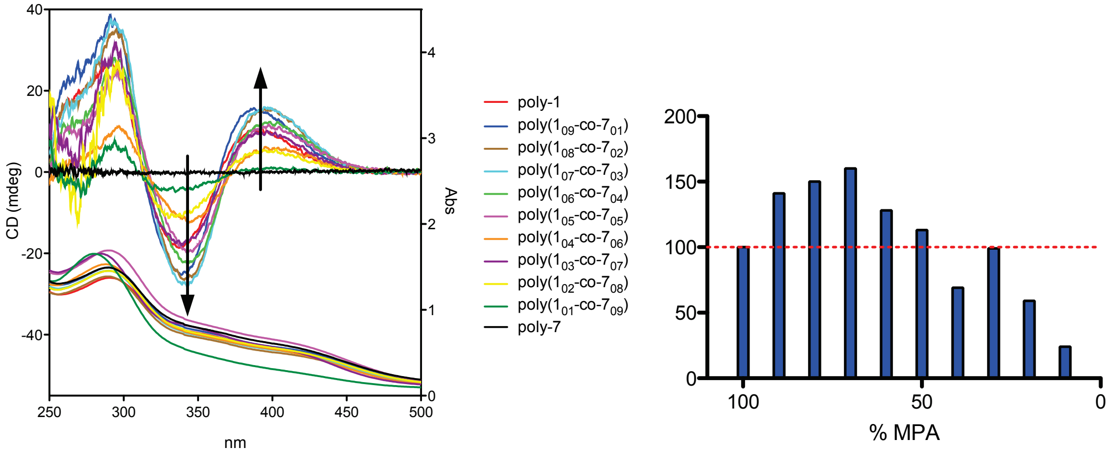

Figure S66. Left: CD and UV spectra and Right: % of CD signal compared to poly-**1** in of a solution of the poly(**1**-*co*-**7**) series (mru)/Co^{2+} ratio of 1.0/0.5 (mol/mol) in $CDCl_3$. [poly(**1**-*co*-**7**)] = 0.3 mg/mL].

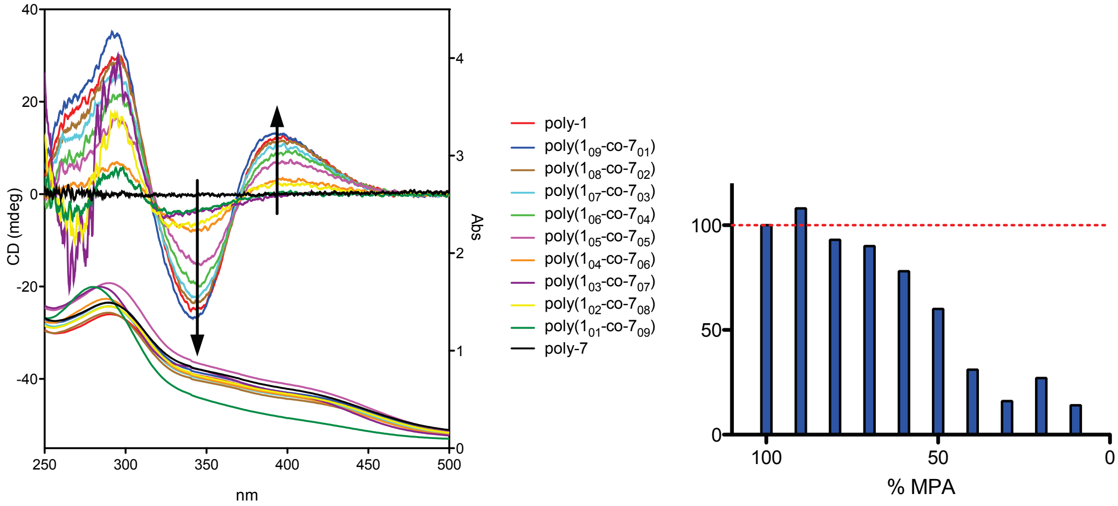

Figure S67. Left: CD and UV spectra and Right: % of CD signal compared to poly-**1** in of a solution of the poly(**1**-*co*-**7**) series (mru)/Mn^{2+} ratio of 1.0/0.5 (mol/mol) in $CDCl_3$. [poly(**1**-*co*-**7**)] = 0.3 mg/mL].

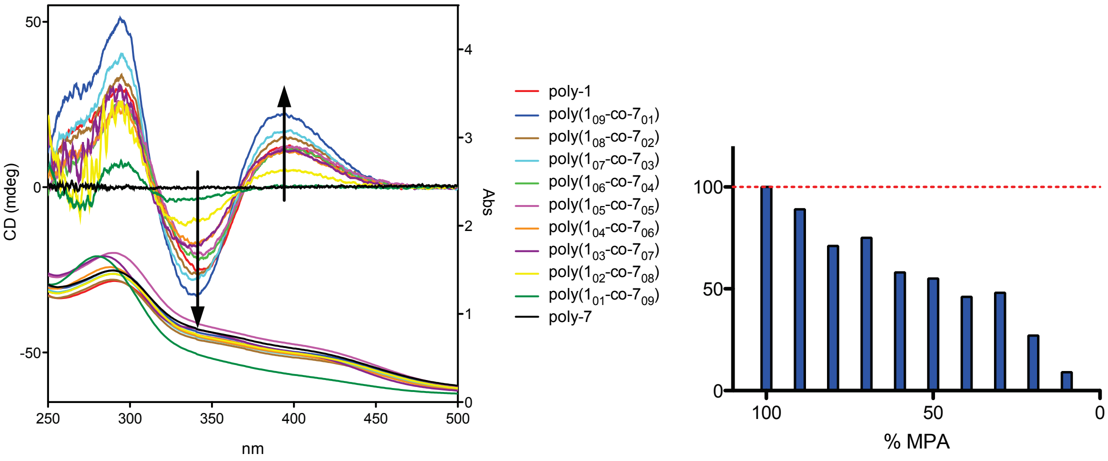

Figure S68. Left: CD and UV spectra and Right: % of CD signal compared to poly-**1** in of a solution of the poly(**1**-*co*-**7**) series (mru)/Ni^{2+} ratio of 1.0/0.5 (mol/mol) in $CDCl_3$. [poly(**1**-*co*-**7**)] = 0.3 mg/mL].

Chiral amplification in poly(1-*co*-7) with monovalent metal ions

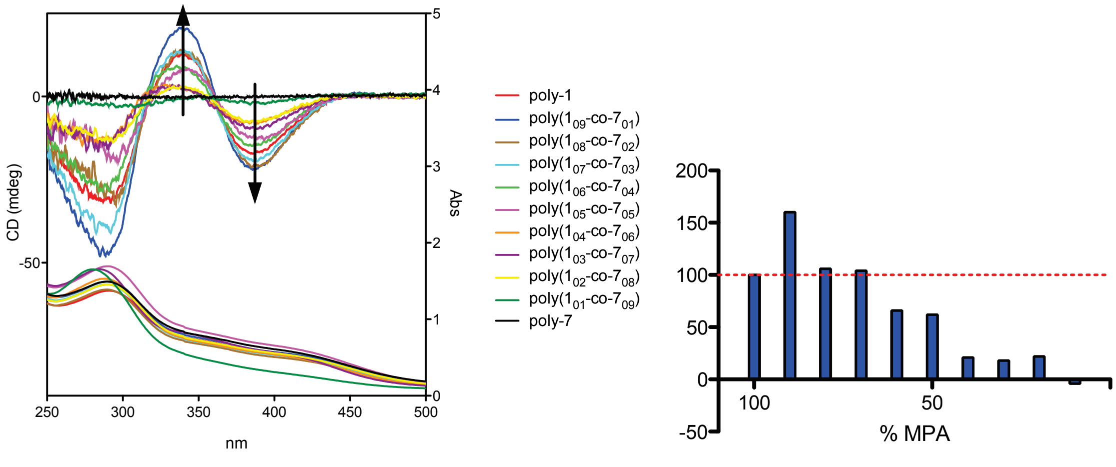

Figure S69. Left: CD and UV spectra and Right: % of CD signal compared to poly-**1** in of a solution of the poly(**1**-*co*-**7**) series (mru)/Ag^{+} ratio of 1.0/0.5 (mol/mol) in $CDCl_3$. [poly(**1**-*co*-**7**)] = 0.3 mg/mL].

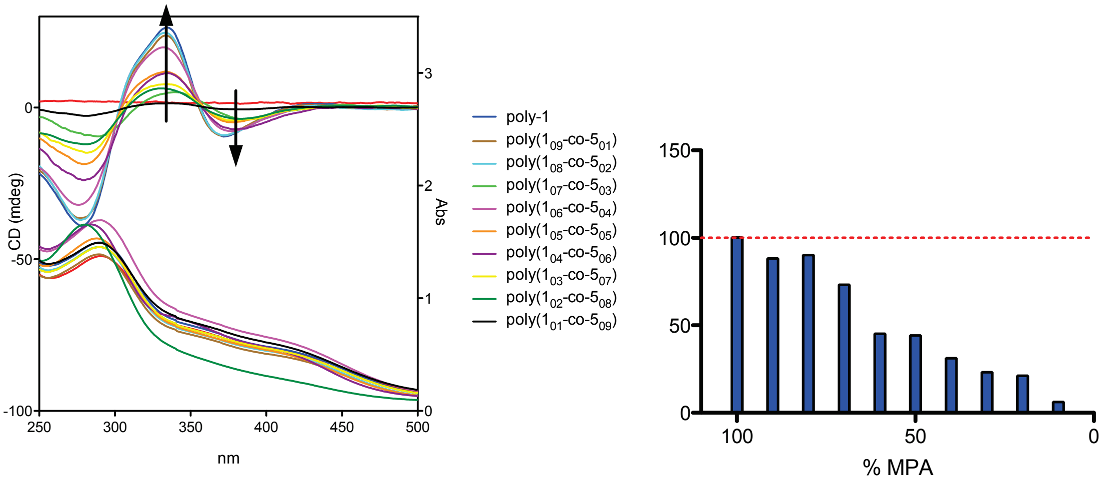

Figure S70. Left: CD and UV spectra and Right: % of CD signal compared to poly-**1** in of a solution of the poly(**1**-*co*-**7**) series (mru)/Li$^+$ ratio of 1.0/0.5 (mol/mol) in CDCl$_3$. [poly(**1**-*co*-**7**)] = 0.1 mg/mL].

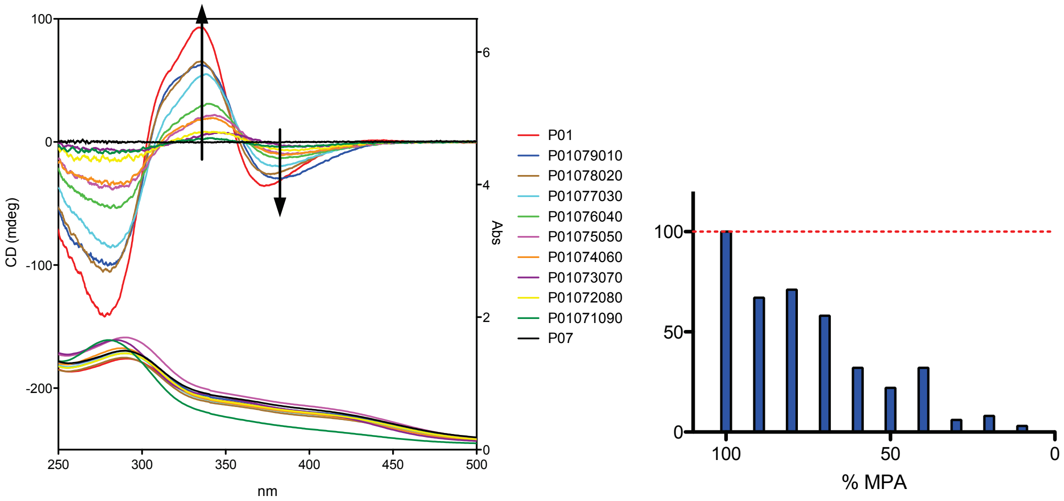

Figure S71. Left: CD and UV spectra and Right: % of CD signal compared to poly-**1** in of a solution of the poly(**1**-*co*-**7**) series (mru)/Li$^+$ ratio of 1.0/0.5 (mol/mol) in CDCl$_3$. [poly(**1**-*co*-**7**)] = 0.3 mg/mL].

Chiral amplification in poly(1-*co*-8) with divalent metal ions

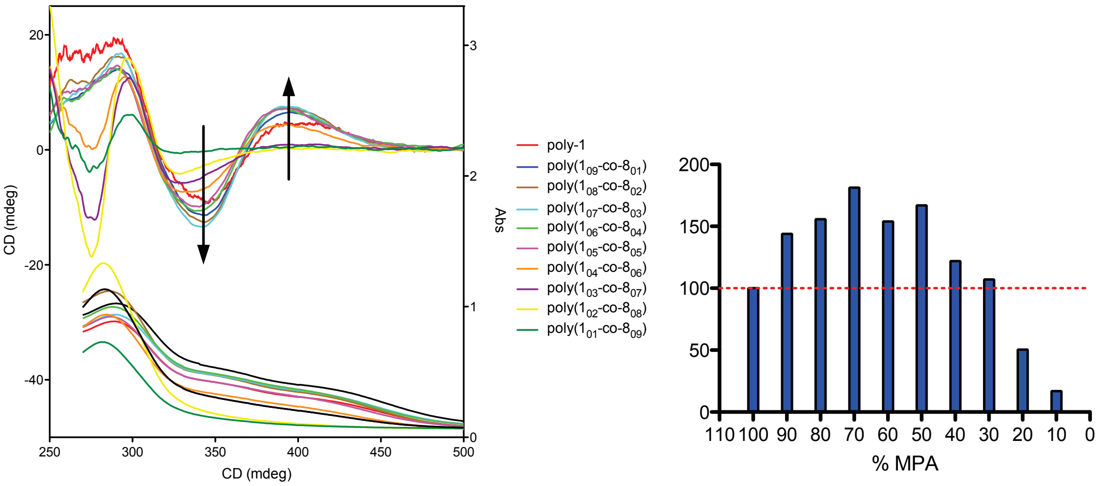

Figure S72. Left: CD and UV spectra and Right: % of CD signal compared to poly-**1** in of a solution of the poly(**1**-*co*-**8**) series (mru)/Ba^{2+} ratio of 1.0/0.5 (mol/mol) in $CDCl_3$. [poly(**1**-*co*-**8**)] = 0.2 mg/mL].

Chiral amplification in poly(1-*co*-8) with monovalent metal ions

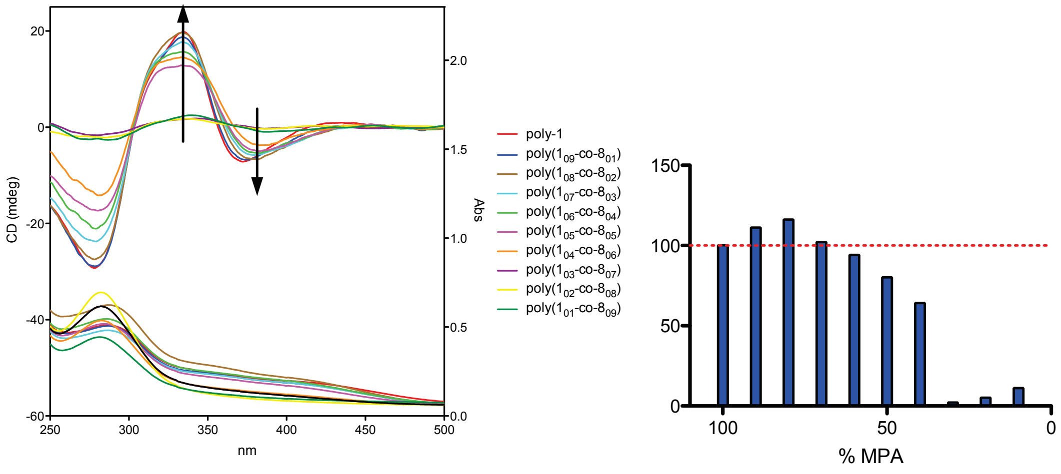

Figure S73. Left: CD and UV spectra and Right: % of CD signal compared to poly-**1** in of a solution of the poly(**1**-*co*-**8**) series (mru)/Li^{+} ratio of 1.0/0.5 (mol/mol) in $CDCl_3$. [poly(**1**-*co*-**8**)] = 0.3 mg/mL].

Chiral amplification in poly(1-*co*-9) with divalent metal ions

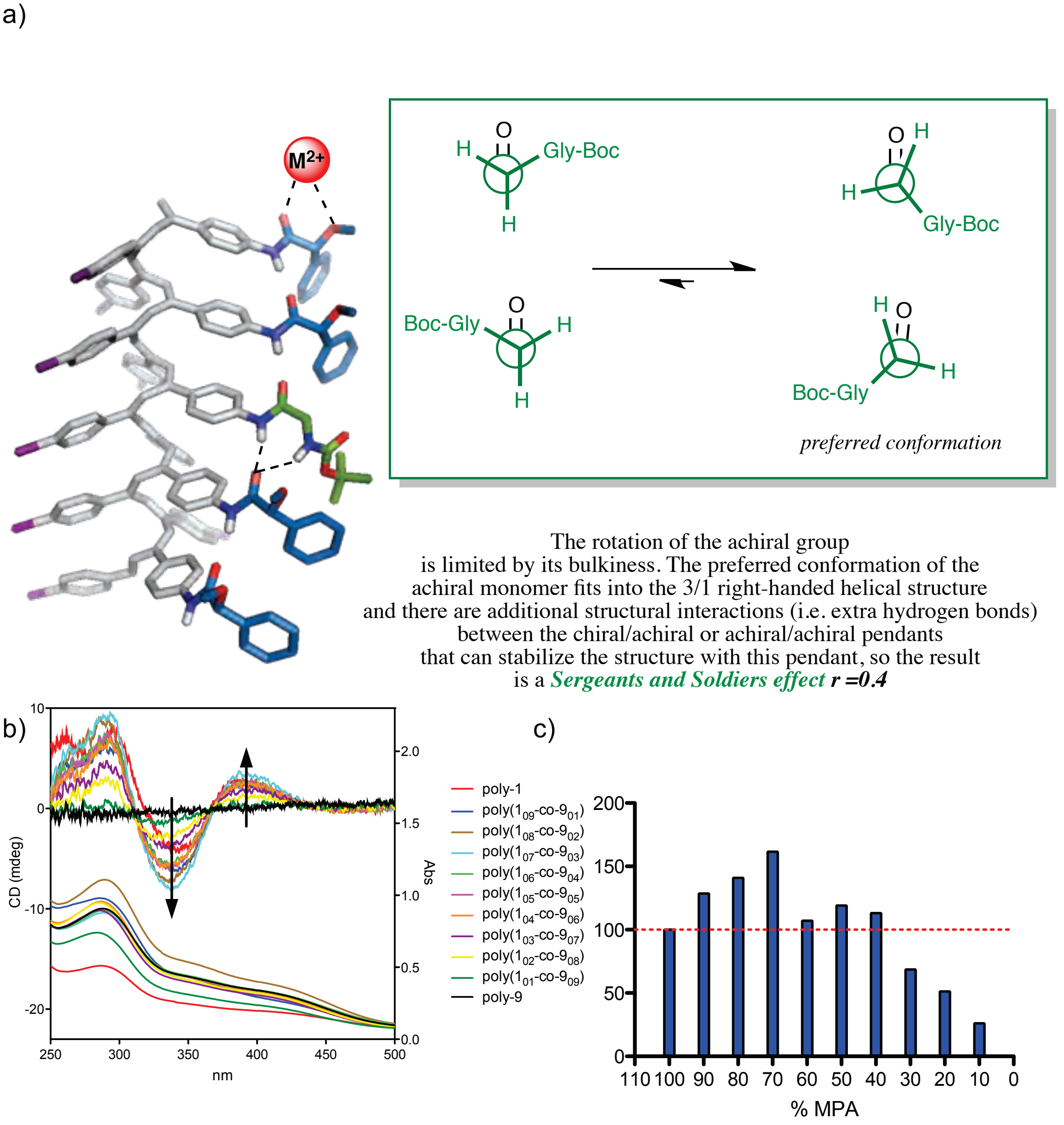

The rotation of the achiral group is limited by its bulkiness. The preferred conformation of the achiral monomer fits into the 3/1 right-handed helical structure and there are additional structural interactions (i.e. extra hydrogen bonds) between the chiral/achiral or achiral/achiral pendants that can stabilize the structure with this pendant, so the result is a ***Sergeants and Soldiers effect*** ***r =0.4***

Figure S74. a) Structural effect of replacing MPA pendants by monomer **09** in poly(**1**-*co*-**9**) and interaction with Ba^{2+}. b) CD and UV spectra .c) % of CD signal compared to poly-**1** in of a solution of the poly(**1**-*co*-**9**) series (mru)/Ba^{2+} ratio of 1.0/0.5 (mol/mol) in CDCl$_3$. [poly(**1**-*co*-**9**)] = 0.1 mg/mL].

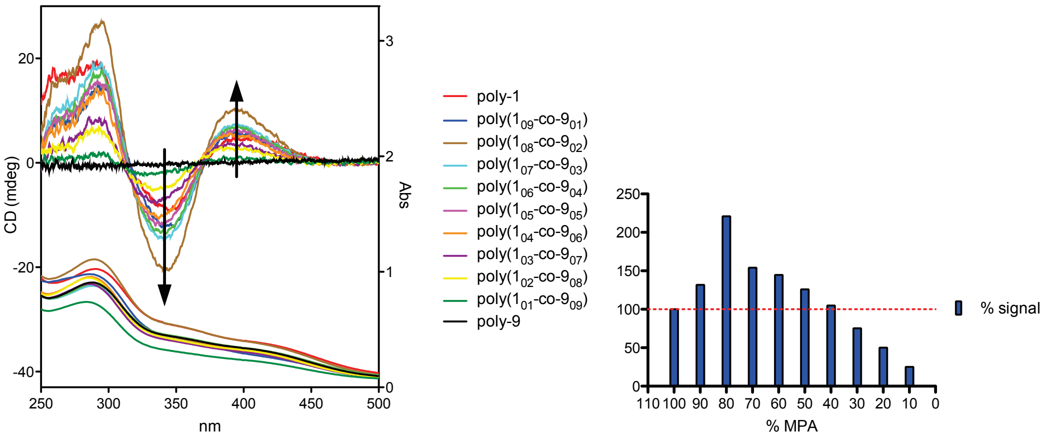

Figure S75. Left: CD and UV spectra and Right: % of CD signal compared to poly-**1** in a solution of the poly(**1**-*co*-**9**) series (mru)/Ba^{2+} ratio of 1.0/0.5 (mol/mol) in $CDCl_3$. [poly(**1**-*co*-**9**)] = 0.2 mg/mL].

Chiral amplification in poly(1-*co*-9) with monovalent metal ions

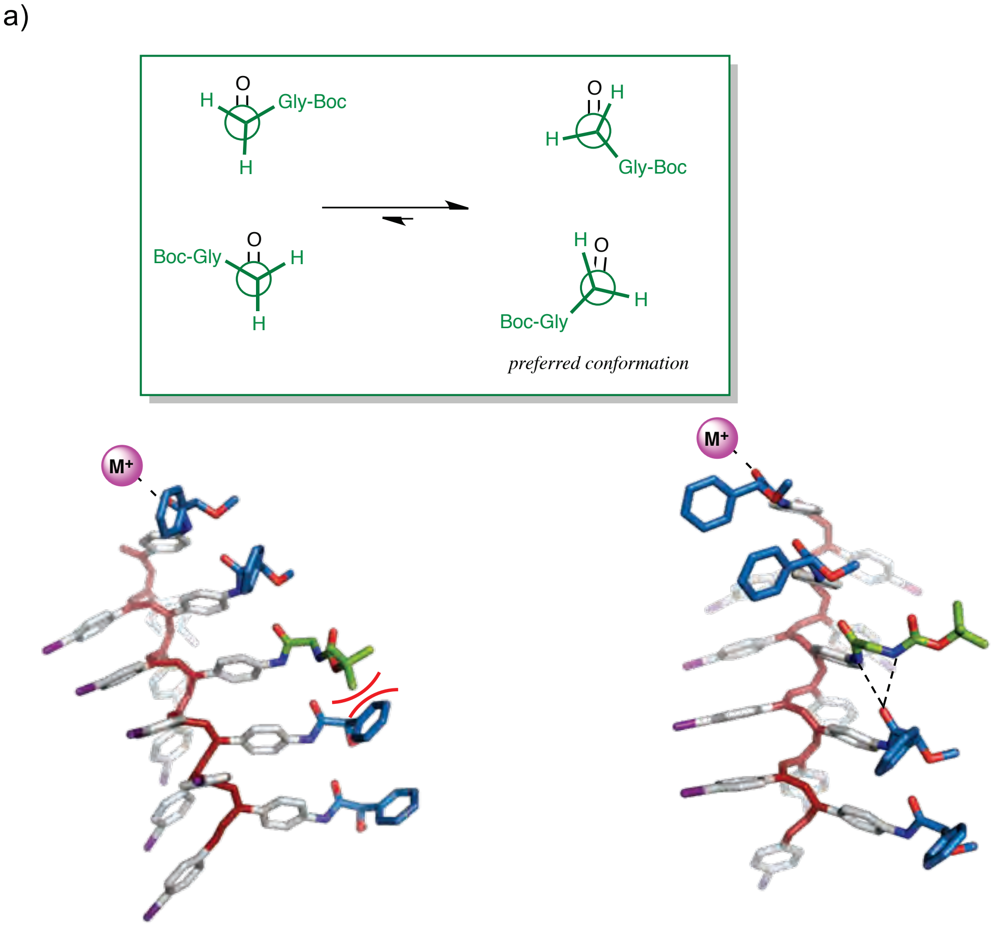

The preferred conformation for the achiral monomer **9**, that should promote the 3/1 helical structure, does not fit into the helical scaffold due to steric interactions with other MPA residues, so the pendant of monomer **9** adopts the alternative minimum energy conformation that places the alkyl chain oriented in a different direction than the MPA pendants, and therefore ***does not promote the Sergeants and Soldiers effect*** **r = 1**

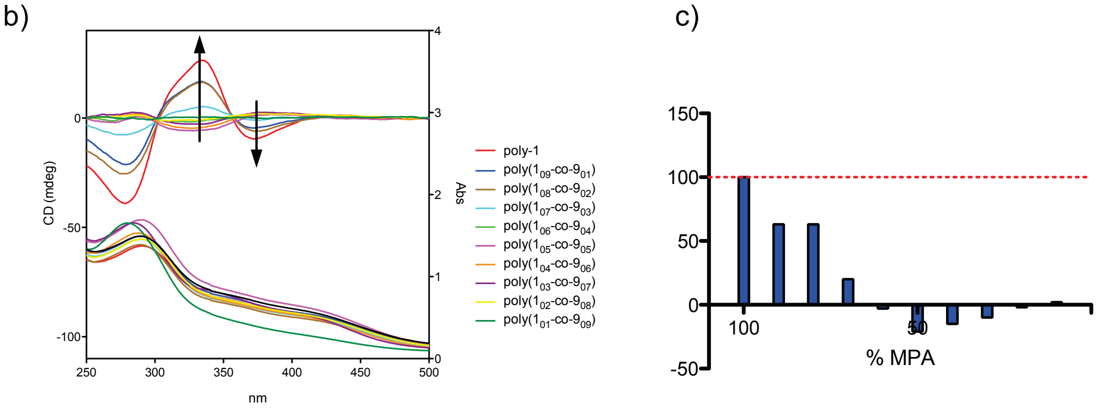

Figure S76. a) Structural effect of replacing MPA pendants by monomer **09** **i**n poly(**1**-*co*-**9**) and interaction with Li^+. b) CD and UV spectra. c) % of CD signal compared to poly-**1** in of a solution of the poly(**1**-*co*-**9**) series (mru)/Li^+ ratio of 1.0/0.5 (mol/mol) in $CDCl_3$. [poly(**1**-*co*-**9**)] = 0.1 mg/mL].

Additional considerations on the complexation of the copolymers

The structural similarity between chiral and achiral pendants allows some complexation of the metal ions with the achiral “Soldiers” (as shown by IR). Nevertheless, this fact does not seem to play any role neither on the amplification of chirality nor on the “Sergeants and Soldiers effect” of these copolymers because homopolymers prepared from **3-9** (“all achiral Soldier” polymers) showed a null CD before and after addition of the metal salt. Therefore, any change in the helical sense of the copolymer upon addition of the ion has to be originated by complexation with the “chiral Soldiers”.

Aggregation and Encapsulation Studies

Dynamic Light Scattering Studies

DLS measurements were performed on a Malvern Nano ZS (Malvern Instruments, U.K.), operating at 633 nm with a 173° scattering angle. Samples were measured at a final concentration of 0.1 mg/mL diluted with $CHCl_3$ with 0.5 equiv. of $Ba(ClO_4)_2$. These studies clearly indicate that the HPMCs form aggregates with a defined structure. The size of these aggregates can be modulated by the addition of different metals or different amounts of the metal.

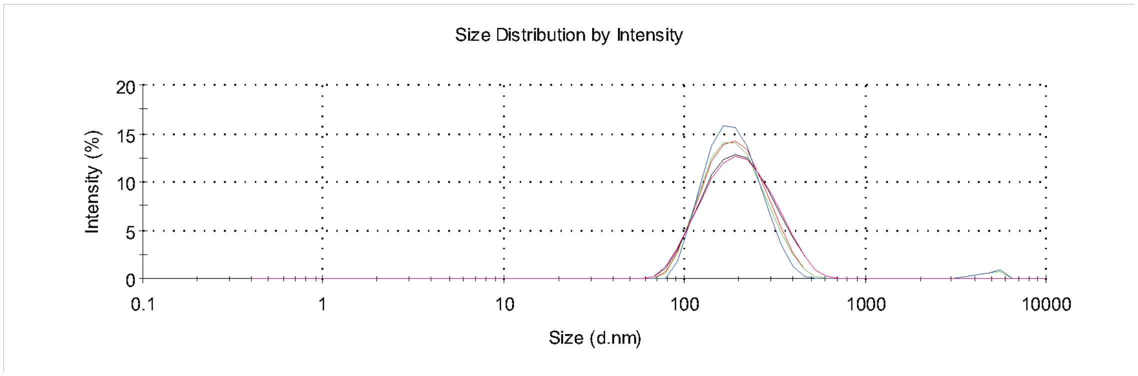

Figure S77. DLS measurements for poly-**1** (mru)/Ba^{2+} ratio of 1.0/0.5 (mol/mol).

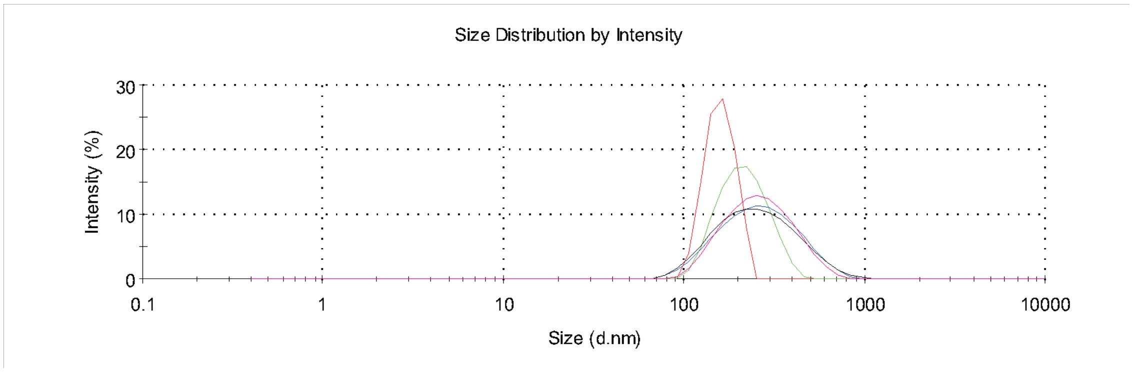

Figure S78. DLS measurements for poly($\mathbf{1}_{0.7}$-*co*-$\mathbf{8}_{0.3}$) (mru)/Ba^{2+} ratio of 1.0/0.5 (mol/mol).

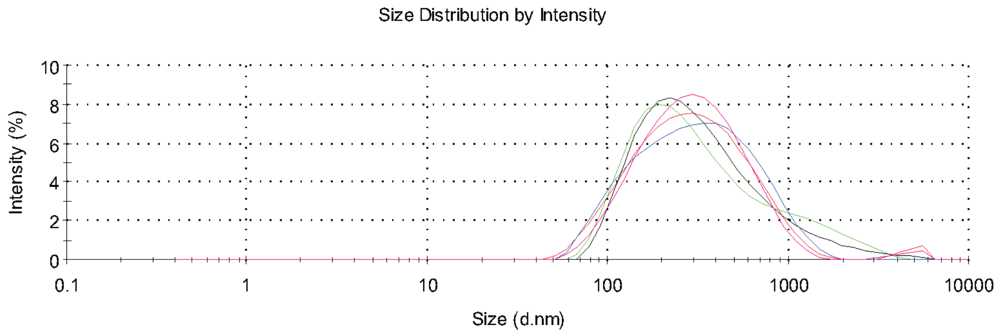

Figure S79. DLS measurements for poly($\mathbf{1}_{0.4}$-*co*-$\mathbf{8}_{0.6}$) (mru)/Ba^{2+} ratio of 1.0/0.5 (mol/mol).

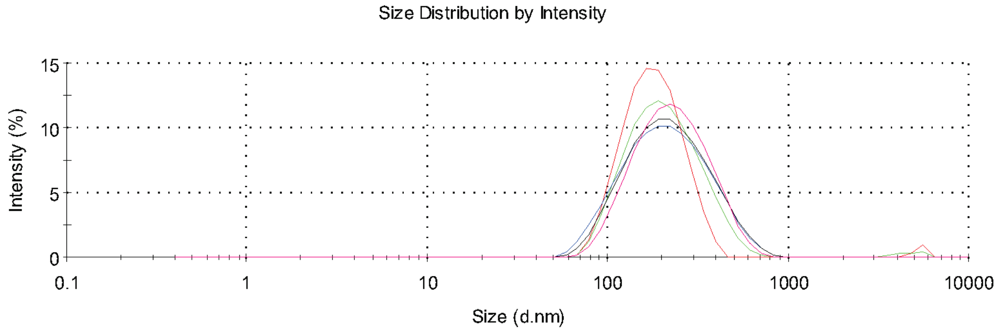

Figure S80. DLS measurements for poly($\mathbf{1}_{0.5}$-*co*-$\mathbf{8}_{0.5}$) (mru)/Ba^{2+} ratio of 1.0/0.5 (mol/mol).

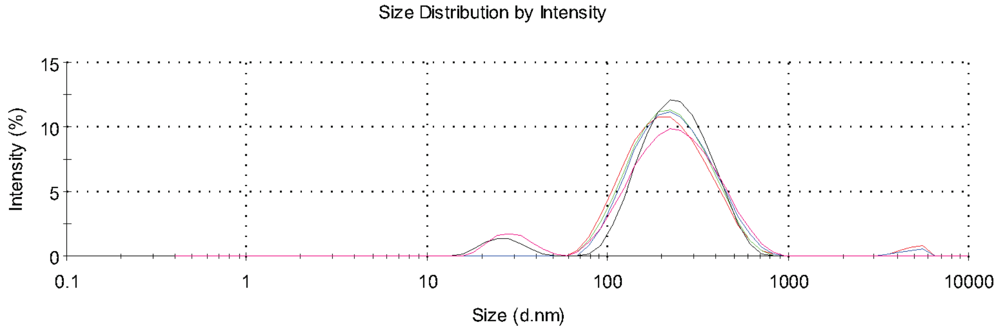

Figure S81. DLS measurements for poly($\mathbf{1}_{0.4}$-*co*-$\mathbf{8}_{0.6}$) (mru)/Ba^{2+} ratio of 1.0/0.5 (mol/mol).

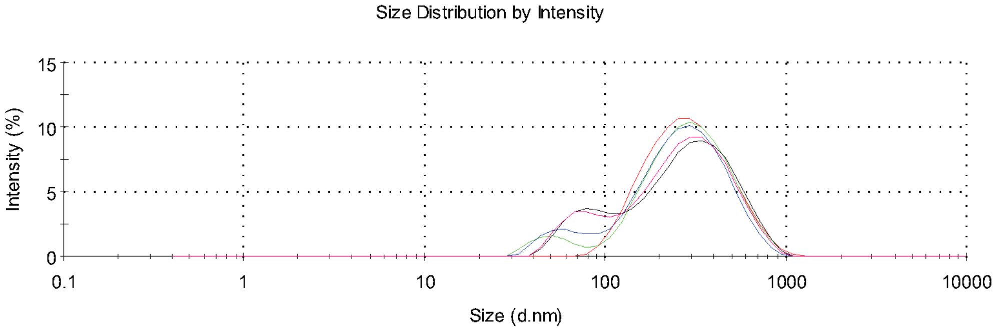

Figure S82. DLS measurements for poly($\mathbf{1}_{0..3}$-*co*-$\mathbf{8}_{0.7}$) (mru)/Ba^{2+} ratio of 1.0/0.5 (mol/mol).

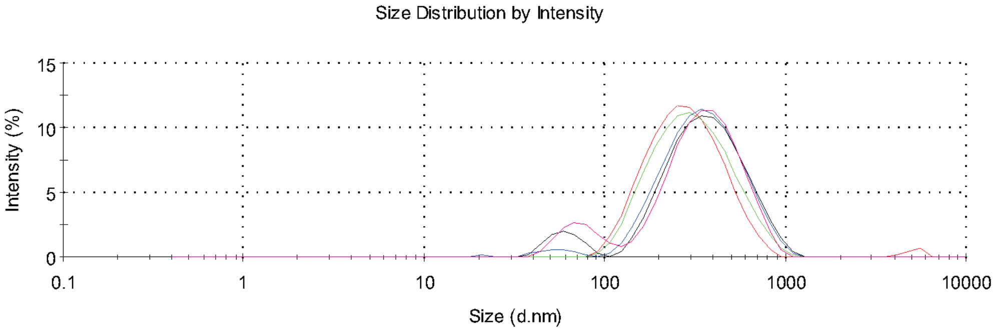

Figure S83. DLS measurements for poly($\mathbf{1}_{0.1}$-*co*-$\mathbf{8}_{0.9}$) (mru)/Ba^{2+} ratio of 1.0/0.5 (mol/mol).

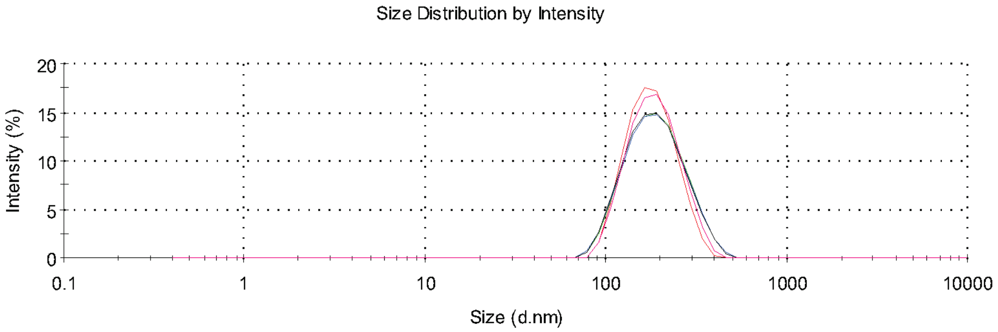

Figure S84. DLS measurements for poly($\mathbf{1}_{0.9}$-*co*-$\mathbf{6}_{0.1}$) (mru)/Ba^{2+} ratio of 1.0/0.5 (mol/mol).

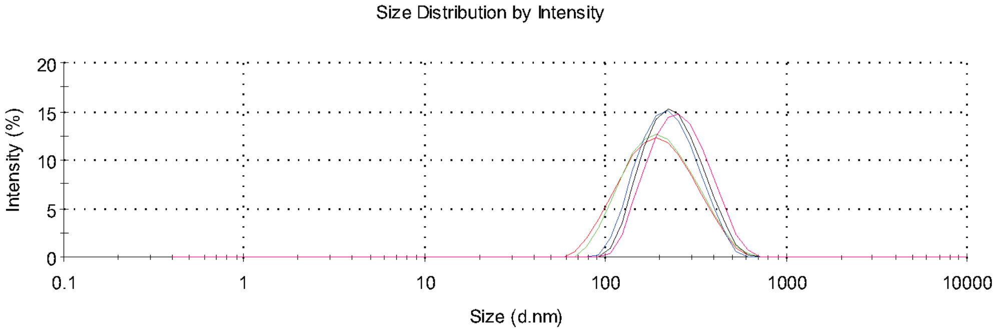

Figure S85. DLS measurements for poly($\mathbf{1}_{0.8}$-*co*-$\mathbf{6}_{0.2}$) (mru)/Ba^{2+} ratio of 1.0/0.5 (mol/mol).

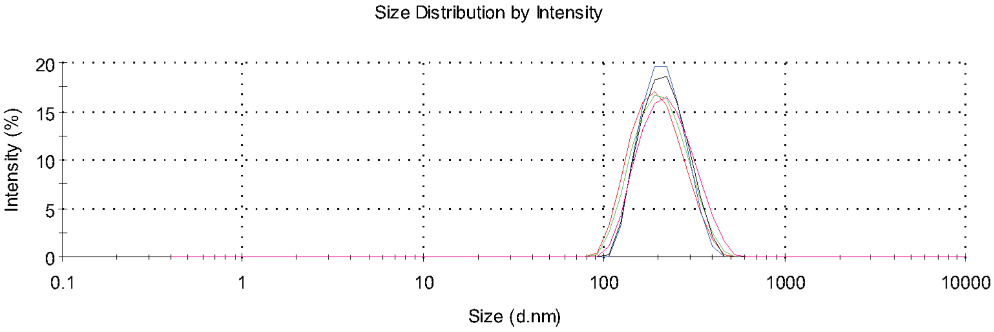

Figure S86. DLS measurements for poly($\mathbf{1}_{0.7}$-*co*-$\mathbf{6}_{0.3}$) (mru)/Ba^{2+} ratio of 1.0/0.5 (mol/mol).

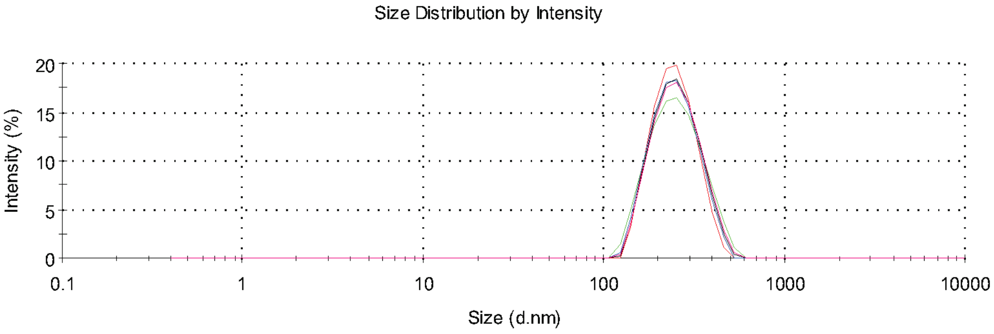

Figure S87. DLS measurements for poly($\mathbf{1}_{0.6}$-*co*-$\mathbf{6}_{0.4}$) (mru)/Ba^{2+} ratio of 1.0/0.5 (mol/mol).

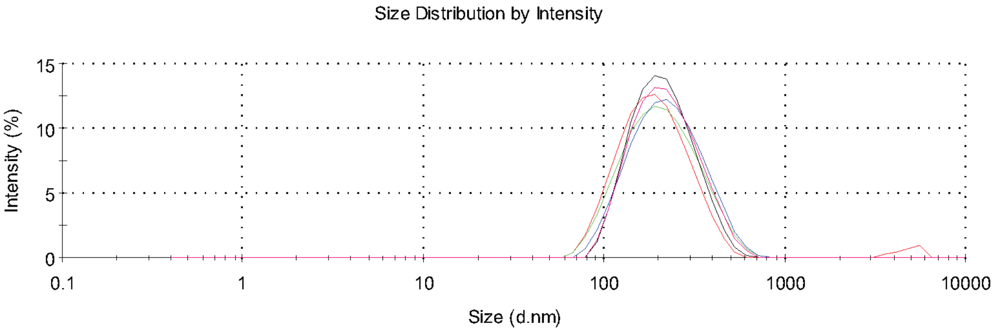

Figure S88. DLS measurements for poly($\mathbf{1}_{0.5}$-*co*-$\mathbf{6}_{0.5}$) (mru)/Ba^{2+} ratio of 1.0/0.5 (mol/mol).

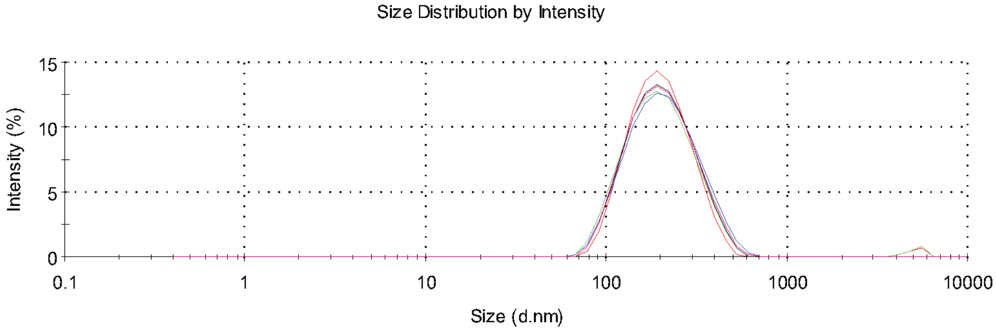

Figure S89. DLS measurements for poly($\mathbf{1}_{0.4}$-*co*-$\mathbf{6}_{0.6}$) (mru)/Ba^{2+} ratio of 1.0/0.5 (mol/mol).

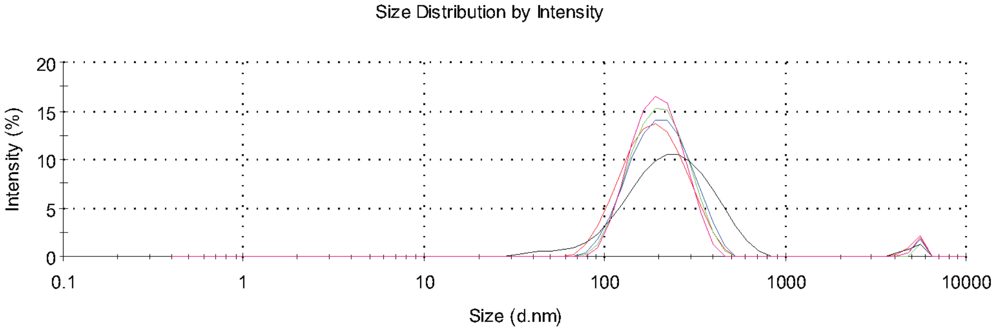

Figure S90. DLS measurements for poly($\mathbf{1}_{0.3}$-*co*-$\mathbf{6}_{0.7}$) (mru)/Ba^{2+} ratio of 1.0/0.5 (mol/mol).

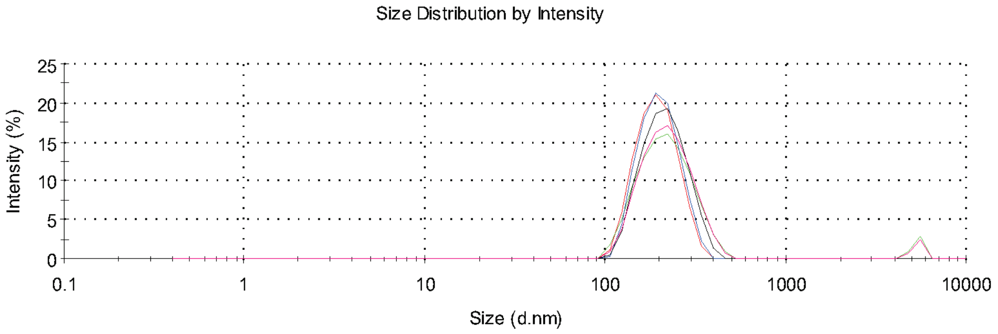

Figure S91. DLS measurements for poly($\mathbf{1}_{0.2}$-*co*-$\mathbf{6}_{0.8}$) (mru)/Ba^{2+} ratio of 1.0/0.5 (mol/mol).

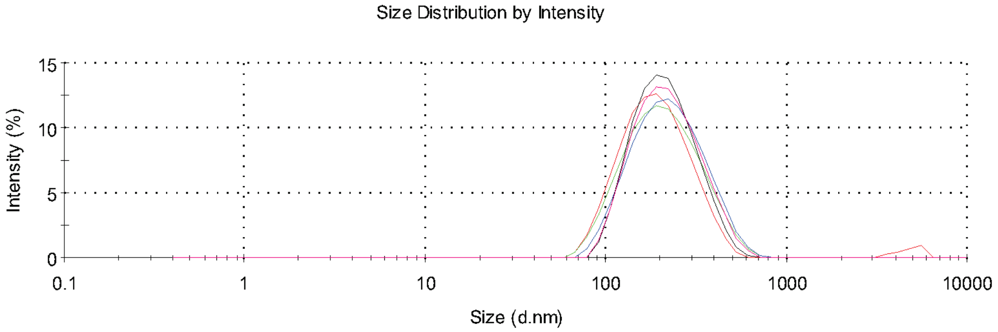

Figure S92. DLS measurements for poly($\mathbf{1}_{0.1}$-*co*-$\mathbf{6}_{0.9}$) (mru)/Ba^{2+} ratio of 1.0/0.5 (mol/mol).

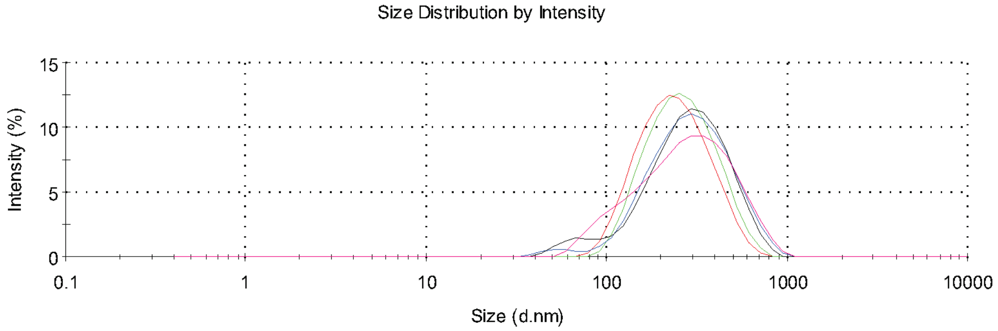

Figure S93. DLS measurements for poly($\mathbf{1}_{0.9}$-*co*-$\mathbf{7}_{0.1}$) (mru)/Ba^{2+} ratio of 1.0/0.5 (mol/mol).

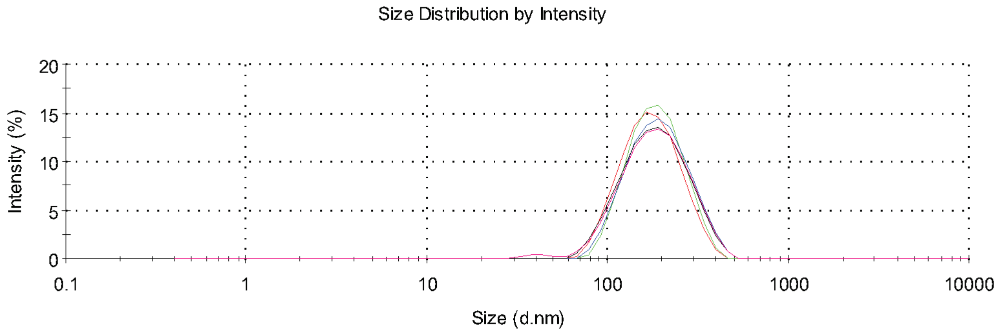

Figure S94. DLS measurements for poly($\mathbf{1}_{0.8}$-*co*-$\mathbf{7}_{0.2}$) (mru)/Ba^{2+} ratio of 1.0/0.5 (mol/mol).

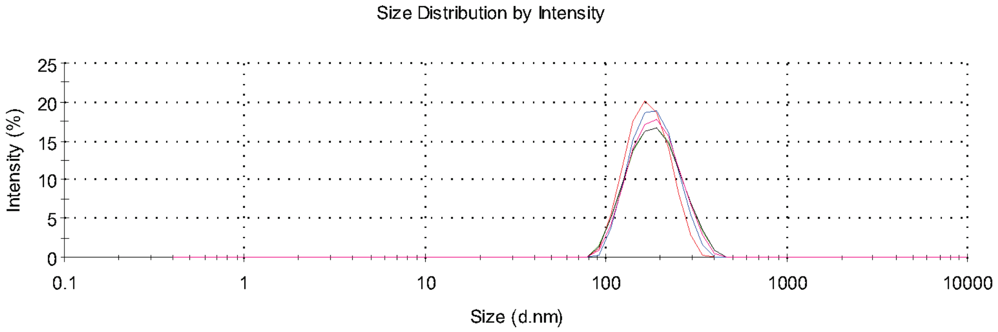

Figure S95. DLS measurements for poly($\mathbf{1}_{0.7}$-*co*-$\mathbf{7}_{0.3}$) (mru)/Ba^{2+} ratio of 1.0/0.5 (mol/mol).

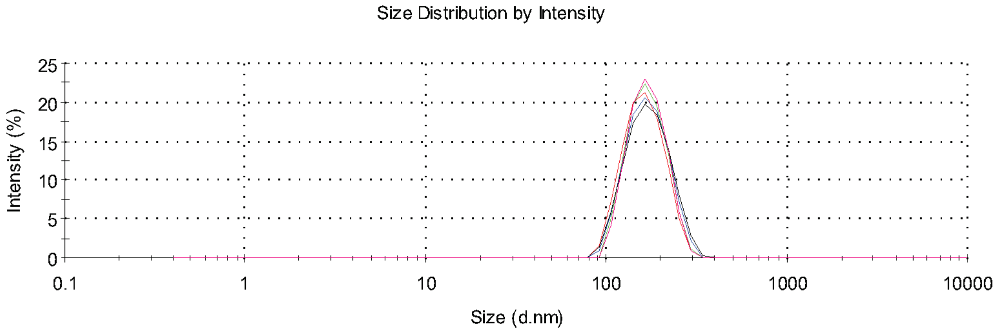

Figure S96. DLS measurements for poly($\mathbf{1}_{0.6}$-*co*-$\mathbf{7}_{0.4}$) (mru)/Ba^{2+} ratio of 1.0/0.5 (mol/mol).

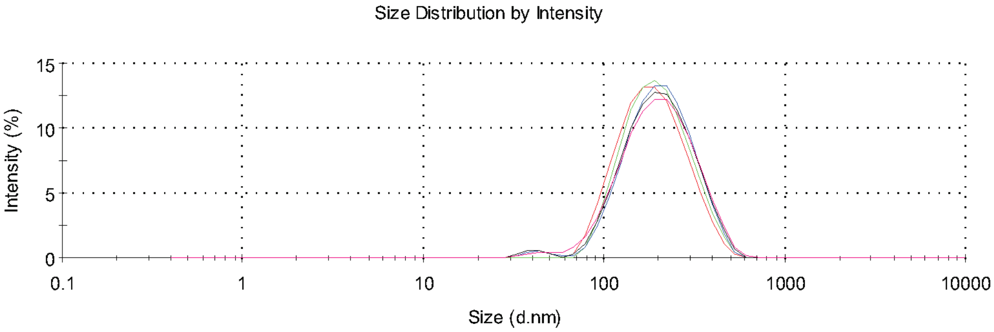

Figure S97. DLS measurements for poly($\mathbf{1}_{0.5}$-*co*-$\mathbf{7}_{0.5}$) (mru)/Ba^{2+} ratio of 1.0/0.5 (mol/mol).

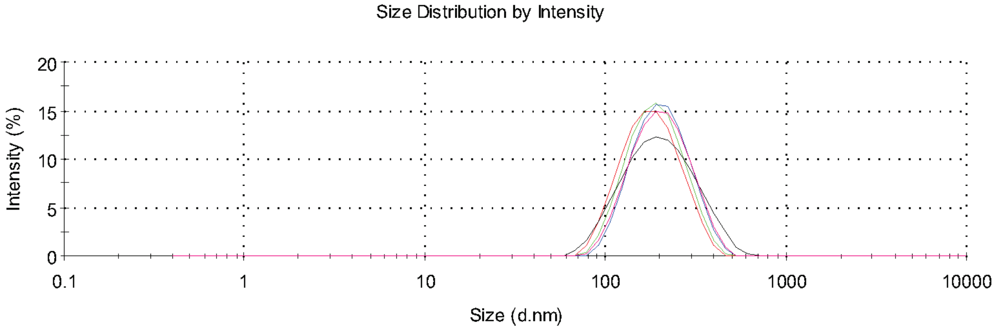

Figure S98. DLS measurements for poly($\mathbf{1}_{0.4}$-*co*-$\mathbf{7}_{0.6}$) (mru)/Ba^{2+} ratio of 1.0/0.5 (mol/mol).

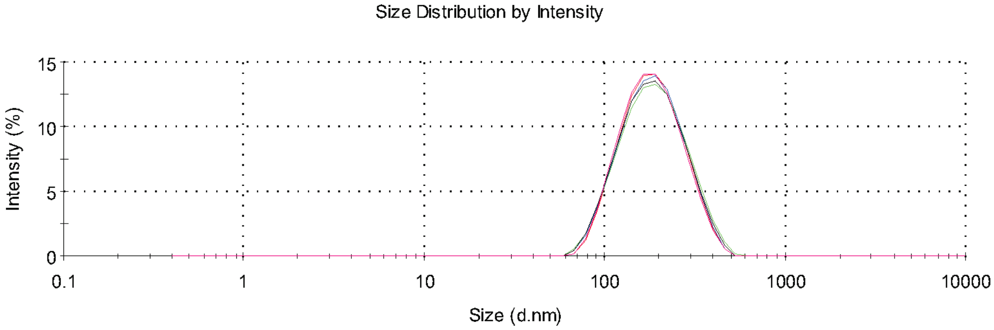

Figure S99. DLS measurements for poly($\mathbf{1}_{0.3}$-*co*-$\mathbf{7}_{0.7}$) (mru)/Ba^{2+} ratio of 1.0/0.5 (mol/mol).

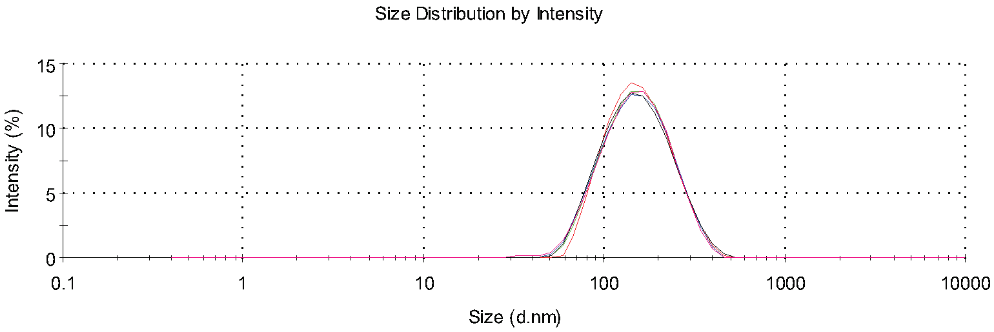

Figure S100. DLS measurements for poly($\mathbf{1}_{0.2}$-*co*-$\mathbf{7}_{0.8}$) (mru)/Ba^{2+} ratio of 1.0/0.5 (mol/mol).

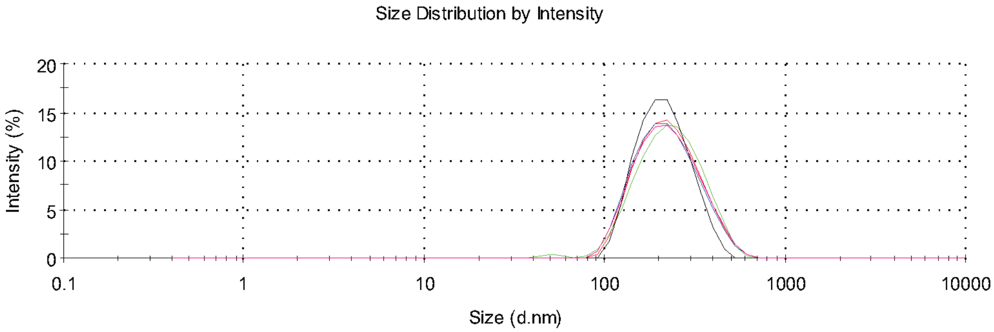

Figure S101. DLS measurements for poly($\mathbf{1}_{0.1}$-*co*-$\mathbf{7}_{0.9}$) (mru)/Ba^{2+} ratio of 1.0/0.5 (mol/mol).

Confocal Microscopy Encapsulation Studies

Images were performed on a Leica TSC-SP2 microscope. Polymer (0.1 mg/mL) with the correspondent fluorescent dyes (5,6-carboxyfluorescein, rhodamine B isothiocyanate) or Quantum Dots [Lumidot CdSe/ZnS (590 nm QD)] solution (10 μL/mL) in $CHCl_3$ and after stirring for 2 min, 5 equivalents of a barium perchlorate metal salt were added to generate the nanospheres. 10 μL of this mixture were dropped in the sample holder.

5,6-Carboxyfluorescein

Figure S102. Confocal images for poly($\mathbf{1}_{0.8}$-*co*-$\mathbf{7}_{0.2}$) (mru)/Ba^{2+} ratio of 1/5 (mol/mol). Left: emission at 505-540 nm, corresponds to polymer and carboxyfluorescein. Middle: emission at 600-700 nm. Right: Sum of the emission at 505-540 plus the emission at 600-700 nm.

Figure S103. Confocal images for poly($\mathbf{1}_{0.4}$-*co*-$\mathbf{7}_{0.6}$) (mru)/Ba^{2+} ratio of 1/5 (mol/mol). Left: emission at 505-540 nm, corresponds to polymer and carboxyfluorescein. Middle: emission at 600-700 nm. Right: Sum of the emission at 505-540 plus the emission at 600-700 nm.

Figure S104. Confocal images for poly($\mathbf{1}_{0.2}$-*co*-$\mathbf{7}_{0.8}$) (mru)/Ba^{2+} ratio of 1/5 (mol/mol). Left: emission at 505-540 nm, corresponds to polymer and carboxyfluorescein. Middle: emission at 600-700 nm. Right: Sum of the emission at 505-540 plus the emission at 600-700 nm.

Figure S105. Confocal images for poly($\mathbf{1}_{0.1}$-*co*-$\mathbf{7}_{0.9}$) (mru)/Ba^{2+} ratio of 1/5 (mol/mol). Left: emission at 505-540 nm, corresponds to polymer and carboxyfluorescein. Middle: emission at 600-700 nm. Right: Sum of the emission at 505-540 plus the emission at 600-700 nm.

Rhodamine B isothiocyanate

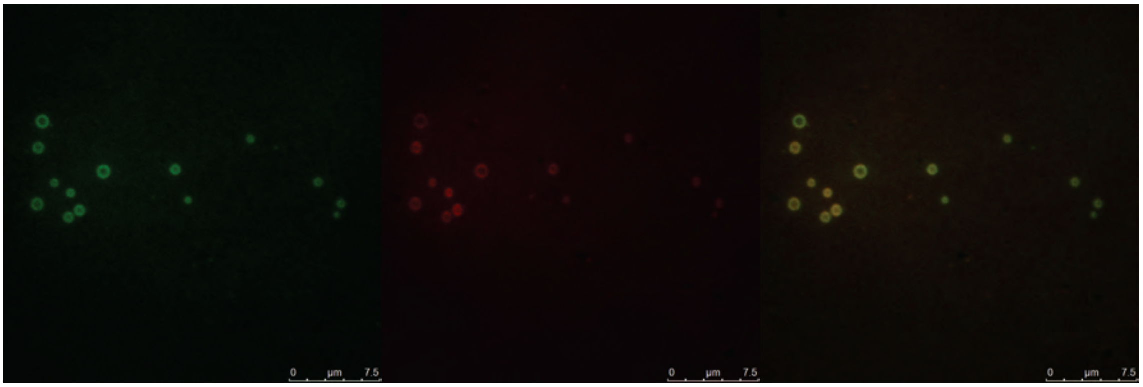

Figure S106. Confocal images for poly($\mathbf{1}_{0.8}$-*co*-$\mathbf{7}_{0.2}$) (mru)/Ba^{2+} ratio of 1/5 (mol/mol). Left: emission at 505-540 nm, corresponds to polymer. Middle: emission at 600-700 nm corresponds to rhodamine. Right: Sum of the emission at 505-540 plus the emission at 600-700 nm.

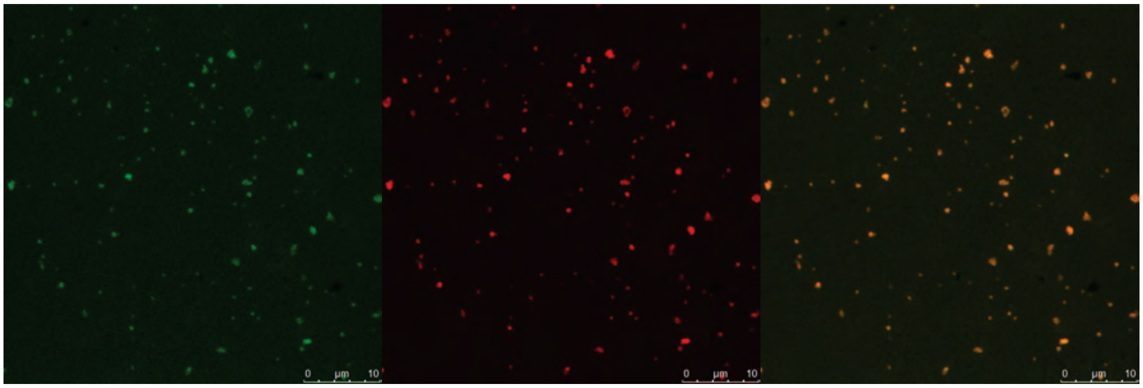

Figure S107. Confocal images for poly($\mathbf{1}_{0.4}$-*co*-$\mathbf{7}_{0.6}$) (mru)/Ba^{2+} ratio of 1/5 (mol/mol). Left: emission at 505-540 nm, corresponds to polymer. Middle: emission at 600-700 nm corresponds to rhodamine. Right: Sum of the emission at 505-540 plus the emission at 600-700 nm.

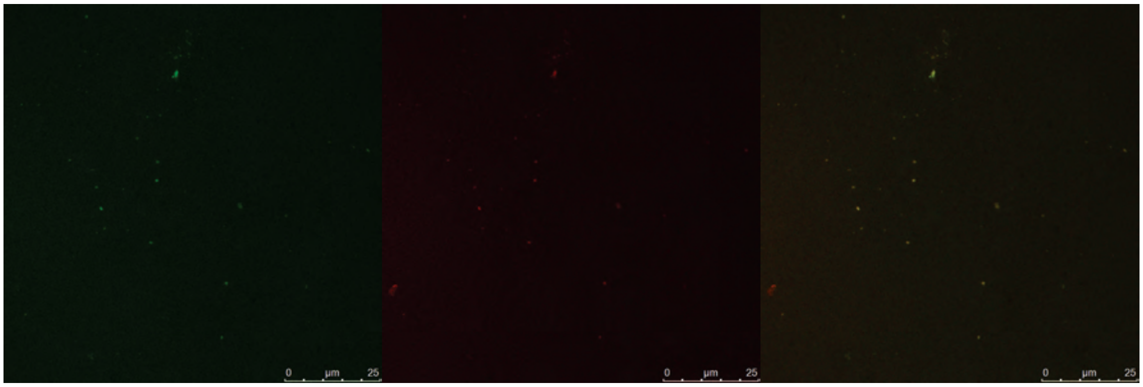

Figure S108. Confocal images for poly($\mathbf{1}_{0.2}$-*co*-$\mathbf{7}_{0.8}$) (mru)/Ba^{2+} ratio of 1/5 (mol/mol). Left: emission at 505-540 nm, corresponds to polymer. Middle: emission at 600-700 nm corresponds to rhodamine. Right: Sum of the emission at 505-540 plus the emission at 600-700 nm.

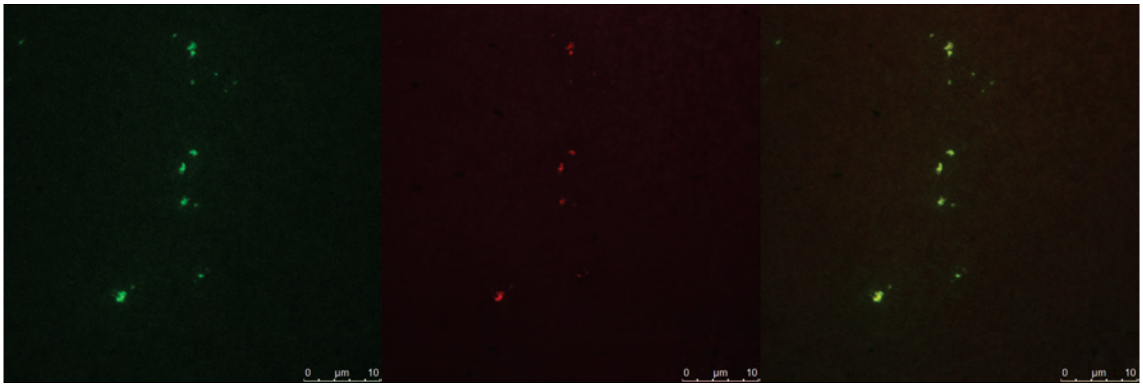

Figure S109. Confocal images for poly($\mathbf{1}_{0.1}$-*co*-$\mathbf{7}_{0.9}$) (mru)/Ba^{2+} ratio of 1/5 (mol/mol). Left: emission at 505-540 nm, corresponds to polymer. Middle: emission at 600-700 nm corresponds to rhodamine. Right: Sum of the emission at 505-540 plus the emission at 600-700 nm.

Quantum Dots [Lumidot CdSe/ZnS (590 nm QD)]

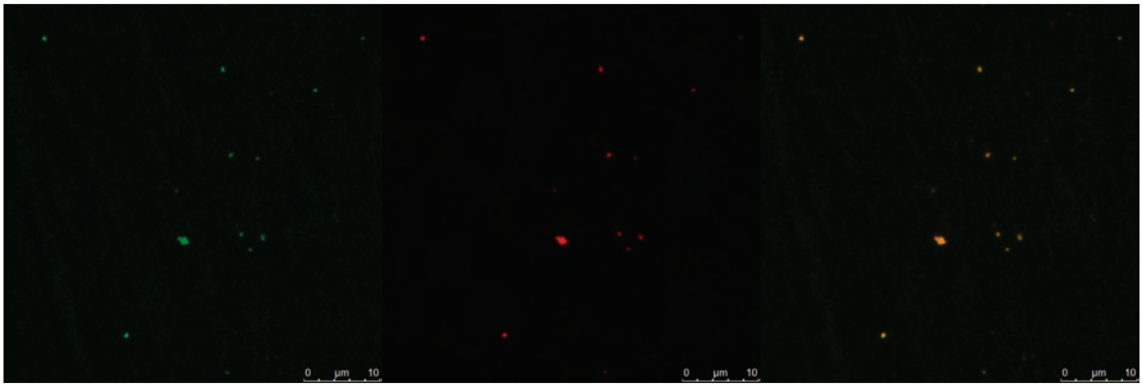

Figure S110. Confocal images for poly($\mathbf{1}_{0.8}$-*co*-$\mathbf{7}_{0.2}$) (mru)/Ba^{2+} ratio of 1/5 (mol/mol). Left: emission at 505-540 nm, corresponds to polymer. Middle: emission at 600-700 nm corresponds to QD. Right: Sum of the emission at 505-540 plus the emission at 600-700 nm.

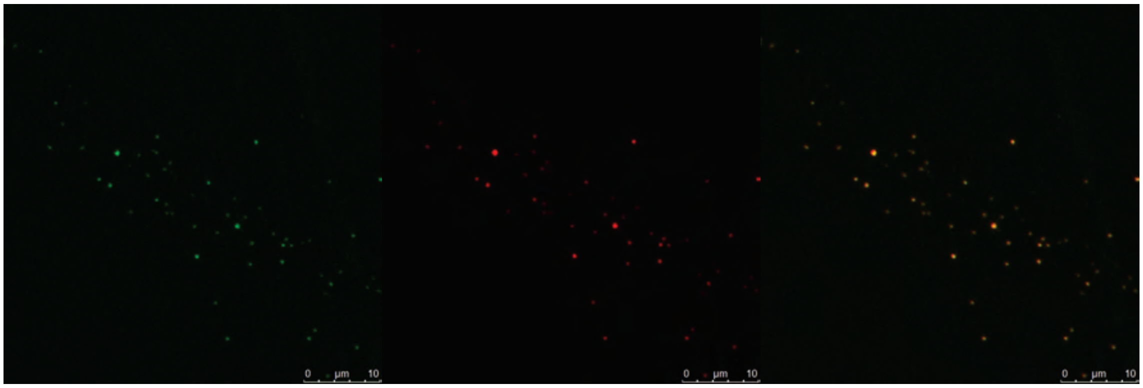

Figure S111. Confocal images for poly($\mathbf{1}_{0.4}$-*co*-$\mathbf{7}_{0.6}$) (mru)/Ba^{2+} ratio of 1/5 (mol/mol). Left: emission at 505-540 nm, corresponds to polymer. Middle: emission at 600-700 nm corresponds to QD. Right: Sum of the emission at 505-540 plus the emission at 600-700 nm.

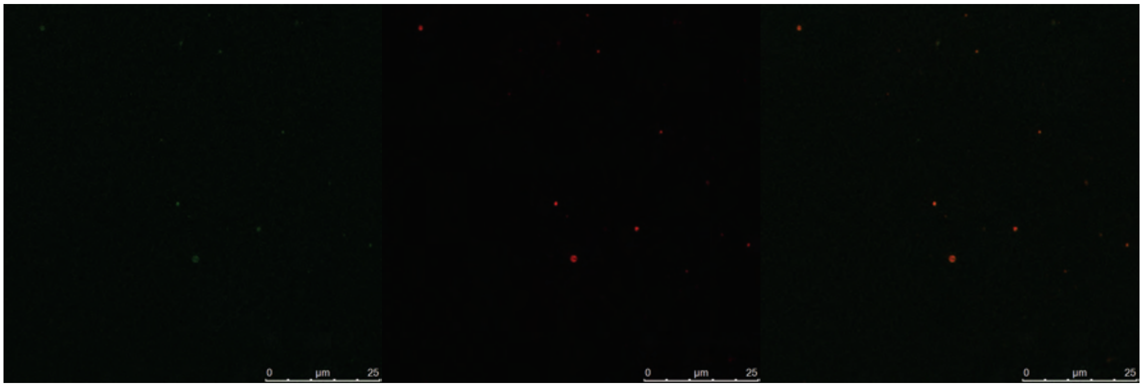

Figure S112. Confocal images for poly($\mathbf{1}_{0.2}$-*co*-$\mathbf{7}_{0.8}$) (mru)/Ba^{2+} ratio of 1/5 (mol/mol). Left: emission at 505-540 nm, corresponds to polymer. Middle: emission at 600-700 nm corresponds to QD. Right: Sum of the emission at 505-540 plus the emission at 600-700 nm.

Surface Electronic Microscopy Studies

SEM measurements were performed on a LEO-435VP electron microscope. A drop of a solution of polymer with 0.5 equivalents of a barium perchlorate (0.1 mg/mL) was settled on a silicon wafer chip, and allowed to dry at rt for 12 h.

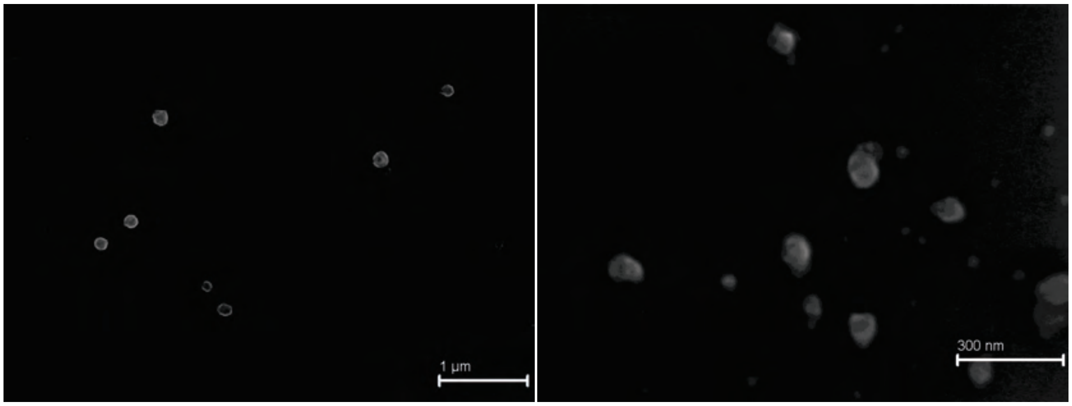

Figure S113. SEM images of nanospheres formed by poly($\mathbf{1}_{08}$-*co*-$\mathbf{7}_{02}$) (mru)/Ba^{2+} ratio of 1.0/0.5 (mol/mol) (left) and poly($\mathbf{1}_{0.4}$-*co*-$\mathbf{7}_{0.6}$) (mru)/Ba^{2+} ratio of 1.0/0.5 (mol/mol) (right).

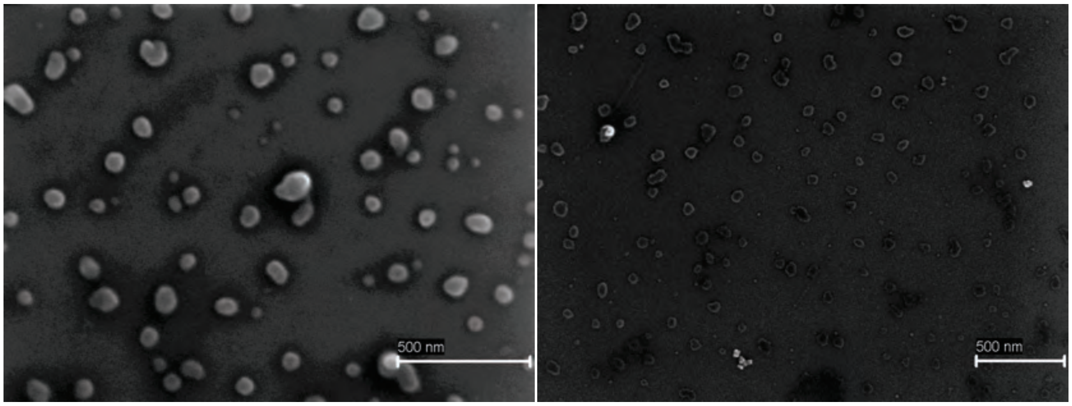

Figure S114. SEM images of nanospheres formed by poly($\mathbf{1}_{0.2}$-*co*-$\mathbf{7}_{0.8}$) (mru)/Ba^{2+} ratio of 1.0/0.5 (mol/mol) (left) and poly($\mathbf{1}_{0.1}$-*co*-$\mathbf{7}_{0.9}$) (mru)/Ba^{2+} ratio of 1.0/0.5 (mol/mol) (right).

Transmision Electronic Microscopy Studies

TEM measurements were performed on a Philips CM-12 electron microscope. A drop of a solution of polymer in $CHCl_3$ with 0.5 equivalents of barium perchlorate (0.1 mg/mL) was settled on a carbon grid, and allowed to dry at rt for 12 h.

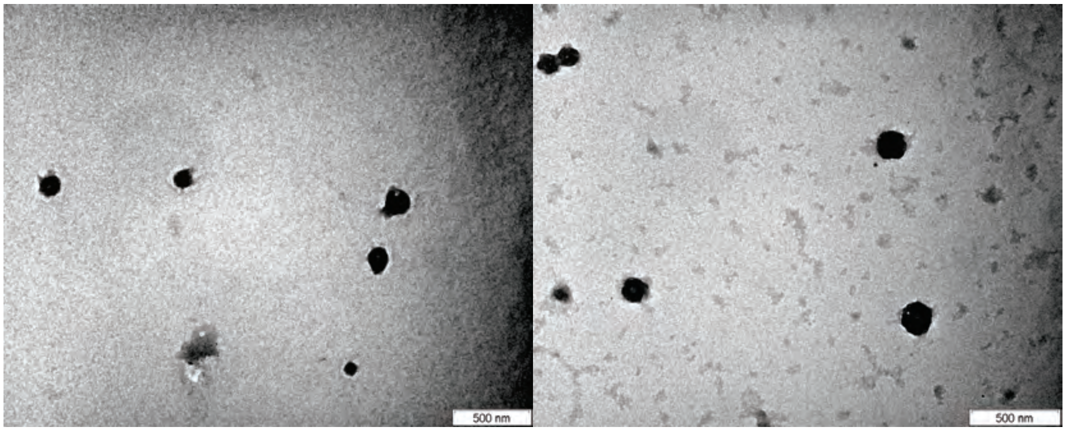

Figure S115. TEM images of nanospheres formed by poly($\mathbf{1}_{0.8}$-*co*-$\mathbf{7}_{0.2}$) (mru)/Ba^{2+} ratio of 1.0/0.5 (mol/mol) (left) and poly($\mathbf{1}_{0.4}$-*co*-$\mathbf{7}_{0.6}$) (mru)/Ba^{2+} ratio of 1.0/0.5 (mol/mol) (right).

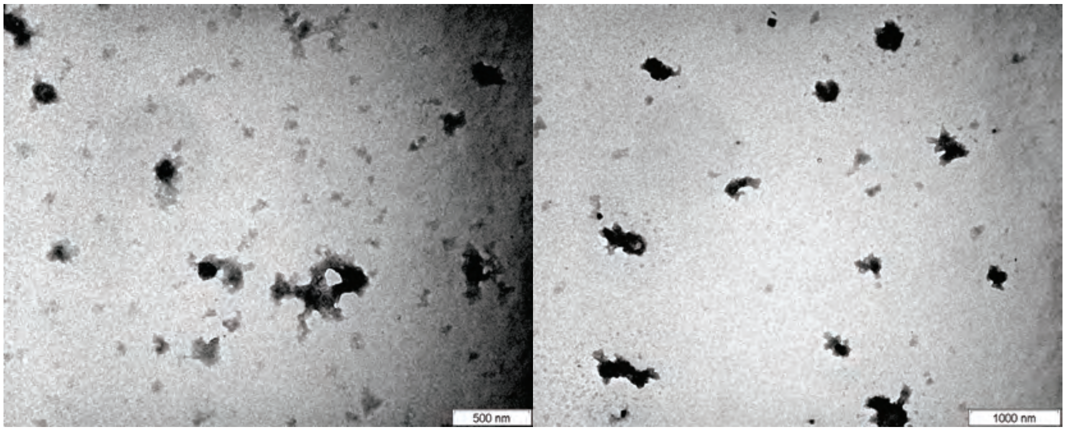

Figure S116. TEM images of nanospheres formed by poly(**1**$_{0.2}$-*co*-**7**$_{0.8}$) (mru)/Ba^{2+} ratio of 1.0/0.5 (mol/mol) (left) and poly(**1**$_{0.1}$-*co*-**7**$_{0.9}$) (mru)/Ba^{2+} ratio of 1.0/0.5 (mol/mol) (right).

Iron Magnets Encapsulation Studies

Polymers in $CHCl_3$ (1 mg/mL) with iron oxide nanoparticles (0,1 mg/mL) were mixed for 15 minutes and then 0,3 equiv. of barium perchlorate were added. Before 2 hours the magnet experiments were performed.

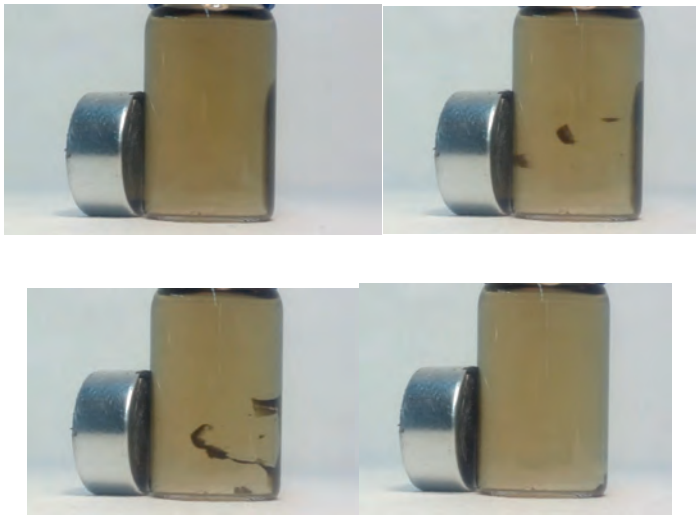

Figure S117. Sequential pictures of the attraction by a magnet of nanospheres of poly(**1**$_{0.8}$-*co*-**7**$_{0.2}$) incorporating magnetic nanoparticles.

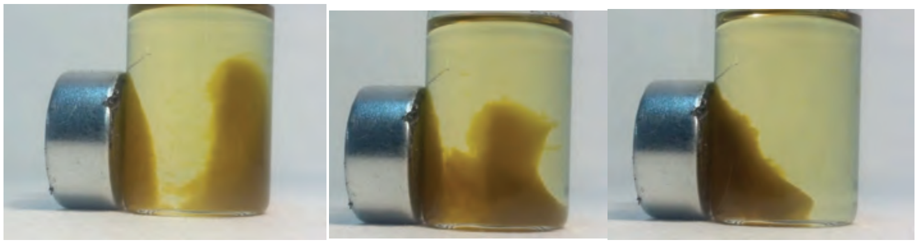

Figure S118. Sequential pictures of the attraction by a magnet of nanospheres of poly($\mathbf{1}_{0.2}$-*co*-$\mathbf{7}_{0.8}$) incorporating magnetic nanoparticles.

Atomic Force Microscopy Studies

Stock solutions of poly($\mathbf{1}_{0.6}$-*co*-$\mathbf{7}_{0.4}$) (1 mg/mL) in $CHCl_3$ were prepared and then diluted until 0.03 mg/mL. A solution of 10 mg/mL of $Ba(ClO_4)_2$ in THF was prepared and 0.2 equiv. of Ba^{2+} were added to a 0.03 mg/mL solution of poly($\mathbf{1}_{0.6}$-*co*-$\mathbf{7}_{0.4}$) in $CHCl_3$. One drop of this mixture(10 μL) was placed on freshly cleaved HOPG and was spin coated at RT at 900 and/or1800 rpm (Figures S136-S138).

All AFM measurements were performed at CACTI (Vigo University, Spain) in a MultiMode V Scanning Probe Microscope (Veeco Instruments) in air at RT with standard silicon cantilevers and super-sharp cantilevers in tapping mode using 12 μm and 1 μm scanners.

Nanoscope processing software and WSxM 4.0 Beta 1.0 [4] (Nanotec Electronica, S.L.) were used for image analysis.

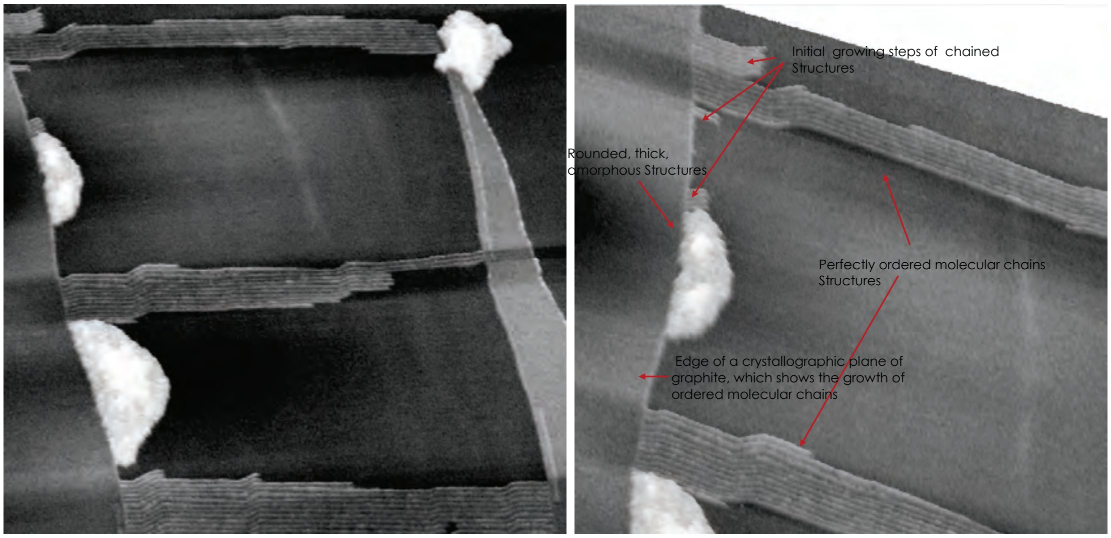

Figure S119. AFM images of poly($\mathbf{1}_{0.6}$-*co*-$\mathbf{7}_{0.4}$) (mru)/Ba^{2+} ratio of 1.0/0.5 (mol/mol)

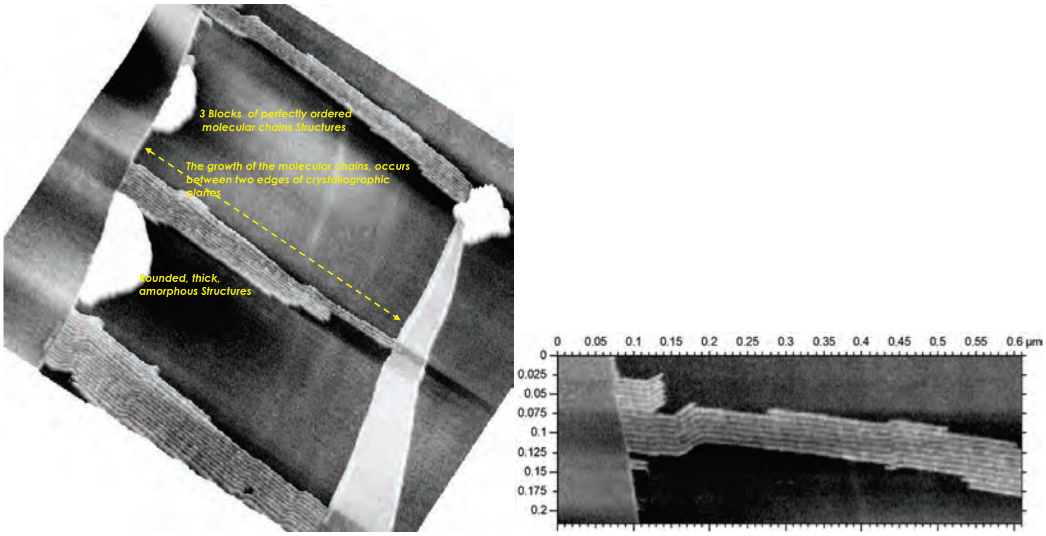

Figure S120. AFM images of poly($\mathbf{1}_{0.6}$-*co*-$\mathbf{7}_{0.4}$) (mru)/Ba^{2+} ratio of 1.0/0.5 (mol/mol)

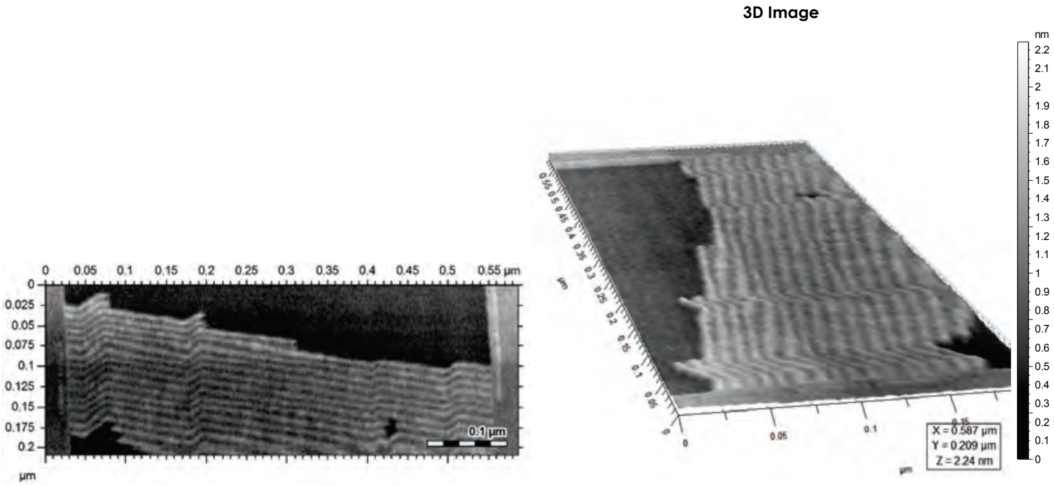

Figure S121. AFM images of poly($\mathbf{1}_{0.6}$-*co*-$\mathbf{7}_{0.4}$) (mru)/Ba^{2+} ratio of 1.0/0.5 (mol/mol).

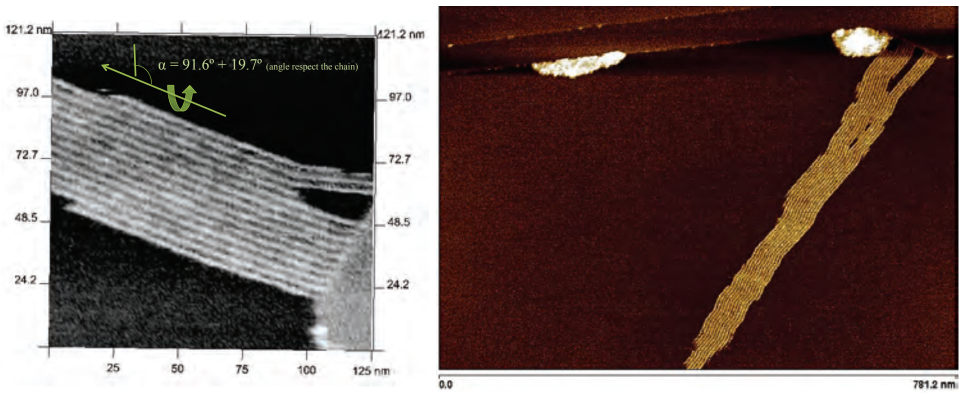

Figure S122. AFM images of poly($\mathbf{1}_{0.6}$-*co*-$\mathbf{7}_{0.4}$) (mru)/Ba^{2+} ratio of 1.0/0.5 (mol/mol)

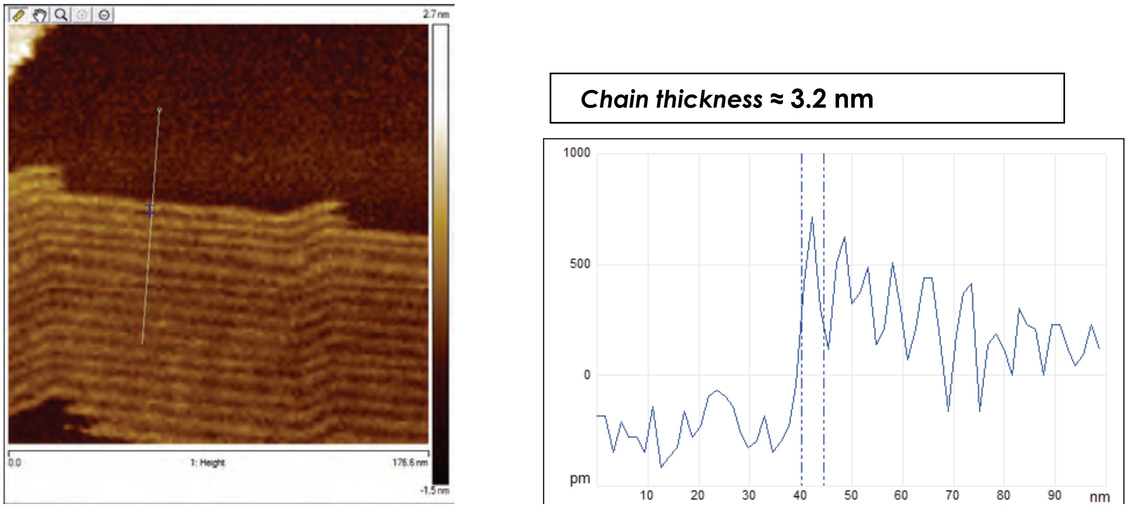
Chain thickness ≈ **3.2 nm**

Figure S123. AFM images of poly($\mathbf{1}_{0.6}$-*co*-$\mathbf{7}_{0.4}$) (mru)/Ba^{2+} ratio of 1.0/0.5 (mol/mol)

Thermal studies

TGA studies

TGA experiments were carried out in a Q5000SA instrument (TA Instruments, New Castle, UK). TGA measurements were performed for homopolymer (poly-**1**) and copolymers [poly($\mathbf{1}_{0.5}$-*co*-$\mathbf{7}_{0.5}$), poly($\mathbf{1}_{0.5}$-*co*-$\mathbf{8}_{0.5}$)]. The studies showed that those polymers started to decompose around 270 ºC.

Analogous experiments were performed for polymer (mru)/Ba^{2+} complexes in a ratio of 1.0/0.5 (mol/mol). It was found that the TGA traces of the polymer and the polymer/metal complexes are different. The decomposition starts in both systems around 270 ºC, but in the case of the polymer/metal complex the degradation is faster than in the single polymer.

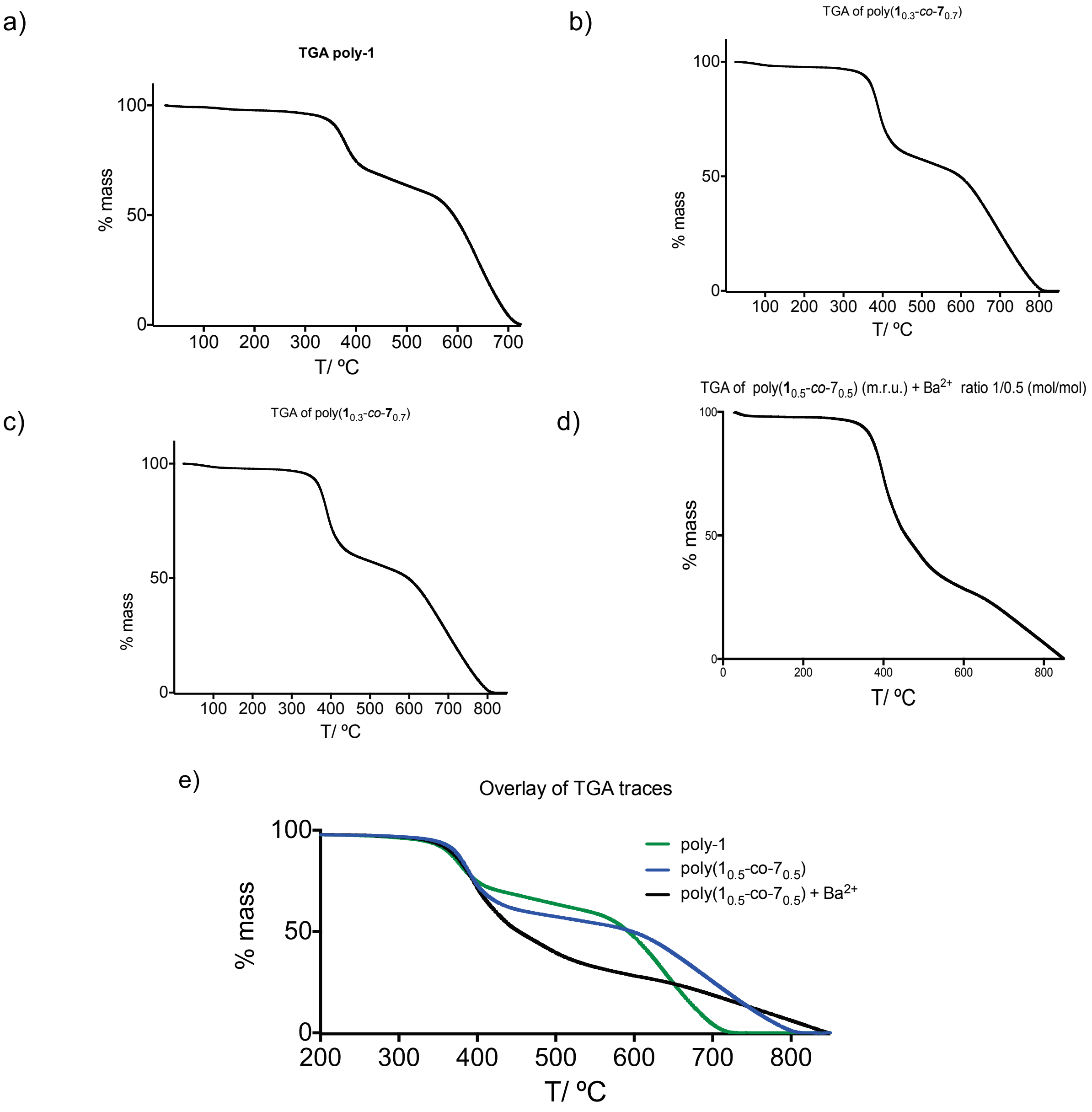

Figure S124. TGA data of (a) poly-**1**, (b) poly($\mathbf{1}_{0.3}$-*co*-$\mathbf{7}_{0.7}$), (c) poly($\mathbf{1}_{0.5}$-*co*-$\mathbf{7}_{0.5}$) and (d) poly($\mathbf{1}_{0.5}$-*co*-$\mathbf{7}_{0.5}$) (mru)/Ba^{2+} ratio of 1.0/0.5 (mol/mol). (e) Overlay showing the TGA traces corresponding to measurements (a), (c) and (d).

DSC studies

DSC measurements were performed in a DSC Q200 Tzero Technology. (TA Instruments, New Castle, UK) equipped with a refrigerated cooling system RCS90 TA Instruments.

DSC experiments were carried out for 3 mg of the homopolymer (poly-**1**) and the copolymers [poly(**1**$_{0.5}$-*co*-**7**$_{0.5}$), poly(**1**$_{0.5}$-*co*-**7**$_{0.5}$) and poly(**1**$_{0.5}$-*co*-**8**$_{0.5}$)].

The DSC trace of poly-**1**, measured at a heating rate of 10 ºC min^{-1} at a temperature range from 0 to 275 ºC, shows an exothermic peak at 200 ºC corresponding to the thermal transition from *cis-cisoidal* to *trans-transoidal* arrangements. Such a transition has been described for other polymers.[vi-ix]

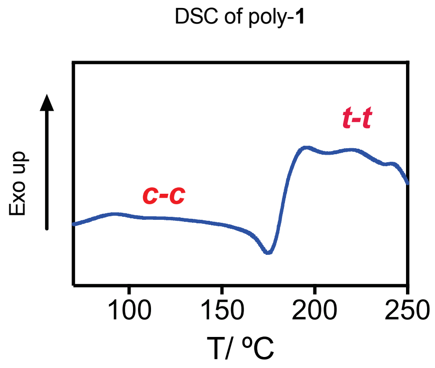

Figure S125. DSC trace of poly-**1**.

Analogous experiments were carried out for the copolymers [poly(**1**$_{0.5}$-*co*-**7**$_{0.5}$), poly(**1**$_{0.5}$-*co*-**7**$_{0.5}$) and poly(**1**$_{0.5}$-*co*-**8**$_{0.5}$)]. All DSC traces show an exothermic peak around 190-200 ºC corresponding to the thermal isomerization of the conjugated double bonds of the backbone from *cis-cisoid* to *trans-transoid*.

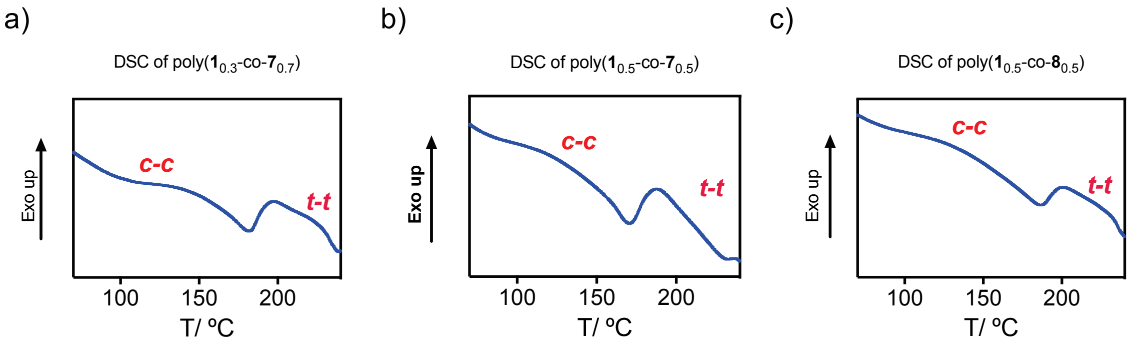

Figure S126. DSC traces of (a) poly(**1**$_{0.3}$-*co*-**7**$_{0.7}$), (b) poly(**1**$_{0.5}$-*co*-**7**$_{0.5}$) and (c) poly(**1**$_{0.5}$-*co*-**8**$_{0.5}$).

DSC traces of the polymer metal complexes [poly(**1**$_{0.5}$-*co*-**7**$_{0.5}$) with Ba^{2+} in a ratio of 1.0/0.5 (mol/mol)] show the exothermic thermal isomerization from *cis-cisoid* to *trans-transoid,* but in this case the isomerization takes place at 240 ºC. So, the arrangement takes place at higher temperatures (a shift of 40ºC) in the presence of the metal ion. This fact is due to the presence the presence of a new material (an aggregate) with higher stability for the *c-c* to *t-t* transition than the single copolymer.

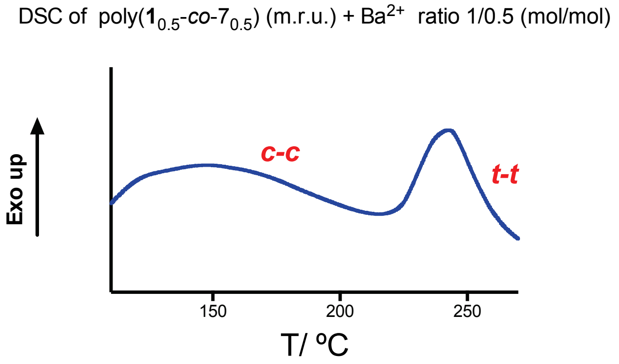

Figure S127. DSC trace of poly(**1**$_{0.5}$-*co*-**7**$_{0.5}$) (mru)/Ba^{2+} in a ratio of 1.0/0.5 (mol/mol).

Supporting References

[i] K. Maeda, M. Muto, T. Sato, E. Yashima, *Macromolecules*, **2011**, *44*, 8343–8349.

[ii] T. Kelen, F. Tüdös, *J. Macromol. Sci. Part A- Chemistry,* **1975**, *9*, 1–27.

[iii] C.I. Simionescu, V. Percec, S. Dumitrescu, *J. Polym. Sci., Polym. Chem. Ed.* **1977**, *15*, 2497–2509.

[iv] M. Tabata, Y. Tanaka, Y. Sadahiro, T. Sone, K. Yokota, I. Miura, *Macromolecules* **1997**, *30*, 5200-5204.

[v] F. Freire, J. M. Seco, E. Quiñoa, R. Riguera, *Angew. Chem. Int. Ed.* **2011**, *50*, 11692-11696.

[vi] F. Freire, J. M. Seco, E. Quiñoa, R. Riguera, *J. Am. Chem. Soc.* **2012**, *134*, 19374-19383

[vii] M. M. Green, N. C. Peterson, T. Sato, A. Teramoto, R. Cook and S. Lifson, *Science*, **1995**, *268*, 1860.

[viii] A. Motoshige, Y. Mawatari, Y. Yoshida, C. Seki, H. Matsuyama and M. Tabata, *J. Polym. Sci., Part A: Polym.Chem.*, **2012**, *50*, 3008.

[ix] L. Liu, T. Namikoshi, Y. Zang, T. Aoki, S. Hadano, Y. Abe, I. Wasuzu, T. Tsutsuba, M. Teraguchi and T. Kaneko, *J. Am. Chem. Soc.*, **2013**, *135*, 602.